Assessment of groundwater environment in a paddy-dominated alluvial fan
- Case study of Tedori River alluvial fan, Japan -

2014

Yumi IWASAKI

Contents

List of figures

List of tables

CHAPTER 1

Introduction

1.1 Background

Groundwater accounts for more than 98% of the Earth's available fresh water; it supplies at least 50% of the potable water, 40% of the industrial water, and 20% of the irrigation water used in the world (Foster and Chilton, 2003). Groundwater is therefore an indispensable and convenient source of water for drinking, industry, and agriculture, and it has supported a wide range of human activities because of its stability in both quality and quantity. However, excessive groundwater use results in declines in groundwater levels, which may have negative impacts on the local environment, such as land subsidence and saltwater intrusion. Until 2009, incidences of foundation subsidence were observed in 64 regions in Japan (Ministry of the Environment, 2011).

In Asian countries, 66% of the paddy and upland fields are irrigated, which corresponds to 12% of the world's agricultural land (Masumoto, 2004). Rice is a staple food for more than half the world's population (IRRI, 2006), and rice cultivation is closely linked with food security, the socioeconomic development of rural society, and conservation of natural resources and the environment. Groundwater recharge is an important process for sustainable groundwater management. Paddy fields are well known for their significant role in groundwater recharge. However, over recent years, the area of the paddy fields in Japan has been decreasing because of socioeconomic factors such as urbanization, increasing the area of fallow fields, and rice yield controls imposed by the government. Controls on rice yields have been implemented in Japan since the 1970s through rotating rice, vegetables, wheat, soybeans, and other crops. Over recent years, paddy-upland crop rotation has been approximately 30% of the total paddy area. Decreases in the area of rice-planted paddy fields may have caused a decrease in the amount of groundwater recharge and a decline in groundwater levels (Sugio et al., 1999; Watanabe et al., 2002; Khan et al., 2010). Clarifying the extent to which the decline in the area of paddy fields affects the groundwater level is important for sustainable groundwater use and paddy farming in the future. Likewise, various studies have been carried out to examine groundwater flows and recharge from paddy fields (Elhassan et al., 2001; Chen and Liu, 2002;

Chen et al., 2002; Anan et al., 2007). However, the effects of land use on groundwater recharge, especially land used for paddy fields as part of a crop rotation system, remain unclear.

Hydrological processes, such as precipitation, evapotranspiration, and interactions with surface water, link groundwater resources and climate change. Although the study area, the Hokuriku region, has a relatively high average temperature, it is subject to heavy snowfall. Accordingly, snowfall in the region is likely to decrease in response to the slight temperature rise predicted for this region due to climate change (Japan Meteorological Agency, 2008). There will therefore be potential long-term impacts on the groundwater environment, such as recharge, storage, and discharge. The Intergovernmental Panel on Climate Change (IPCC) (2007) suggested that there was a lack of studies addressing the impacts of climate change on groundwater. Hydrological simulations linked with General Circulation Models (GCMs) that predict future climate conditions can be used to investigate future impacts of climate change on groundwater resources. Several studies using groundwater models and GCMs have shown that climate change will have negative impacts on groundwater environments (Eckhardt and Ulbrich, 2003; Scibek and Allen, 2011; Sulis et al., 2011). To date, however, there have been few studies on the potential effects of climate change on groundwater in Japan (Koizumi, 2009).

Sustainable management of groundwater resources requires an understanding of how groundwater responds to natural and socioeconomic changes, such as land use, groundwater use, and climate change. However, groundwater environments are specific and unique in terms of, among other factors, topography, meteorology, land use, irrigation practice, and groundwater use. Furthermore, limited availability of data for groundwater level, groundwater use, hydrogeology, and soil characteristics constricts our ability to develop sophisticated groundwater flow models. A groundwater study for evaluating the factors that influence groundwater environments should therefore be an illustrative case study.

1.2 Research problem

Groundwater recharge is water that reaches the groundwater body by moving through the unsaturated (vadose) zone, the area between the land surface and the groundwater table. The zone below the groundwater table is called the saturated zone. Groundwater recharge from irrigated paddy fields is an important part of the hydrological cycle in agricultural fields in Japan. It is difficult to develop a groundwater flow model for irrigated paddy field areas, as irrigated paddy fields have specific soil structures, comprising the puddled topsoil layer, the plough zone, the underlying subsoil layer, and irrigation regimes that include managing the ponding water and intermittent irrigation. The possibility of applying a coupled physically based unsaturated

model and groundwater flow model to several land uses, including the rice-planted paddy, crop-rotated paddy, and upland fields, and to large areas of hydrogeological interest and relatively deep groundwater tables, must be examined. Furthermore, field observations of the hydrological cycle and hydrogeological conditions are needed to improve understanding of the processes involved, and to develop accurate models.

1.3 Research objectives

The objective of this study is to evaluate groundwater environments, through an examination of groundwater levels, recharge, flow, and storage in an alluvial fan where irrigated paddy fields dominate, by integrating unsaturated/saturated modeling, hydrological observations, and hydrochemical observations. The study area is the Tedori Alluvial Fan in Ishikawa Prefecture, Japan. Specific objectives of the study are as follows:

1) Identification of the effects of land use, mainly dominated by irrigated paddy fields, and groundwater-river water interactions on the groundwater level.

2) Development of a groundwater flow model that considers paddy water management and crop rotation in the paddy fields, in which the unsaturated flow model is adapted to evaluate the impacts of climate change on groundwater environments.

3) Quantitative assessment of the factors influencing groundwater recharge and groundwater-level changes.

4) Estimation of the mechanisms of groundwater recharge and groundwater flow paths from hydrochemical observations of multiple tracers (major dissolved ions, large number of elements, and oxygen, hydrogen and strontium isotopes).

1.4 Structure of this thesis

This thesis consists of nine chapters, and its structure is shown in Figure 1-1. The outline of each chapter is as follows.

The introductory chapter presents the background to the study, along with the study objectives and challenges associated with the study.

Chapter 2 is a review of relevant groundwater literature. It provides a discussion of recent studies of groundwater environments in paddy fields and alluvial fans, along with studies that evaluated the impacts of climate change on groundwater environments. Recent research reporting methods for estimating groundwater recharge are included. Finally, recent studies describing groundwater flow models and methods for coupling physical-based unsaturated groundwater models and groundwater flow models are discussed.

Chapter 3 includes a summary of information relating to the hydrological processes in the study area. Hydrological data were collected for the study site to provide information on the distribution of groundwater levels and groundwater flow paths as the basis for suitable groundwater models. Information about seasonal and annual groundwater fluctuations, based on the continual groundwater-level observations at some wells, is presented. The groundwater flow and distribution of the groundwater levels are delineated by groundwater-level contours, which have been obtained from simultaneous groundwater-level observations. Interactions between groundwater and river water, and the amounts of the water exchanged, are estimated from discharge observations of the Tedori River.

Chapter 4 contains an evaluation of the direct relationship between groundwater levels and the area of the paddy fields. Through spatial analysis using GIS (Geographical Information Systems), the relationship between increments in groundwater levels at the beginning of the irrigation period and the ratio of the paddy field area to the total area around the sampled wells is examined. In addition, the question of how the distance between paddy fields and the sampled wells influences changes in groundwater levels is considered.

Chapter 5 describes the development of the groundwater model using MODFLOW, based on the hydrological observations collected during the irrigation period. In this model, factors influencing groundwater-level changes during the irrigation period are assessed using steady state groundwater flow analysis, and scenarios of past, present and future land use and groundwater use. The steady state model is used to examine how groundwater levels might be effectively protected using hypothetical scenario analysis.

In Chapter 6, the steady state model is extended to include a transient model that can estimate the quantitative effects of different land use conditions, such as paddy and upland fields (including crop-rotated paddy fields), on groundwater recharge and groundwater levels. The transient model consists of a 1-D unsaturated model (HYDRUS-1D) that can estimate groundwater recharge and a 3-D groundwater model (MODFLOW). Land use is modeled at a high resolution using a 400 m × 400 m model grid. Based on groundwater flow simulations from 1975 to 2009, relationships between temporal changes in groundwater levels and artificial or natural factors are evaluated.

Chapter 7 provides predictions of groundwater levels for 2010–2090 from the newly developed transient groundwater flow model and predicted meteorological variables. The future meteorological changes are already available at a daily time step; these are generated for multiple GCM (Global Circulation Model) and GHG (Greenhouse Gas) emission scenarios. An investigation of the sensitivities of groundwater levels in paddy-dominated areas to climate change is included.

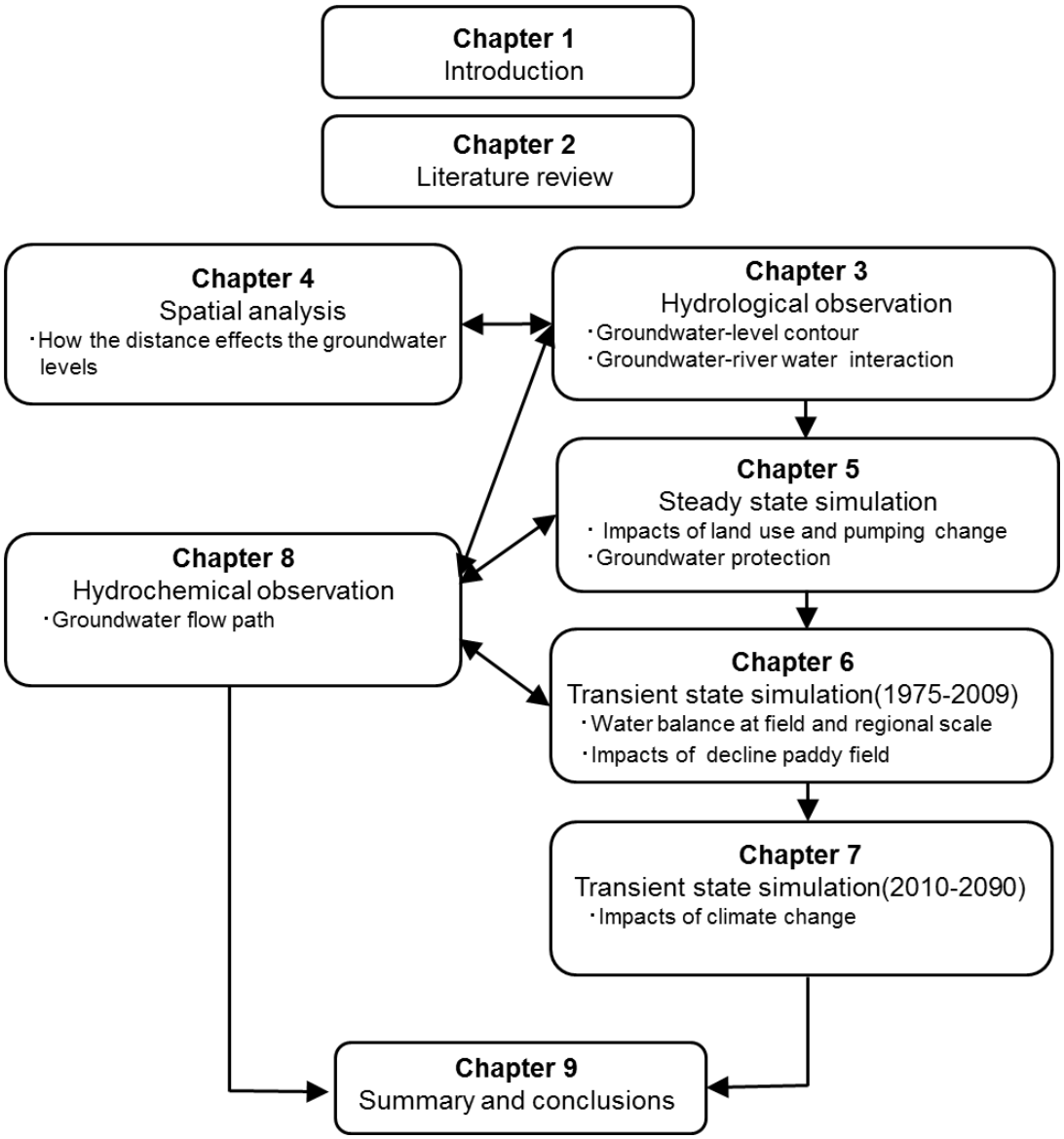

Figure 1-1 Structure of this thesis.

In Chapter 8, the sources and flow paths of groundwater in the paddy-dominated alluvial fan are investigated using a multi-tracer technique. Water samples collected simultaneously at 83 sites, including 63 groundwater sites, 12 river water sites, two spring water sites, and five paddy water sites, are analyzed for major dissolved ions, a wide range of elements, and stable isotopes (oxygen, hydrogen, and strontium). The consistency between hydrological observations and the numerical flow simulations is examined. The groundwater recharge sources defined in Chapters 4 and 5, and groundwater flow paths defined in Chapters 3 and 4, are reconsidered based on the distributions of the multi-tracer concentrations.

Chapter 9 is a summary of the results from the preceding chapters.

References

Anan M, Yuge K, Nakano Y. Saptomo S, Haraguchi T. 2007. Quantification of the effect of rice paddy area changes on recharging groundwater. Paddy Water Environ 5: 41–47.

Chen SK, Liu CW. 2002. Analysis of water movement in paddy rice fields (I) experimental studies. J Hydrol 260: 206-215.

Chen SK, Liu CW, Huang HC. 2002. Analysis of water movement in paddy rice fields (II) simulation studies. J Hydrol 268: 259-271.

Eckhard K, Ulbrich U. 2003. Potential impacts of climate change on groundwater recharge and streamflow in a central European low mountain range. J Hydrol 284: 244-2582.

Elhassan AM, Goto A, Mizutani M. 2001. Combining a tank model with a groundwater model for simulating regional groundwater flow in an alluvial fan. Trans of JSIDRE 215: 21–29.

Foster SSD, Chilton PJ. 2003. Groundwater: the processes and global significance of aquifer degradation. Phil Trans R Soc Lond B 358: 1957-1972.

Intergovernmental Panel on Climate Change (IPCC). 2007. Climate change 2007: the Physical Science Basis. Cambridge University Press, Cambridge.

IRRI. 2006. Bringing hope, improving lives: Strategic plan 2007-2015. p. 61.

Khan S, Rana T, Corroll J, Gabriel. 2010. Assessment of rice hydraulic loading impacts on groundwater and salinity levels. Paddy Water Environ 8: 23-29.

Koizumi R. 2009. Evaluation of groundwater environment in Toyohira River Alluvial Fan using groundwater flow analysis. Proceedings of Japanese Society of Physical Hydrology, http://rikusui.sci.hokudai.ac.jp/rikuken/media/2009sapporo/09abst18.pdf (in Japanese).

Masumoto T. 2004. Muti-functional roles of paddy irrigation in monsoon Asia. Jour JSIDRE 72(7): 559-564 (in Japanese)

Ministry of the Environment. 2011. 2009 Conspectus of subsidence problems in Japan. http://www.env.go.jp/press/file view.php ?serial=16543&hou id=13187 (in Japanese).

Scibek J, Allen DM. 2006. Modeled impacts of predicted climate change on recharge and groundwater levels. Water Resour Res 42: W11405.

Sugio S, Eto M, Imayama K, Deguchi C, Suharyanto A. 1999. Fall of unconfined groundwater level caused by change of ground cover condition in Miyazaki city. Journal of Groundwater Hydrology 41(4): 253-262 (in Japanese with English abstract).

Sulis M, Paniconi C, Rivard C, Harvey R, Chaumont D. 2011. Assessment of climate change impacts at the catchment scale with a detailed hydrological model of surface-subsurface interactions and comparison with a land surface model. Water Resour Res 47: W01513.

Watanabe S, Yoneda M, Morisawa S, Yokoyana T. 2002. Simulation of groundwater level fluctuation and recharge estimation in Kagamihara groundwater basin, Gifu prefecture.

Journal of Groundwater Hydrology 44(3): 199–211 (in Japanese with English abstract).

CHAPTER 2

Literature review

2.1 Groundwater environment at paddy field area

Paddy rice is the major food source in Japan, Taiwan, Korea, as well as other rice-growing countries in Monsoon Asia. It is recognized that water infiltration from the paddy fields during irrigation periods contributes significantly to groundwater recharge because paddy rice requires the standing water during the most of its growth period. There are also multi-functionalities of paddy field; irrigation of flood, nitrogen cycle control, mitigation of local climate and so on. (Haung et al., 2006; Kim et al., 2006; Masumoto et al., 2004; Matsuno et al., 2006; Mitsuno et al., 1982).

Many studies for quantitative evaluation of groundwater recharge by paddy fields have been carried out with groundwater monitoring or simulation methods. Horino et al. (1989) pointed out that groundwater storage in the Echi River alluvial fan in Shiga Prefecture, Japan, where much paddy field occupy, plays role as storage reservoir. Tanaka et al. (2010) quantified the amount of water recharged from paddy fields and other lands in the Shira River basin in Kumamoto Prefecture, Japan. The estimated annual recharge was as high as 15,300 mm. Elhassan et al. (2001) investigated the water balance in the Nasunogahara alluvial fan in Tochigi Prefecture, Japan, based on the groundwater flow model combined with a tank model. The proportion of the groundwater recharge from paddy fields to the total recharge was 27% in spite of the paddy fields area ratio was less than 40% and the irrigation period was limited in four months of the year.

Various studies examine the impact of the decline in the paddy field area on the groundwater level. Fujihara and Ohashi (2000) investigated groundwater level changes with and without paddy irrigation using a 3-D groundwater model in the Dogo Paine in Ehime Prefecture, Japan. Under the no paddy irrigation condition, the maximum declines of groundwater levels during the irrigation period in a dry year and in normal year were 56 cm and 96 cm, respectively. The no paddy irrigation condition also resulted in the decline of groundwater levels during the non-irrigation period in a dry year. Anan et al. (2007) simulated changes in groundwater levels when all farmlands were ponded in the left bank of the Chikugo River, Fukuoka Prefecture,

and showed that the groundwater level and groundwater storage would increase by 0.5-1.0 m and 20% from the present condition, respectively. Kiriyama and Ichikawa (2004) concluded that the groundwater recharge decline in about half of that of 25 years ago in Kumamoto city, Kumamoto Prefecture, because of decreasing the rice-planted paddy field, which was affected by the urbanization and rice-upland crop rotation system. Sugio et al. (1999) reported that the decline of groundwater levels was consistent with changes in the impervious area based on a tank model simulation in Miyazaki City, Miyazaki Prefecture. Watanabe et al. (2002) indicated that the groundwater level declined by about 5 m when the paddy field transformed to a mixture field of the paddy and upland field, and the declines could not be recovered only by the groundwater recharge from precipitation in the Kagamihara City, Gifu Prefecture. Khan et al. (2010) described that the decrease of the paddy field by 50% and 75% from the present caused to groundwater level declined in 1 m in Australia.

2.2 Groundwater environment in alluvial fan

Alluvial fan is one of the major landforms in Japan. Based on the classification of landforms, alluvial fan occupies 8% of the whole area and 45% of whole lowland in Japan (Seto, 1986). In addition, 38% of paddy field exist on alluvial fans. Alluvial fans are often characterized by permeable, coarse texture soils. Alluvium deposits along streams constitute shallow aquifers and are capable of significant recharge. Groundwater and surface water interactions, such as water exchange between the groundwater and river water through the riverbed (river water infiltration to groundwater and groundwater flow to the river), and spring water in downstream of the fan, frequently occur. The above interaction is an essential part of hydrological water cycles influenced significantly by many factors: geology, landform, climate, and human activities (Sophocleous, 2002). Kalbus et al. (2006) provide a review of measuring methods for aquifer-river interaction. Various methods have been used, for example, Darcy equation, environmental tracers, heat tracer, and hydrograph separation. For hydraulically connected aquifer-river system, the exchange flow is a function of the difference between groundwater level and river water level. A simple approach to estimate the exchange flow is to consider the flow between the groundwater and river water to be controlled by the Darcian law. Sanz et al. (2011) calculated aquifer recharge from the river under various intensities of groundwater pumping using numerical model based MODFLOW and quantitatively assessed river recharge induced by groundwater pumping. This method has also been successfully used in some studies (Imagawa et al., 2012; Zume and Tarhule, 2008).

2.3 Impacts of climate change on groundwater environments

Climate change is probably one of the most challenging issues facing water resources. Groundwater resources are related to climate change through hydrological processes including precipitation, evapotranspiration, recharge processes, and interaction with surface water resources (rivers and lakes). Recently, a number of GCM were developed to enable understanding and prediction of climate change and future meteorological factors. Groundwater flow simulation with GCMs is a novel methodology to assess the effects of climate change on groundwater. In impact analysis, it is important to give the well-understood uncertainties of climate change projections, which are mainly associated with use of GCM, and multi-GCM analysis is applied to assess of the uncertainty (Portmann et al., 2013). Physical-based hydrological models for estimation of groundwater recharge must take into account unsaturated water flow to accurately assess the impacts of climate on groundwater. During the last decade, several studies evaluated the effects of climate change on regional groundwater recharge and groundwater level and showed that climate change will have positive or negative impacts on groundwater levels. Goderniaux et al. (2011) indicated that predicted groundwater levels in eastern Belgium tended to decrease between 2010 and 2085 under increasing precipitation during summer and decreasing precipitation during winter. The decline of the groundwater levels ranged from 2 m to 21 m. In the contract, Brouyere et al. (2004) reported that there is no enhancement of the seasonal changes in groundwater levels in eastern Belgium. Scibeck and Allen (2006) reported that groundwater recharge in southwest Canada will increase from spring to summer, with a maximum increase of 0.5 m occurring from 2040-2069. Crosbie et al. (2013) pointed out that predicted groundwater recharge will increase and decrease by approximately 10% by 2050 based on 16 GCMs in the high plains region of the United States. They also reported that areas with high current groundwater recharge levels are less sensitive to changes in precipitation. Various studies evaluating impacts of climate change on groundwater environments have been attempted (Allen et al., 2004; Holman, 2006). Predicted climate change and the groundwater response to climate change differed from place to place. Climate change may also affect land use and agricultural practices such as the amount of available water resources, irrigation water demand, and cultivation management (Watanabe and Kume, 2009). Toewa and Allen (2009) predicted that groundwater levels in Canada would increase due to application of increased amounts of irrigation water, which will contribute to groundwater recharge under warmer temperature conditions. Fiklin et al. (2010) indicated that changes in evapotranspiration, plant growth (irrigation timing), and irrigation demand, which were caused by the climate change, mainly would affect groundwater recharge in western United State. Therefore, quantifying the impact of climate change on groundwater resources requires not only

reliable forecasting of changes in major climate variables, but also adequate estimation of various factors influenced by climate change.

2.3 Methods for estimating groundwater recharge

2.3.1 Modeling methods

Groundwater recharge is the water, which reaches the groundwater body moving through the unsaturated zone. Groundwater recharge fluctuates both temporally and spatially due to various factors, such as soil permeability, land use condition, topography, amount of rainfall, amount of snowfall, timing of snowmelt, and irrigation management. Especially, groundwater recharge from irrigated paddy fields depends on the soil structure and irrigation management. The soil is puddled before transplanting to reduce percolation losses by decreasing the hydraulic conductivity of paddy soils. Then, paddy soil presents stratified layers that consist of the top puddled layer, muddy layer, plow sole (also, called hardpan) layer, and underlying subsoil layer (Liu et al., 2001; Tournebize et al., 2006). Furthermore, several paddy irrigation managements are carried out in accordance with the growth stage of rice, such as a puddling, mid-summer drainage, and intermittent irrigation. Consequently, many factors influence groundwater recharge from paddy fields, such as top and subsoil thickness, hydraulic conductivity of plow sole layer, ponding water depth and soil pudding intensity (Chen and Liu, 2002; Kukal and Aggarwal, 2002; Lin et al., 2013).

Accurate quantification of groundwater recharge is important for proper management of groundwater resources. Because field measurements cannot accurately evaluate the amount of groundwater recharge, groundwater recharge is commonly estimated using several methods. Water balance methods estimate recharge as the residual of precipitation (and irrigation water) minus runoff, lateral seepage, and evapotranspiration (Don et al., 2006; Imaizumi et al., 2006). The advantages of water balance methods are that they can estimate from readily available data. Other conceptual methods are based on field measurements of runoff and precipitation or percolation and precipitation. Fujihara and Ohashi (2000) calculated 2 mm/d as groundwater recharge at irrigated paddy field considering percolation and precipitation. The tank model was proposed by Sugawara (1974) and was one of the applicable and widely used as rainfall-runoff models in Japan. Elhassan et al. (2001) coupled a paddy tank and two-layer non-paddy tanks to calculate the percolation rate for irrigation and non-irrigation periods from the upper tanks to the shallow aquifer. Raneesh and Thampi (2013) developed three-layer tank model whose first layer is the surface layer with associated some land uses (paddy, farm, forest and urban fields). Various tank models have been developed to simulate groundwater recharge from agricultural

fields (e.g. He et al., 2008; Kiriyama et al., 2000; Watanabe et al., 2002). Water table fluctuation method is based on the assumption that rises in groundwater level in unconfined aquifers are due to recharge water arriving at the water table (e.g. Kerchum et al., 2000).

The majority of currently available unsaturated models is based on either the Richards equation (Richards, 1931) or the kinematic wave equation (Smith and Hebbert, 1983). While the Richards equation considers flow due to capillary and gravity forces, the kinematic wave considers only gravity forces. Typical physically based model solves the Richards equation (Tournebize, 2006; Kaushal et al., 2009).

These methods for groundwater recharge estimation often require some calibration parameters and the estimated groundwater recharge is limited by the model structure. Groundwater model calibration or inversion is also used to estimate the recharge from information regarding hydraulic conductivity, hydraulic heads, and other parameters (e.g. Nettasana et al., 2012). Certain studies have made use of chemical/isotope concentrations (Zhu, 2000; Štuopis et al., 2012).

2.3.1 Water quality methods

The chemical, isotopic and gaseous tracer methods are widely used for the estimation of groundwater recharge source and its spatial variability. Stable oxygen (^{16}O and ^{18}O) and hydrogen (^{1}H and ^{2}H) isotopes are an ideal tracer for delineating hydrological processes because they are constituent water molecule themselves. The oxygen and hydrogen isotopes, which are expressed as $\delta^{18}O$ and δD, exhibit spatial and temporal variations as a result of isotope fractionations that accompany water-cycle phase changes and mixing processes (Gibson et al., 2005). In Japan, several studies investigated groundwater source and groundwater-river water interactions using the $\delta^{18}O$ and δD (Komiyama et al., 2003; Wakui and Yamanaka, 2006; Tsuchihara et al., 2010).

The combination of major element concentrations of groundwater and land use data helps to determine the sources of groundwater recharge. Geological tracers, such as sodium, nitrate, silica, aluminum and strontium, often delineate the groundwater flow path. To separate the river flow components, mixing models or mixing diagram based on the conservation of mass are applied. Strontium (Sr) isotope in water, which is expressed as the $^{87}Sr/^{86}Sr$ ratio, is only controlled by water-rock interactions and mixing processes. The concentration of ^{87}Sr increases over time as radioactive ^{87}Rb decays while the concentrations of the other isotopes (^{84}Sr, ^{85}Sr, and ^{86}Sr) remain constant. Older rocks, therefore, have higher $^{87}Sr/^{86}Sr$ ratios than younger rocks with the same initial Rb/Sr ratio. Over geologic time, the $^{87}Sr/^{86}Sr$ in rocks with a high Rb/Sr becomes higher than rocks with a lower Rb/Sr. Thus, the ratios are indicators of both age and geochemical origin (Capo et al., 1998). The $^{87}Sr/^{86}Sr$ ratio have been used successfully in groundwater-surface

water interaction studies to distinguish different sources of groundwater recharge and help identify likely flow paths (Banks et al., 2011; Han et al., 2010; Petelet-Giraud et al., 2007; Uliana et al., 2007; Xie et al., 2013). Furthermore, the Sr isotope ratio has been used to assess the impacts of agricultural activities on groundwater (Böhike and Horan, 2000; Jiang, 2011; Hosono et al., 2007; Nakano et al., 2008).

Groundwater flow models were developed using multiple preexisting and field observation data, such as topography, geology, and borehole, to reproduce the hydrogeological conditions as precisely as possible. The developed model was verified by observed groundwater levels. However, there is often difficulty in measuring the groundwater levels at fine spatial and temporal when a target area is relatively wide. Hydrochemical observations, such as dissolved ions, stable isotopes, and radioactive isotopes of various origins of water, can provide to information about groundwater sources, groundwater flow paths, and age of the groundwater. Thus, the reconsideration of conceptual models, model structures, and hydrogeological settings etc. based on the hydrochemical observations is important validation processes.

2.4 Groundwater flow model

The numerical simulation attempts to reproduce complexity by integrating components of the hydrogeological system, climatic effects, and anthropogenic issues. Groundwater flow models have been used for investigating groundwater system dynamics, for evaluating recharge, discharge and storage of aquifer, and for predicting future conditions or impacts of human activities, groundwater development, and groundwater management (Zhou and Li, 2011).

Natural processes and human activities affect groundwater environment, such as recharge, flow paths, and discharge. Groundwater models attempt to reproduce complexity by integrating components of the hydrogeological system, climatic effects, and anthropogenic issues. If models can reasonably reproduce past and present groundwater environments, they can predict the future changes in the groundwater environments. Future predictions are important information for the exploration of sustainable groundwater use and the decision-making of groundwater management. The models should be validated well based on the hydrogeological and hydrological observations.

Many numerical models have been developed. Some numerical modeling software has been widely used; such as Finite Element subsurface FLOW system (FEFLOW, Diersch, 1996) and MODular three-dimensional finite-difference groundwater FLOW model (MODFLOW, Harbaugh and McDonald, 1996). MODFLOW has separate package to resolve special hydrogeological problems. Groundwater modeling requires complex information concerning hydrogeology, topography, soil, land use, and groundwater use. In recent years, a

large number of studies using GIS as pre-process and post-process. GIS is a beneficial tool for handling the complexity of different spatial physical and hydrogeological data, and for integrating data of various sources. GIS helps develop such a distribution type model easily.

Estimating groundwater recharge, which is the upper boundary condition of the groundwater flow model, is an important issue for constructing a reliable groundwater model. However, for regional groundwater modeling, the groundwater recharge and evapotranspiration process are often simplified. For example, in some traditional groundwater flow models such as FEFLOW, these fluxes are often imposed by the modeler and estimated independently from the model. In MODFLOW, the groundwater recharge is often directly specified by users as flux, and evapotranspiration is treated as a head-dependent flux boundary, using a linear or a piecewise linear relationship between water table depth and evapotranspiration rate.

2.5 Coupling of unsaturated-saturated model

Coupled models using an unsaturated model and a groundwater model are distinguished on the basis of differences in their structures and coupling strategies. Firstly, general coupled models are classified into the following types; a combination of a physically based unsaturated flow model and a conceptual groundwater model, a combination of a conceptual unsaturated flow model and a physically based groundwater model, and physically based approaches that fully integrate unsaturated and groundwater flows. Coupling scheme is generally characterized as follows: (1) sequential or one way coupling, in which the unsaturated outputs are inputs in the groundwater flow models and the models are independently calculated at each time step; and (2) full or two way coupling scheme, which means that two models are coupled by the internal boundary condition and this boundary condition is updated using the groundwater model result until convergence criteria are achieved. Details of numerical coupling methods concerning with the boundary conditions of the unsaturated model have been reported by Furman (2008). The one-way coupling methods are generally used when the unsaturated zone is thick. Boggard and van Asch (2002) used 1-D unsaturated model and 3-D groundwater model. Munévar and Mariño (1999) used 2-D unsaturated model (2-D Richards equation) and 2-D groundwater flow model in an alluvial fan where thickness of the unsaturated zone range were relatively deep (from 31 to 42 m).

Combined models of both physically models for unsaturated and saturated zone have been applied to many studies. Lateral flux is much smaller than vertical water flux in agricultural field (Chen et al., 1994; Zhu et al., 2012), therefore, it may be an alternative method to couple a 1-D unsaturated flow model into groundwater flow models (Twarakvi et al., 2008; Šimůnek and Bradford, 2008). This method has also been successfully applied in some studies (Hollanders et

al., 2005; Zhu et al., 2012). Recently, some models linking an existing unsaturated flow model with a groundwater model have been developed. This study mainly focuses on MODFLOW. Niswonger et al. (2006) provided the unsaturated-zone flow (UZF1) package for MODFLOW. Seo et al. (2008) combined simplified HYDRUS-1D and MODFLOW called HYDRUS package for MODLOW. Twarakivi (2008) provided a comparison of the HYDRUS package with other MODFLOW package that evaluated processes in the unsaturated zone, and presented a field application demonstrating the functionality of the package. Leterme et al. (2012) modified HYDRUS package to allow the excess water to be removed as seepage. Xu et al. (2012) tested the coupled MODFLOW-2000 with the SWAP (Soil - Water - Atmosphere - Plant) package in an arid irrigation district on a regional scale and van Walsum and Groenendijk (2008) also integrated SWAP and MODFLOW. Several studies have presented the coupling of SWAT (Soil and Water Assessment Tool) and MODFLOW (Pisinaras et al., 2012; Ke, 2013). Some researchers have employed the same model combination (e.g. MIKE SHE, Refsgaard et al., 1995).

Physically based models simulate the unsaturated water flow processes and estimate the recharge and discharge using 3-D Richards equations, e.g. MODFLOW SURFACT (Hydro GeoLogic Inc., 1996), VSF package for MODFLOW (Thoms et al., 2006), HydroGeoSphere (HGS) (Therrien et al., 2006) , InHM (VanderKwaak et al., 2001), CATHY(Camporese et al., 2010), ParFlow (Kollet et al., 2006; Maxwell et al., 2008), MODHMS(Panday et al., 2004), and HYDRUS (2D/3D) (Šimůnek et al., 2006). These models have some disadvantages. Models for watershed-scale modeling are often hampered by the numerical solution of Richards equation in the unsaturated zone. Richards equation is difficult to solve due to its parabolic form and the nonlinear relationships between soil water pressure head, hydraulic conductivity, and water content. Because of the requirement of much finer temporal and spatial discretization, heavily available computational resources are required (van Walsum and Groenendijk, 2008). Furthermore, some models do not reasonably consider the effects of vegetation growth and meteorological factors on groundwater recharge and evapotranspiration (such as VSF package), which have significant impacts on water flow in the unsaturated zone. When the coupling of unsaturated-saturated model is used at the paddy fields, however, it may cause some problems because it is not able to completely represent the characteristics of fields and address complicated the irrigation water managements: e.g. the standing water.

2.6 Summary

To reproduce the groundwater recharge and groundwater level at the paddy and crop rotated paddy fields considering the meteorological changes and irrigation managements, coupling of the 1-D unsaturated flow model and 3-D groundwater model can become effective technique.

However, the possibility of application of the coupled model at paddy and crop rotated paddy fields is unclear. When using the available data, which is provided gratis with GIS base, and hydrological observations, the model precision is limited by the spatial and temporal resolutions of used data. The model precision is therefore needed to be exanimated beforehand. This study selects HYDRUS-1D for the unsaturated flow model and MODFLOW for 3-D groundwater flow model because of a large number of various application studies. The integrated approaches of unsaturated/saturated flow modeling, hydrological observations, and hydrochemical observations try to estimate groundwater environments.

References

Anan M, Yuge K, Nakano Y. Saptomo S, Haraguchi T. 2007. Quantification of the effect of rice paddy area changes on recharging groundwater. Paddy Water Environ 5: 41–47.

Allen DM, Mackie DC, Wei DC. 2004. Groundwater and climate change: a sensitivity analysis for Grand Forks aquifer, southern British Columbia, Canada. Hydrogeol J 12: 270-290.

Banks EW, Simmons CT, Love AJ, Shand P. 2011. Assessing spatial and temporal connectivity between surface water and groundwater in a regional catchment: Implications for regional scale water quantity and quality. J Hydro 404: 30-49.

Boggard, TA, van Asch TWJ. 2002. The role of the soil moisture balance in the unsaturated zone on movement and stability of the Beline landslide, France. Earth Surf Proc Lnd 27: 1177-1188.

Böhlke JK, Horan M. 2000. Strontium isotope geochemistry of groundwaters and streams affcted by agriculture, Locust Grove, MD. Appl Geochem 15: 599-609.

Brouyère S, Carabin G, Dassrgues A.2004. Climate change impacts on groundwater resources: modelled deficits in a chalky aquifer, Geer basin, Belgium. Hydrogeol J 12: 123-134.

Camporese M, Paniconi C, Putti M, Orlandini S. 2010. Surface-subsurface flow modeling with path-based runoff routing, boundary condition-based coupling, and assimilation of multisource observation data. Water Resour Res 46: W02512.

Capo RC, Stewart BW, Chadwich OA. 1998. Strontium isotopes as tracers of ecosystem process: theory and methods. Geoderma 82: 197-225.

Chen SK, Liu CW. 2002. Analysis of water movement in paddy rice fields (I) experimental studies. J Hydrol 260: 206-215.

Chen SK, Liu CW, Huang HC. 2002. Analysis of water movement in paddy rice fields (II) simulation studies. J Hydrol 268: 259-271.

Chen Z, Govindaraju RS, Kavvas ML. 1994. Spatial averaging of unsaturated flow equations

under infiltration conditions over areally heterogeneous fields-1. Development of models. Water Resour Res 30(2): 523–534

Crosbie RS, Scanlon BR, Mpelasoka FS, Reedy RC, Gates JB, Zhang L. 2013. Potential climate change effects on groundwater recharge in the High Plains Aquifer, USA. Water Resour Res 449: 3936-3951.

Diersch HJG. 1996. Interactive, graphics-based finite-element simulation system FEFLOW for groundwater flow, contaminant mass and head transport processed. FEFLOW User's Manual Version 4.50, Berlin.

Don NC, Hang NTM, Araki H, Yamanishi H, Koga K. 2006. Groundwater resources and management for paddy field irrigation and associated environmental problems in an alluvial coastal lowland plain. Agr Water Manage 84: 295-304.

Elhassan AM, Goto A, Mizutani M. 2001. Combining a tank model with a groundwater model for simulating regional groundwater flow in an alluvial fan. Trans. of JSIDRE 215: 21-29.

Eaneesh KY, Thampi SG. 2013. A simple semi-distributed hydrologic model to estimate groundwater recharge in a humid tropical basin. Water Resour Manage 27: 1517–1532.

Fucklin DL, Luedeling E, Zhang M. 2010. Sensitivity of groundwater recharge under irrigated agriculture to changes in climate , CO_2 concentrations and canopy structure. Agr Water Manage 97: 1039-1050.

Fujihara M., Ohashi G. 2000. A numerical estimation of the effect on groundwater surface elevation by irrigation water in Dogo Plain. Trans. of JSIDRE 208: 155–1630 (in Japanese).

Furman A. 2008. Modeling coupled surface-subsurface flow processed: a review. Vadose Zone J. 7: 741–756.

Gibson JJ, Edwards TWD, Birks SJ, st Amour NA, Buhay WM, MCEacher P, Wolfe BB, Peters DL. 2005. Progress in isotope tracer hydrology in Canada. Hydrol Process 19: 303-327.

Goderniaux P, Brouyere S, Blenkinsop S, Burton A, Fowler HJ, Orban P, Dassargues A (2011) Modeling climate change impacts on groundwater resources using transient stochastic climate. Water Resour Res 47: W12516.

Harbaugh AW, McDonald MG. 1996. User's documentation for MODFLOW-96, an update to the USGS modular finite-difference ground-water flow model. USGS Open-File Report 96-485, p.56.

He B, Takese K, Wang Y. 2008. A semi-distributed groundwater recharge model for estimating water - table and water-balance variables. Hydrogeol J 16: 1215-1228.

Holman IP. 2006. Climate change impacts on groundwater recharge – uncertainty, shortcomings, and the way forward?. Hydrogeol J 14: 637-647.

Horino H, Watanabe T, Maruyama T. 1989. Studies on the Role of Groundwater in Water Used for Irrigation. Trans. of JSIDRE 144: 9-16 (in Japanese).

Hosono T, Nakano T, Igeta A, Tayasu I, Yanaka T, Yachi S. 2007. Impacts of fertilizer on a small watershed of Lake Biwa: Use of sulfur and strontium isotopes in environmental diagnosis. Sci Total Environ 384: 342-354.

Hollanders P, Schulz B, Shaoli W, Lingen AC. 2005. Drainage and salinity assessment in the huinong canal irrigation district, Ningxia, China. Irrig and Drain 54: 155-173.

Huang CC, Tsai MH, Lin WT, Ho YF, Tan CH. 2006. Multifunctionality of paddy fields in Taiwan. Paddy Water Environ 4(4): 199–204.

HydroGeoLogic. 1996. MS-VMS Software (Version 1.2) Documentation. HydroGeoLogic, Inc., Herndon.

Imagawa C, Takeuchi J, Kawachi T, Ishida K, Chono S, Buma N. 2011. A hydroenvironmental watershed model improved in canal-aquifer water exchange process. Paddy Water Environ 9(4): 425–439.

Imaizumi M, Ishida S, Tsuchihara T. 2006. Long-term evaluation of the groundwater recharge function of paddy fields accompanying urbanization in the Nobi Plain, Japan. Paddy Water Environ 4: 251-263.

Kaushal KG, Bhabani SD, Mohamman S, Pratap BSB. 2009. Measurement and modeling of soil water regime in a lowland paddy field showing preferential transport. Agr Water Manage 96: 1705–1714.

Kalbus E, Reinstorf E, Schimer M. 2006. Measuring methods for groundwater, surface water and their interactions: a review. Hydrol Earth Syst Sci Discuss 3: 1809-1850.

Ke KY. 2013. Application integrated surface water-groundwater model to mult-aquifers modeling in Choushui River alluvial fan, Taiwan, Hydrol Process. Published online in Wiley Online Library.

Kerchum NJ, Donovan JJ, Avery WH .2000. Recharge characteristics of a phreatic aquifer as determined by storage accumulation, Hydrogeol J 8(6): 579-593.

Khan S, Rana T, Carroll J, Gabriel H. 2010. Assessment of rice hydraulic loading impacts on groundwater and salinity levels. Paddy Water Environ 8: 23–29.

Kim TC, Gim US, Kim JK, Kim DS. 2006. The multi-functionality of paddy farming in Korea, Paddy Water Environ 4(4): 169–179.

Kiriyama T, Ichikawa T. 2004. Reservation of groundwater basin recharch by paddy field. Annu J Hydraul Eng JSCE 48: 373-378 (in Japanese with English abstract).

Kiriyama T, Ichikawa T, Hoshida Y. 2000. Conjecture of groundwater level using tank model in Kumamoto area. Annu J Hydraul Eng JSCE 44: 223-228 (in Japanese and English abstract).

Komiya H, Malaya S, Masuda H, Kusakabe M. 2003. Groundawter flow system in the central and south part of Matumoto basin, Nagano, estimated from Oxygen and Hydrogen stable isotope ratios and water quality. Journal of Groundwater Hydrology 45(2): 145-168 (in Japanese with

English abstract).

Kukal SS, Aggarwal GC. 2002. Percolation losses of water in relation to puddling intensity and depth in a sandy loam rice (Oryza sativa) field. Agr Water Manage 57: 49-59.

Leterme B, Gedeon M, Jacques D. 2013. Groundwater recharge modeling in the Nete catchment (Belgium) with HYDRUS-1D – MODFLOW package, In: Šimůnek, J., M. Th. van Genuchten, and R. Kodešová (eds.), Proc. of the 4th International Conference "HYDRUS Software Applications to Subsurface Flow and Contaminant Transport Problems", Invited paper, March 21-22, 2013, Dept. of Soil Science and Geology, Czech University of Life Sciences, Prague, Czech Republic, ISBN: 978-80-213-2380-3, pp. 235-244.

Liu CW, Chen SK, Jou SW, Kuo SF. 2001. Estimation of the infiltration rate of a paddy field in Yun-Lin, Taiwan. Agri Sys 68: 41-54.

Lin L, Zhang ZB, Janssen M, Lennartz B. 2013. Infiltration properties of paddy fields under intermittent irrigation. Paddy Water Environ (published online).

Matsuno Y, Nakamura K, Masumoto T, Matsui H, Kato T, Sato Y. 2006. Prospects for multifunctionality of paddy rice cultivation in Japan and other countries in monsoon Asia. Paddy Water Environ 4: 189-197.

Maxwell RM, Kollet SJ. 2008. Quantifying the effects of three-dimensional subsurface heterogeneity on Hortonian runoff processes using a coupled numerical, stochastic approach. Adv Water Resour 31(5): 807–17.

Mitsuno T, Kobayashi S, Maruyama T. 1982. Groundwater recharge function of paddy field: a case of groundwater balance analysis in Nobi Plain. Jour. JSIDRE 50(1): 11-18 (in Japanese).

Munévar A, Mariño MA. 1999. Modeling analysis of ground water recharge potential on alluvial fans using limited data. GROUND WATER 34(5): 649-659.

Nakano T, Tayasu I, Yamada Y, Hsono T, Igeta A, Hyodo F, Andoo A, Saitoh Y, Tanaka T, Wada E, Yachi S. 2008. Effect of agriculture on water quality of Lake Biwa tributaries, Japan. Science of the total environment 389: 132-148.

Niswonger RG, Prudic DE, Regan RS. 2006. Documentation of the Unsaturated-Zone Flow (UZF1) Package for modeling unsaturated flow between the land surface and the water table with MODFLOW-2005: U.S. Geological Survey Techniques and Methods 6-A19, 62 p.

Nettasana T, Craing J, Tolson B. 2012. Conceptual and numerical models for sustainable groundwater management in the Thaphra area, Chi River Basin, Thailand. Hydrogeol J 20: 1355-1374.

Panday S, Huyakorn PS. 2004. A fully coupled physically-based spatially-distributed model for evaluating surface/subsurface flow. Adv Water Resour 27(4): 361–82.

Petelet-Giraud E, Négrel Ph, Gourcy L, Schmidt C, Schirmer M. 2007. Geochemical and isotopic constraints on groundwater-surface water interactions in a highly anthropized site.

The Wolfen/Bitterfeld megasite (Mulde subcachment, Germany). Environ Pollut 148: 707-717.

Pisinaras V, Petalas C, Tsihrintzis VA, KAratzas GP. 2012. Integrated modeling as a decision-aiding tool for groundwater managements in a Mediterranean agricultural watershed, Hydrol Process. Pubished online in Wiley Online Library.

Portmann FT, Döll P, Eisner S, Flörke M. 2013 Impact of climate change on renewable groundwater resources: assessing the benefits of avoided greenhouse gas emissions using selected CMIP5 climate projections. Environ Res Lett 8: 1-14.

Richards LA. 1993. Capillary conduction of liquids through porous mediums. Physics, NY.

Raneesh KY, Thampi SG. 2013. A simple semi-distributed hydrologic model to estimate groundwater recharge in a humid tropical basin. Water Resour Manage 27: 1517-1532.

Refsgaard JC, Storm B. 1995. MIKE SHE. In Computer Models of Watershed Hydrology, Singh VP (eds.). Water Resources Publications, pp. 809-846.

Sanz D, Castaño S, Cassiraga E, Sahuquillo A, Gómez-Alday JJ, Peña S, Calera A. 2011. Modeling aquifer-river interactions under the influence of groundwater abstraction in the Mancha Oriental System. Hydrogeol J19: 475-487.

Scibek J, Allen DM, (2006) Modeled impacts of predicted climate change on recharge and groundwater levels. Water Resour Res . 42: W11405.

Seo HS, Šimunek J, Poeter EP, 2007. Documentation of the HYDRUS package for MODFLOW-2000, the U.S. Geological Survey modular ground-water model. GWMI 2007-01. Int. Ground Water Modeling Ctr., Colorado School of Mines, Golden. p. 98.

Seto R. 1986. Land use by landform classification in Japan –Analysis with the data of grid square basis-. Journal of the Japan cartographers association 24(4): 1-11 (in Japanese).

Šimůnek J, van Genuchten MT, Šejna M. 2006. The HYDRUS-1D Software Package for Simulating the One-Dimensional Movement of Water, Heat, and Multiple Series 1, Department of Environmental Sciences, University of California Riverside, Riverside. p. 270.

Šimůnek J, Bradford SA. 2008. Vazose zone modeling: Introduction and importance. Vadose Zone Journal. 7(2): 581-586.

Sophocleous M. 2002. Interactions between groundwater and surface water: the state of the science. Hydrogeol J 10: 52-67.

Štuopis A, Juodkazis V, Mokrik R. 2012. The quandary aquifer system flow model by chemical and tritium isotope data: case of south-east Lithuania. Baltica 25(2): 91-98.

Sugawara M, Ozaki E, Watanabe I, Katsuyama Y. 1974. Tank model and its application to Bird creek, Wollombi Brook, Bikin River, Sanaga River and Nam Mune, Research notes of National. Research center for disaster prevention, Tokyo.

Simith RE, Hebbert RHB. 1983. Mathematical simulation of interdependent surface and

subsurface hydrologic processes. Water Resour Res 19(4): 987-1001

Tanaka K, Funakoshi Y, Hokamura T, Yamada F. 2010. The role of paddy rice in recharging urban groundwater in the Shira River Basin. Paddy Water Environ 8: 217-226.

Therrien R, McLaren RG, Sudicky EA, Panday SM. 2006. Hydrogeosphere. Waterloo, Canada: Groundwater Simulations Group. University of Waterloo, Waterloo.

Toews MW, Allen DM. 2009. Simulated response of groundwater to predicted recharge in a semi-arid region using a scenario of modelled climate change. Environ Res Lett 4: 035003.

Thoms RB, Johnson RL Healy RW. 2006. User's guide to the variably saturated flow (VSF) process for MODFLOW . Techniques and Methods 6-A18.

Tournebize J, Watanabe H, Takagi K, Nishimura T. 2006. The development of a coupled model (PCPF-SWMS) to simulate water flow and pollutant transport in Japanese paddy fields. Paddy Water Environ 4: 39-51.

Tsuchihara T, Yoshimoto S, Ishida S, Minakawa H, Masumoto T, Imaizumi M. 2010. Environmental Isotope-based Investigation of Hydrological Aspects of Groundwater Recharge and Discharge in Tedori Alluvial Fan. Applied Hydrology 22: 11-20 (in Japanese).

Twarakavi NKC, Šimunek J, Seo S. 2008. Evaluating Interactions between Groundwater and Vodose Zone Using the HYDRUS-Based Flow package for MODFLOW. Vadose Zone J 7: 757-768.

Uliana MM, Banner JL, Sharp Jr. JM. 2007. Regional groundwater flow paths in Trans-Pecos, Texas inferred from oxygen, hydrogen, and strontium isotopes. J Hydrol 337: 334-346.

VanderKwaak JE, Loague K. 2001. Hydrologic-response simulations for the R-5 catchment with a comprehensive physics-based model. Water Resour Res 37(4): 999–1013

van Walsum PEV, Groenendijk P. 2008. Quasi steady-state simulation of the unsaturated zone in groundwater modeling of lowland regions. Vadose Zone J 7(2): 769-781.

Watanabe S, Yoneda M, Morisawa S, Yokoyama T. 2002. Simulation of groundwater level fluctuation and recharge estimation in Kagamihara groundwater basin, Gifu prefecture. Journal of Groundwater Hydrology 44(3): 199-211 (in Japanese).

Watanabe T, Kume T. 2009. A general adaptation strategy for climate change impacts on paddy cultivation: special reference to the Japanese context. Paddy Water Environ 7: 313-320.

Wakui H,Yamanaka T. 2006. Surfaces of groundwater recharge and their local differences in thecontral part of Nasu fan as revealed by stable isotopes. Journal of Groundwater Hydrology 48(2): 263-277 (in Japanese with English abstract).

Xie X J, Wang Y X, Ellis A, Su C, Li J, Li M, Duan M. 2013. Delineation of groundwater flow paths using hydro chemical and strontium isotope composition: a case study in high arsenic aquifer systems of the Datong basin, northern China. J Hydrol 476(7): 87-96.

Xu X, Huang G, Zhan H, Qu Z, Huang Q. 2012. Integration of SWAP and MODFLOW-2000 for

modeling groundwater dynamics in shallow water table areas. J Hydrol 412: 170–181.
Zhou Y, Li W. 2011. A review of regional groundwater flow modeling. Geoscience frontiers 2(2): 205-214.
Zhu C. 2000. Estimate of recharge from radiocarbon dating of groundwater and numerical flow and transport modeling. Water Resour Res 36(9): 2607–2620.
Zhu Y, Shi L, Lin K, Yang J, Ye M. 2012. A fully coupled numerical modeling for regional unsaturated-saturated water flow. J Hydrol 475: 188-203.
Zume JT, Tarhule A. 2008 Simulating the impacts of groundwater pumping on stream–aquifer dynamics in semiarid northwestern Oklahoma, USA. Hydrogeol J 16: 797–810.

CHAPTER 3

Hydrological observation

3.1 Introduction

In the study area, some researchers have examined the interactions between groundwater and river water; studies have focused on both river water infiltration to groundwater, and groundwater flow to the river through hydrological observations (Futamata et al., 2005; Morita et al., 2008; Tsujimoto et al., 2005). Ishikawa Prefecture and Kokusai Kogyo Co., LTD. (1995) examined the distribution of groundwater levels. Nevertheless, no feasible research has been carried out for developing a numerical groundwater flow simulation for identifying long-term changes in groundwater environments in recent years in this study area.

In this chapter, firstly summary of data for estimating hydrological processes in the study area is given. Secondly, the properties of seasonal and annual groundwater fluctuations were examined based on the continual groundwater observation. The groundwater flows and distribution of the groundwater levels were delineated by groundwater-level contours, which were obtained by the simultaneous groundwater observations. Finally, the interaction between groundwater and river water was examined using the discharge observations of the Tedori River.

These measurement data were used to develop and calibrate the groundwater model introduced in the Chapter 5. The hydrochemical observations were mentioned in Chapter 8.

3.2 Study area

3.2.1 Location and Topography

The study site is the Tedori River Alluvial Fan in Ishikawa Prefecture, Japan (Figure 3-1, 3-2). The center of the fan is located at North 36° 31′, East 136° 34′ (WGS 84). The alluvial fan was formed by the Tedori River and has the typical topographical shape of alluvial fans. The Tedori River, which has a total length of 72 km, originates in Mt. Hakusan (elevation 2,702 m asl). The Tedori River basin area extends over 807 km^2. The Sai River, which has a total length of 35 km, originates in Mt. Naradake (elevation 1,644 m asl) and its basin area is 256 km^2.

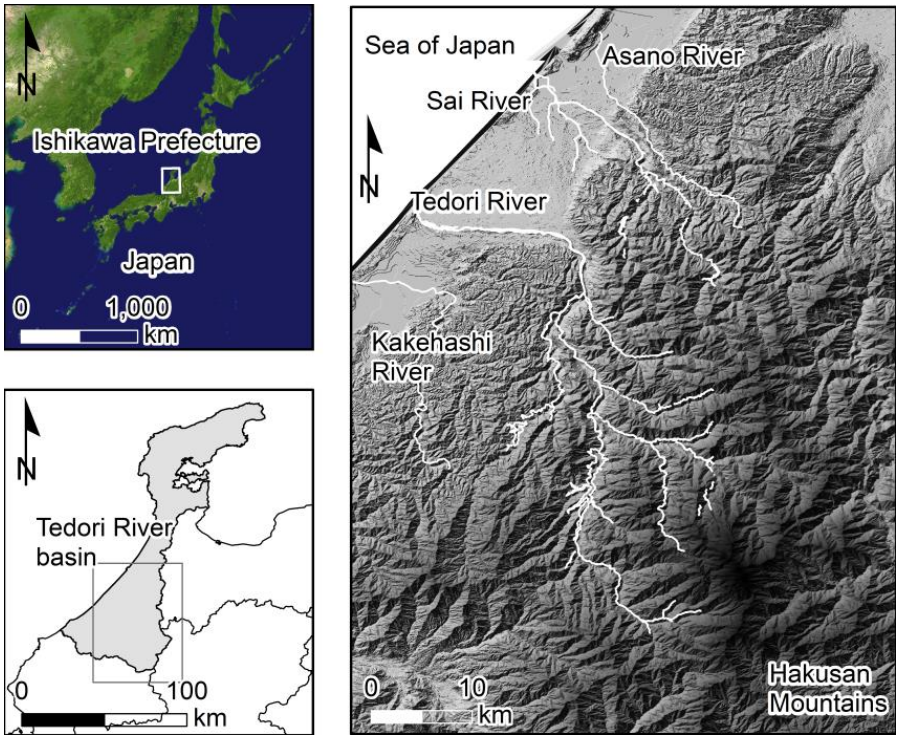

Figure 3-1 Map of the Tedori River basin.

Note: The white lines represent rivers.

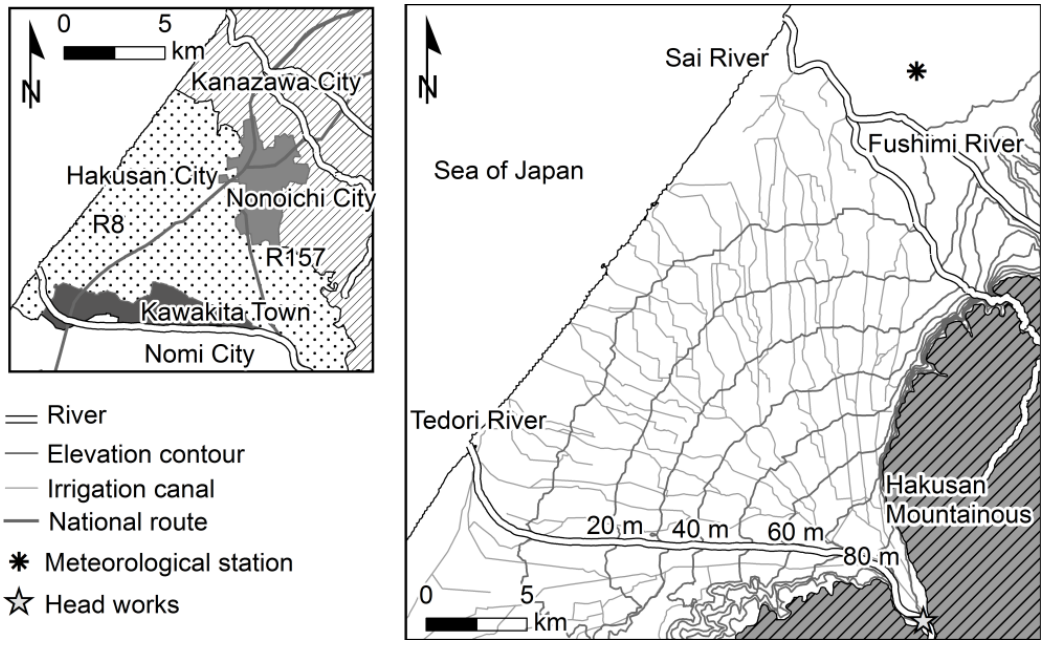

Figure 3-2 Map of the Tedori River alluvial fan.

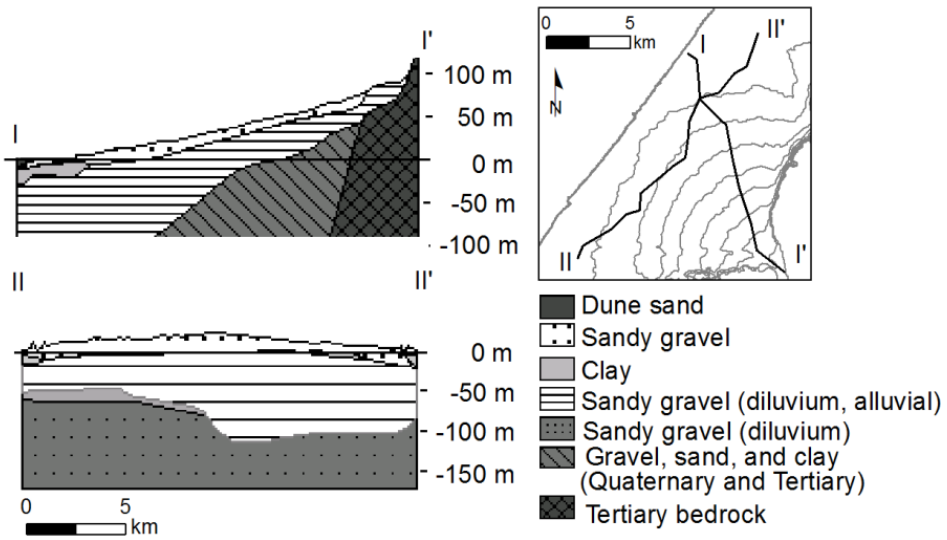

Figure 3-3 Hydrogeological conditions across the study area (Modified From Hokuriku Regional Agricultural Administration Office 1977).

The right side of the fan is wider than the left because the northeast area overlaps with the Sai River and the Asano River Alluvial Fan (Hokuriku Regional Agricultural Administration Office, 1977). The study area is the right side of the fan, bounded by the Tedori River to the south, the Sai River and the Fushimi River (a branch of the Sai River) to the northeast, the Sea of Japan to the west, and the Hakusan mountains to east. The northeast boundary is hereafter referred to as the Sai River. The study area is about 16 km from north to south and 12 km from west to east, covering a total of about 140 km^2. The top of the fan is about 80 m above sea level (asl) and the average slope is 1/140 (the fan is relatively steep).

3.2.2 Hydrogeology

Figure 3-3 illustrates the hydrogeological conditions across the study area. The main geological deposit is sandy gravel with a depth of over 130 m in the middle of the fan. In the middle and upper parts of the fan, the aquifer is confined by alluvium composed of alternate layers of sandy gravel (diluvium and alluvium) and sandy gravel and clay (Quaternary and Tertiary) (Hokuriku Regional Agricultural Administration Office, 1977). Underlying the alluvium is Tertiary bedrock. Along the coastline of the Sea of Japan, a clay layer is wedged into the gravel layer. In this study, the sandy gravel layer and the sandy gravel and clay layer are regarded as aquifer materials. According to seamless digital geological map of Japan (Geological Survey of Japan, 2012), the surface geology at the middle part of the Tedori River basin is composed of rhyolite rocks (Neogene) and that of the upper part is composed of some older rocks: sandstone (Cretaceous) and mafic gneiss (middle to late Paleozoic).

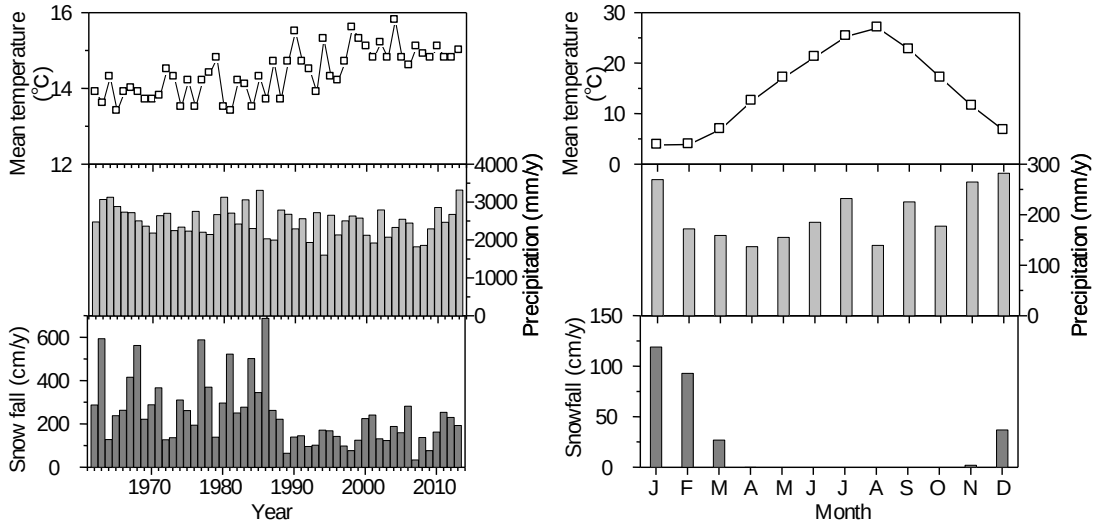

(a) (b)

Figure 3-4 Annual and monthly (average climate during 1981-2010) changes in precipitation, mean temperature, and snowfall: (a) annual changes, and (b) monthly changes.

3.2.3 Meteorology

The study area is located in a humid region with a monsoon-dominated climate, where precipitation exceeds evapotranspiration, and the surplus water becomes groundwater recharge and river water discharge (Shimada, 2012).

The meteorological data were collected at the Kanazawa Local Meteorological Observation Station, which locates 2 km east of the study area. Figure 3-4 shows annual and monthly changes in mean temperature, precipitation, and snowfall. According to annual average climate data for 30 years (1981–2010), the annual precipitation and annual snow depth are 2,399 mm and 281 cm, respectively, and the average annual temperature is 14.6 °C. Monthly precipitation from November to January is relatively high partly due to the snowfall that occurs during this period (Figure 3-4 (b)). Snowfall is likely to be decreased by the slight temperature rise expected for the region as a result of climate change (Japan Meteorological Agency, 2008). The snowfall depth has decreased to an average of 141 cm since the late 1980s (Figure 3-4 (a)).

3.2.4 Land use

Figure 3-5 illustrates changes of land use conditions using 100 m mesh data. Paddy fields are the dominant land use in the study area. Land use data (100 m grid) are available from the National

Land Numerical Information download service (the Ministry of Land, Infrastructure, Transport and Tourism, 2011). The paddy field areas were 70%, 62%, 61%, 58%, 52% and 45% of the total area in 1976, 1987, 1991, 1997, 2006 and 2009, respectively. The land use of the area in 2009 consisted of paddy, upland, urban (building), river, and other land covering 45%, 2%, 39%, 4%, and 10% of the total, respectively. There are also many business entities in the study area of the fan (e.g., food factories, breweries, and precision machine factories), which require a high volume of clean groundwater. The upland field is about 2%, and this has changed very little over time. Upland fields are primarily distributed only in the coastal zone near the Sai River. The area of urban area has increased considerably around the central part of Kanazawa, the prefectural capital, which is located on the northeast portion of the fan, and along Route 8. The increases in urban area have been almost equal to decreases in paddy field area. The population is about 80 million. The crop rotated paddy fields in the study area increased from 4.9% of the total paddy fields in 1976 to 25% in 2009. Since 1998, the ratios have fluctuated between 25% and 33%.

3.2.5 Irrigation practice

The rice irrigation period, when irrigation water is allocated from the Tedori River, is from mid-April to early September in the study area. Rice is planted at the beginning of May and a mid-summer drainage is conducted during June to temporarily dry the paddy soils, after which intermittent irrigation is conducted. In paddy fields, growers typically adopt the rice-upland crop rotation system, in which soybean is grown in the summer (from June to October) and barley in the winter (from November to May).

3.2.6 Groundwater use

Figure 3-6 shows the spatial distribution of annual groundwater use (using a 1km grid) in 1987, 1993, and 2008. The amount of pumping discharge is large in the downstream section of the Tedori River and in central parts of Kanazawa. Annual groundwater use in the Tedori River fan was 1.01×10^8 m^3 in 2009 (Ishikawa Prefecture, 2010), of which industrial water, city water, snowmelt water, irrigation water, and building maintenance water accounted for 59%, 30%, 4%, 4%, and 3%, respectively (Figure 3-7). Groundwater for snowmelt is groundwater applied to the road in order to melt freshly fallen snow on the road by ejecting groundwater (sometimes artificially heated) through pipelines laid under the road using heat energy of groundwater of groundwater use to the total drinking water supply was 35% in the fan (Ishikawa Prefecture, 2012). In addition, about 32% of quantity of the drinking water is supplied by deep wells from the confined aquifer. Figure 3-7 shows the changes in annual groundwater use. Annual

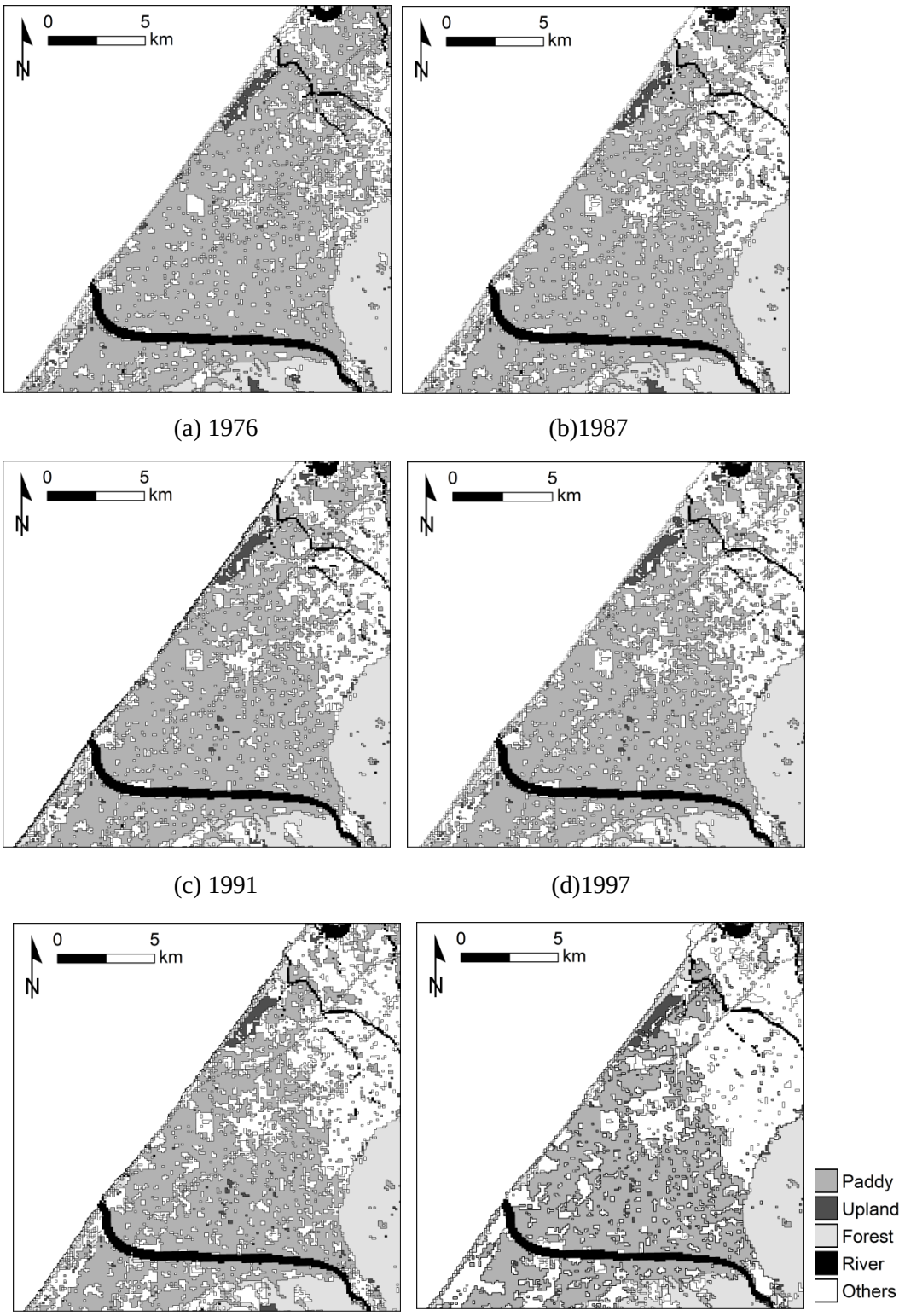

(a) 1976 (b)1987

(c) 1991 (d)1997

(e) 2006 (f) 2009

Figure 3-5 Changes in land uses (100 m grid): (a) in 1976, (b) in 1987, (c) in 1991, (d) in 1997, (e) in 2006, and (f) in 2009.

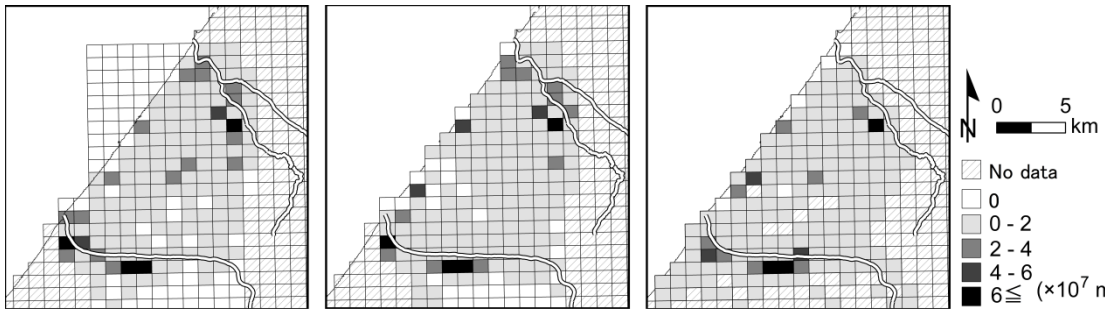

(a) 1987 (b) 1993 (c) 2008

Figure 3-6 Changes in annual groundwater use (1 km grid): (a) in 1987, (b) in 1993, and (c) in 2008.

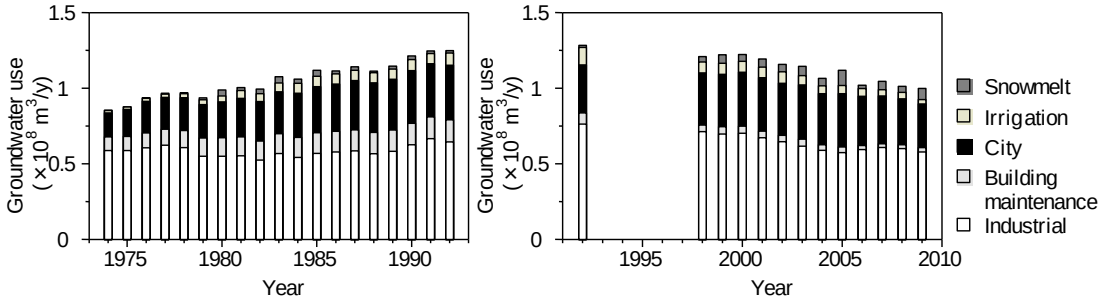

(a) (b)

Figure 3-7 Changes in annual groundwater use for each purpose: (a) in nine cities and towns, and (b) in six cities and towns in the study area.

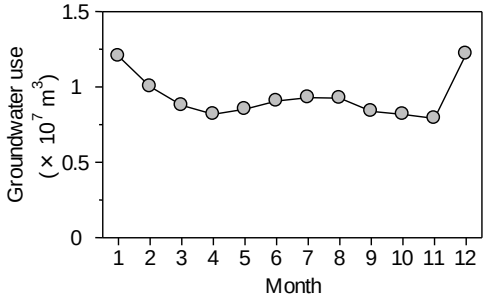

Figure 3-8 Changes in monthly groundwater use in the study area in 2005.

groundwater use increased until 1992 because of increasing drinking water requirements but showed little change from 1992 to 2005 by the regulation of groundwater overdraft (Ishikawa Prefecture, 2010). Figure 3-8 shows monthly changes in 2005. The monthly groundwater use was highest in December due to melting snow purpose, while the lowest was in November.

3.3 Continual groundwater level observation

Groundwater levels are monitored at 11 sites (wells A-K in Figure 3-9) in the fan. Two wells with different strainer depths exist at 2 points (E and J in Figure 3-9), so there are 13 monitoring wells in total, details of which are summarized in Table 3-1. Seven of these wells (C-I wells in Figure 3-9) are located within the right side of the fan (model domain). The groundwater levels have been monitored with automatic pressure type or float type water-level gauges by the prefectural government since 1974 with some exceptions to 2006 for A-C wells and to 2009 for the others with 3-hour interval groundwater levels averaged every 24 hours.

Figure 3-10 shows fluctuations in the decade-average groundwater levels at E well. The seasonal pattern of fluctuation observed in the wells (other than H and J (Deep) wells) showed first that a substantial increase of the groundwater level from the end of April to early May (the beginning of the irrigation period). This is due to the paddy fields being plowed and irrigated before the rice seedlings are transplanted. Second, during July to September (the irrigation period), groundwater levels remain high and stable. Third, during September to October (the beginning of the non-irrigation period), groundwater levels decrease dramatically. Finally, during November to April (the non-irrigation period), groundwater levels fluctuate influenced by rainfall, snowfall, and snowmelt. At H and J (Deep) wells, clear changes in groundwater level were not apparent because groundwater use by pumping was relatively large in the areas near these observation wells. The increments of groundwater levels at the beginning of the irrigation period are considered to be typical pattern of groundwater level changes in the paddy irrigation area (Horino et al., 1989; Imaizumi et al., 2006).

Figure 3-11 shows the annual changes in groundwater level. Most of wells, the lowest decade-averaged groundwater level was observed in the 1990s, while the groundwater levels increased slightly during the 2000s, probably because of a reduction in annual groundwater use. Aoyama (2013) reported that the maximum foundation subsidence during 1974-2007 was 0.45 m Around the Kanazawa City and the subsidence had been caused by the decline of the groundwater levels.

3.4 Simultaneous groundwater-level observation

The groundwater-level contours were obtained from mapping and kriging of groundwater levels, which were observed temporally at 113 wells in December of 1993 (Ishikawa Prefecture and Kokusai Kogyo Co., LTD., 1995), 87 wells in November of 2009, and 86 wells in June of 2010, which are used ordinarily Figure 3-12 shows the groundwater-level contours.

Comparisons of the groundwater levels during the irrigation period in 2010 and the

Table 3-1 Characteristics of the observation wells.

Well	Elevation (m)	Depth of well (m)	Depth of strainer (m)
A	7.40	150	137-145
B	1.91	150	58-80, 113-131, 137-145
C	9.67	150	123-128, 134-150
D	3.85	200	134-151
E	8.93	82/200*	23-32, 43-55/160-172, 183-189*
F	24.08	30	21-27
G	23.20	150	123-139
H	5.78	200	120-139
I	42.73	100	72-88
J	7.99	70/150*	24-42/78-93*
K	23.84	60	11-22, 38-49

*(asterisk) Depth of the strainer at E and J refers to shallow well/deep well.

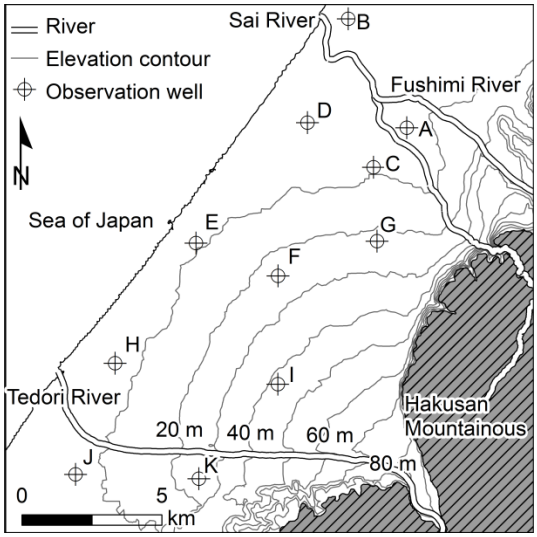

Figure 3-9 Map of of the locations of observation wells.

non-irrigation period in 2009 (Figure 3-12(a)) indicate that distributions of the water level during the irrigation period was 5 m higher than that of the non-irrigation period. Amount of the groundwater use in June, however, was 9% larger than that of in November. These results indicated that the groundwater recharge from the paddy field effected on the groundwater levels for the entire area.

Additionally, the groundwater level during the non-irrigation period declined 5 m over

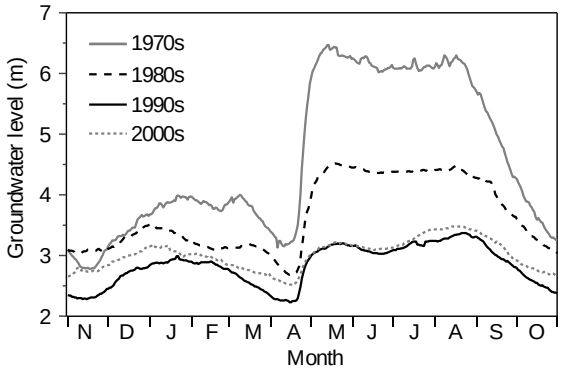

Figure 3-10 Fluctuation in the decade-average groundwater level at E well.

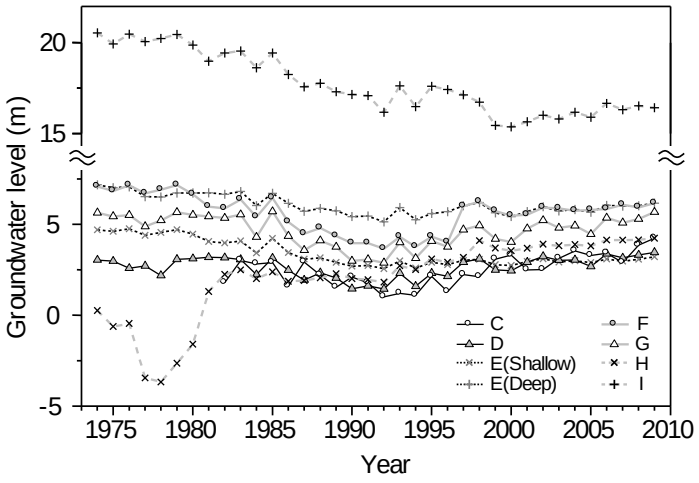

Figure 3-11 Annual changes in groundwater level.

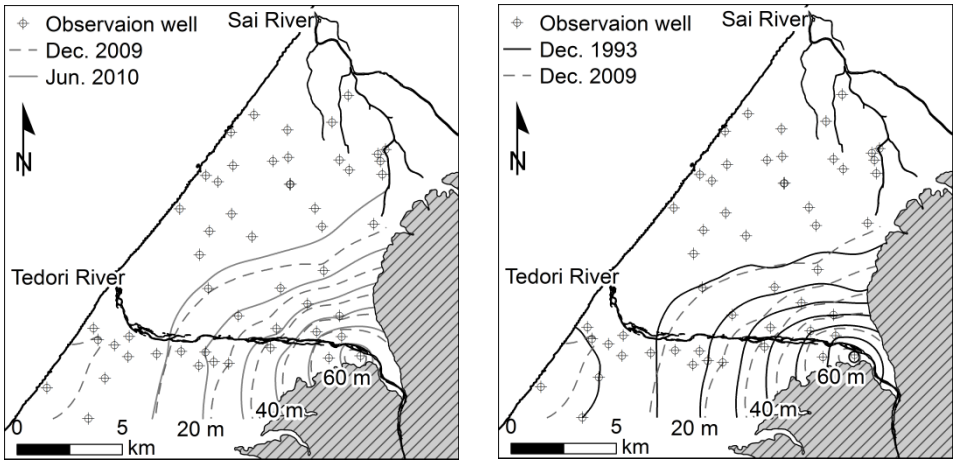

(a) (b)

Figure 3-12 Comparisons of measured groundwater levels during (a) the recent irrigation period and non-irrigation period, and (b) non-irrigation periods of 1993 and 2009.

17 years (from 1993 to 2009) in the middle part of the fan (Figure 3-12(b)). The groundwater-level contour maps showed that the groundwater flows from the upper zone of the fan to the northwest side, and flow lines perpendicular to contours point in the downstream direction, indicating that they are controlled by the topographic gradient of the land surface (1/140) and seepage water from the Tedori River. Lateral flow from the mountain front is not observed in the study area. The depth of groundwater-table varied from 2 m to 45 m spatially during the non-irrigation period in 1993, and was deeper in the upper region of the fan than the lower region.

3.5 Discharge observations of the Tedori River

To determine groundwater–river water exchange volumes, river flow amounts at eight points along the Tedori River and inflow amounts entering the river (10 points) were measured, and the amount of water flowing from the river to groundwater or from groundwater to the river in each observation interval was calculated considering a water balance between the neighboring observation points. The measurements were conducted in the irrigation (2009 June) and non-irrigation (2009 December) periods. The measurement range was from 1.1 km to 16.4 km from the river mouth. Figure 3-13 shows the net exchange water volume between groundwater and the Tedori River per km along the river during the irrigation and non-irrigation period in 2009. At the irrigation period, groundwater flowed to the river (gaining river) in the downstream section located between 1.1 km and 2.2 km from the river mouth, and in the section located between 11.8 km and 14.3 km from the river mouth. Seepage water recharged to the groundwater (losing river) in the sections located between 2.2 km and 11.8 km and between 14.3 km to 16.4 km from the river mouth. At the non-irrigation period, the groundwater flows to the river was observed only in the downstream section from at 1.1 km to 2.2 km from the river mouth and seepage water was observed in the section 2.2 km to 16.4 km from the river mouth. Futamata et al. (2005) reported that the Tedori River was gaining river in the downstream and upper stream sections of the river and was losing river in the mid-stream section of the river. Their observation result mostly agreed with obtained results. Total inflows from the river to groundwater for duration of the irrigation period and the non-irrigation period were 4.1×10^6 m^3/d and 5.1×10^6 m^3/d, respectively. Total outflows from groundwater to the river for duration of the irrigation period and the non-irrigation period were 1.1×10^6 m^3/d and 7.5×10^5 m^3/d, respectively.

Figure 3-14 shows the deepest river bed level and groundwater levels along the Tedori River, which were interpolated by observed groundwater levels in 1993, 2009, and 2010. In the section located between the river mouth and 2.5 km from the mouth, the groundwater

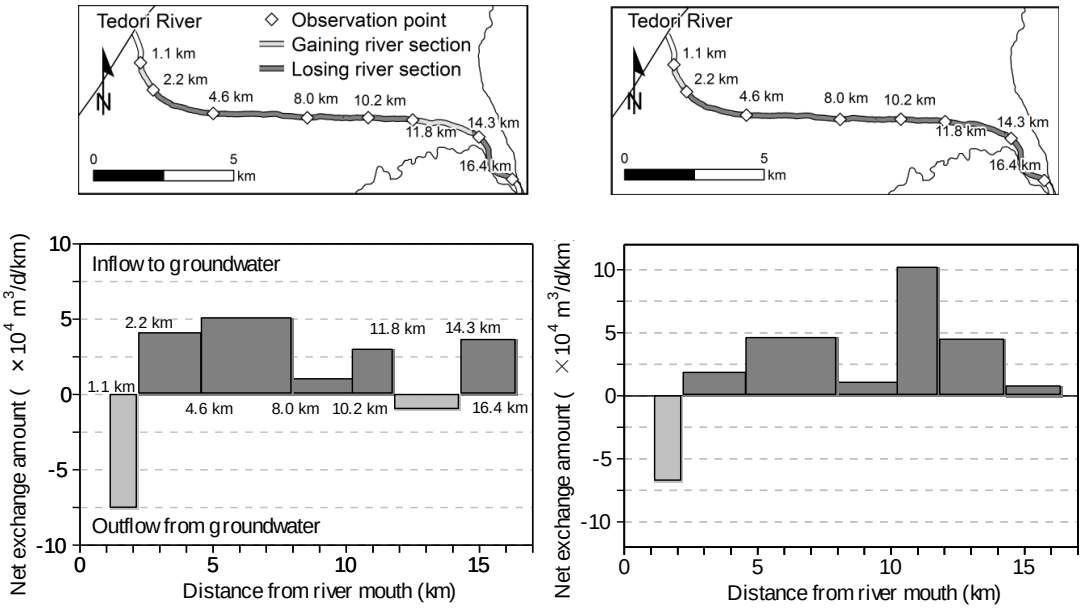

(a) (b)

Figure 3-13 Location map of the water flow observation points along the Tedori River and net exchange water volume per km for each observation section: (a) during the irrigation period in 2010, and (b) during the non-irrigation period in 2009.

Noto: Positive values indicate inflow from the Tedori River to groundwater and negative values indicate outflow from groundwater to the Tedori River.

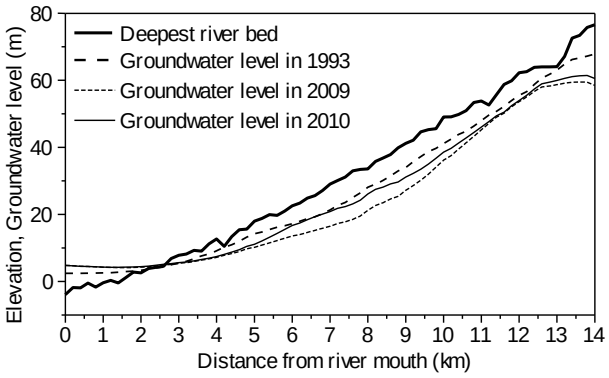

Figure 3-14 Relation between the deepest river bed level and groundwater levels in 1993, 2009, and 2010 along the Tedori River.

levels were higher than the deepest river bed level. At the upper stream section from 2.5 km, the groundwater levels turn to be lower than the deepest river bed level. This figure is consistent with the sections of losing and gaining river estimated by the river discharge observations.

3.6 Conclusions

This chapter shows groundwater environments by some hydrological observations. Noticeable results in the hydrological observations were as follows:

1) Comparisons of groundwater level observations during the irrigation and the non-irrigation periods revealed that distributions of the groundwater levels during the irrigation period are about 5 m higher than during the non-irrigation period, which implies that paddy irrigation water contributes significantly to groundwater level.

2) Comparisons of groundwater level observations during the non-irrigation period in 1993 and 2009, distributions of the groundwater levels in the upper and middle parts of the fan have declined 5 m during 1993–2009.

3) Discharge observations of the Tedori River during the irrigation and non-irrigation periods confirm that much river water infiltrates into shallow groundwater almost along the river. In the downstream section, which is 1.1 km and 2.2 km from the river mouth, along the river, groundwater flowed into the river.

References

Aoyama S. 2013. Groundwater pumping-up and foundation subsidence in the Kanazawa plain, In Normal hydrological cycle as a core of irrigation water - Case study in the Tedori River basin assuming the climate change-, Maruyama T. and Hayase Y. (eds.). Ishikawa Prefectural University Press: Ishikawa, pp. 181-190 (in Japanese).

Futamata K, Takahashi I, Inoue M. 2005. Influence of river stream on groundwater and recharge in the Tedori River alluvial fan areas. Research Report of the Hokuriku Regional Office, Ministry of Construction, pp. 209-212 (in Japanese).

Geological Survey of Japan, AIST (eds.). 2012. Seamless digital geological map of Japan 1: 200,000. Jul 3, 2012 version. Research Information Database DB084.

Hokuriku Regional Agricultural Administration Office. 1977. Hydraulic geology and groundwater in Ishikawa prefecture (in Japanese).

Horino H, Watanabe T, Maruyama T .1989. Studies on the Role of Groundwater in Water Used for Irrigation. Trans. JSIDRE 144: 9-16 (in Japanese with English abstract).

Imaizumi M, Ishida S, Tsuchihara T .2006. Long-term evaluation of the groundwater recharge function of paddy fields accompanying urbanization in the Nobi Plain, Japan. Paddy Water Environ 4: 251-263.

Ishikawa Prefecture. 2010. Environmental white book 2009 in Ishikawa Prefecture, Ishikawa. http://www.pref.ishikawa.lg.jp/kankyo/shiryo/hakusyo/documents/h21hakusyo.pdf.(in

Japanese).

Ishikawa Prefecture. 2012. List of amount of intake water by water service facilities. Statistical survey of water service in 2010. http://www.pref.ishikawa.lg.jp/mizukankyo/shiryo/suidou/h22.html. (in Japanese).

Ishikawa Prefecture, Kokusai Kogyo Co., LTD. 1995. Report on groundwater in Tedori Rive alluvial fan. p.145 (in Japanese).

Japan Meteorological Agency. 2008. Global warming projection 7. http://ds.data.jma.go.jp/tcc/tcc/products/gwp/gwp7/index-e.html. (in Japanese).

Kayane I. 1980. Groundwater use for snow melting on the road. GeoJournal 4.2: 173-181.

Ministry of Land, Infrastructure, Transport and Tourism. 2011. National Land Numerical Information Download Service. http://nlftp.mlit.go.jp/ksj/.

Morita K, Honda T, Nishiura T. 2008. For planning of normal discharge of Tedori River. Technical Report of Hokuriku Regional Office of Construction, Ministry of Construction and Transportation. http://www.hrr.mlit.go.jp/library/happyoukai/h20/pdf/c/cj_15kanazawa.pdf. (in Japanese).

Shimada J. 2012. Sustainable groundwater managements considering potential groundwater recharge in Monsoon Asia. Journal of Japanese Association of Hydrological Sciences 42(2): 33-42 (in Japanese with English abstract)

Tsujimoto T, Futamata H, Qing X, Sumi T. 2005. Relation between instream flow and underground water in fluvial fan discussed in river management of the Tedori River. Journal of River Engineering 11: 529–534 (in Japanese with English abstract).

CHAPTER 4

Relationship between increment of groundwater level at the beginning of irrigation period and paddy field area

4.1 Introduction

The groundwater level is an important parameter for evaluating spatial and temporal changes in groundwater environments, particular groundwater recharge. The groundwater level is governed by various factors such as topography, geological structure, land use, groundwater use, and climate conditions. At the site used in this study, there are some non-negligible factors influencing the groundwater level, including groundwater use for drinking and industrial water, and the interaction between the groundwater and river water including both river water infiltration to groundwater and groundwater flow to the river. In this first stage of a wider study, the direct relationship between groundwater levels and paddy field areas is evaluated. In this chapter, the relationship between differences in the depth of groundwater from just before the irrigation period to just after the soil puddling at paddy fields (hereafter called increments of groundwater levels) and paddy field area ratios to total area around the sampled wells is examined, and used circular buffer zone analysis to investigate how the distance of paddy fields from the sampled wells influences changes in groundwater levels.

4.2 Spatial analysis

4.2.1 Data sets

Daily groundwater levels were available for 13 wells from 1974 to 2006 for the wells A-C and to 2009 with some exception. In the study, we divided the fan into three parts. The area within 5 km of the crest of the fan is described as the upper part, from 5 km to 10 km of the crest is the middle part, and the farthest 10 km is the lower part (Figure 4-1). There are four observation wells in the middle part and nine observation wells in the lower part.

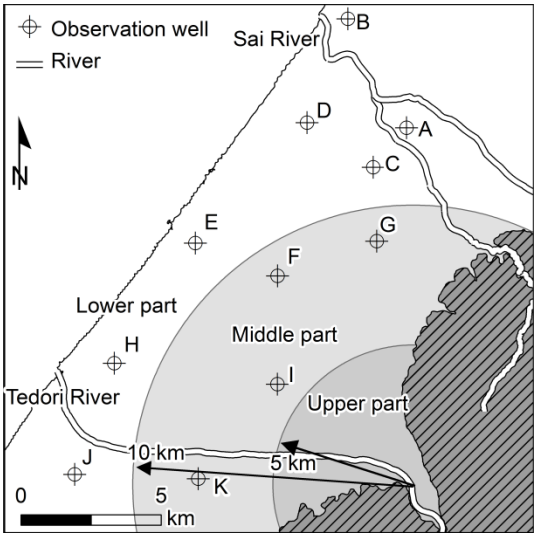

Figure 4-1 Three partitions of the model domain.

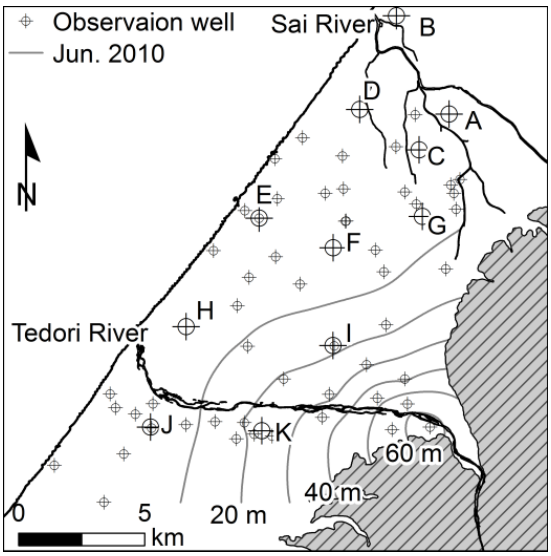

Figure 4-2 Spatial distribution of groundwater level in the irrigation period in 2010.

Figure 4-2 shows the spatial distribution of groundwater levels measured in the irrigation period (June 2010). The groundwater level contours indicate that the groundwater flows from the upper zone of the fan to the northwest side. Depths of the groundwater level were 15－25 m at F, G and I wells which are located in the middle part of the fan, and 0－10 m at the other wells in the lower part. Underlying the area along the coastline is a clay layer 2－44 m below the surface. Considering results from bore explorations (Hokuriku Regional Agricultural Administration Office, 1977) and depths of the strainer in the observation wells (Table 4-1), the shallow wells at E and J wells may be measuring the shallow groundwater level in the unconfined aquifer. The other wells are considered to be measuring the deep groundwater level

of the aquifer.

The land use data are 100 m grid data produced by the National Land Numerical Information download service (the Ministry of Land, Infrastructure, Transport and Tourism, 2011) for 1976, 1987, 1991, 1997, and 2006.

4.2.2 Data Analysis

A substantial increase of the groundwater level from the end of April to early May (the beginning of the irrigation period) was observed in the wells (other than H and J (Deep) wells). The increments of groundwater levels at the beginning of the irrigation period are considered to be typical of the pattern of groundwater level changes in the paddy irrigation area. In this chapter, the relationship between increments of groundwater levels of the observation wells and paddy field area ratios to total area around the sampled wells were examined. Increments were calculated by subtracting the weekly mean groundwater level before irrigation from that after the first irrigation. The low stable-level period is considered to be from April 13 to April 19 and the high stable-level period from May 1 to May 7 every year. At B and J wells, however, the low stable-level appeared later, so weekly mean groundwater levels before irrigation for these wells were derived for the period from April 22 to April 28.

This spatial analysis used the GIS tool. Paddy field area ratios were calculated within circular buffer zones, which were delineated in 0.2 km intervals from 0.2 km to 2.0 km centered on each observation well. As described later in this paper, there were indeed only a few changes in the correlation coefficients between the increments of groundwater level and the paddy field area ratio for the buffer radius lager than one plus decimal km. This supports and rationalizes the maximum buffer radius range (2.0 km) were set. I recognize that the buffer zone may not necessarily be circular. However, I assume that a circular buffer zone with a radius of 2.0 km is sufficient for considering the effect of the infiltrated water from paddy fields on the groundwater level at a well located at the center of the circular zone and that the simplification in using a circular buffer zone will not significantly affect consequent discussions. At near-coastal wells at B, D, E, and H wells, large circular buffer.

4.3 Results and Discussion

4.3.1 Increments of groundwater levels

Figure 4-3 shows changes in the increments of groundwater levels at the beginning of the irrigation period. At F, G, and I wells in the middle part of the fan, the increments were about 3

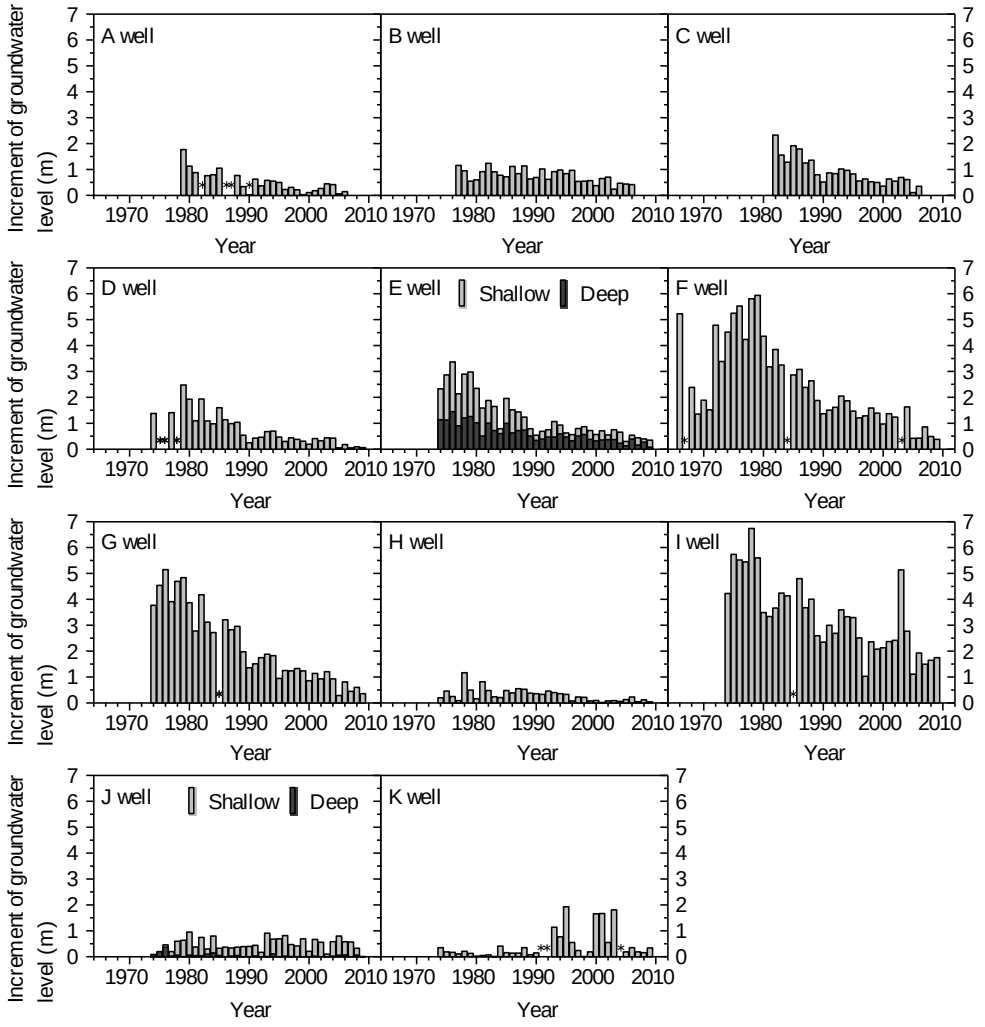

Figure 4-3 Changes in the increments of groundwater levels in the observation wells. *(asterisk) means missing value.

－5 m in around 1980 and declined to about 1－3 m until 2009. Similarly, some observation wells in the urban area (A, B, C and D) show decreases from 1－2m to 0.5 m of the increment of groundwater level. At E (Shallow), E (Deep) and H wells in the lower part of the fan, the increments also decrease J (Shallow). Groundwater levels at the J (Deep) well do not show seasonal pattern of fluctuation and the increment of groundwater levels at the J (Deep) well is very little typically less than 0.1 m. The K well, which is located near the Tedori River in the middle part of the fan, showed little increment during 1980s, but the increment increased around 2000. It is considered to be due to the decrease of groundwater pumping in the area near the K well (Figure 3-6).

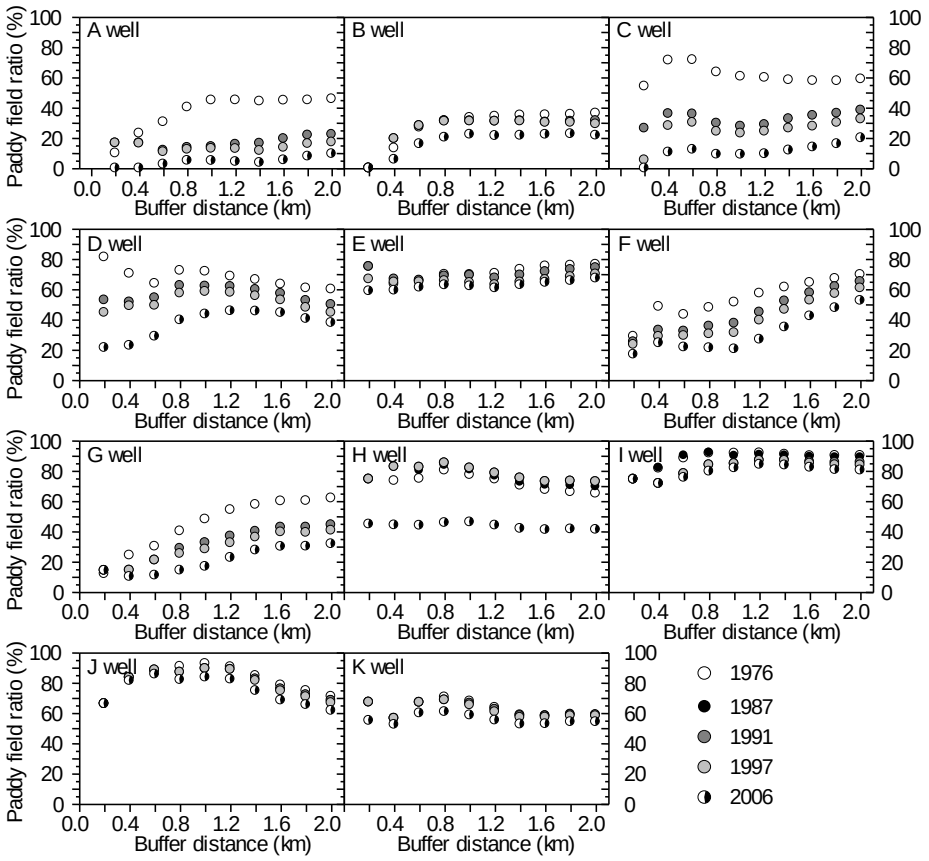

Figure 4-4 Changes in paddy field area ratios in the buffer zone for the observation wells.

4.3.2 Paddy field area ratio

Paddy field area ratios in each buffer zone have decreased over the past thirty years, from 1976 to 2006, as shown in Figure 4-4. In particular, at A, C and D wells located near the urban area and at F, G and H wells are surrounded by many paddy fields, the temporal changes of paddy field area ratio were larger than for other wells. For the C and D wells especially, as the buffer distance is large the amount of temporal change in the paddy field area becomes smaller because the land use change is averaged in the case of large buffer zones.

4.3.3 Relationship between the increments of groundwater level and the paddy field area ratio

Figure 4-5 shows relationships between the increments of the groundwater levels and the paddy field area rate for a buffer distance of 1.6 km. At most wells, a good linear relationship was found for all buffer zones and correlation coefficients mostly exceeded 0.7. However, at

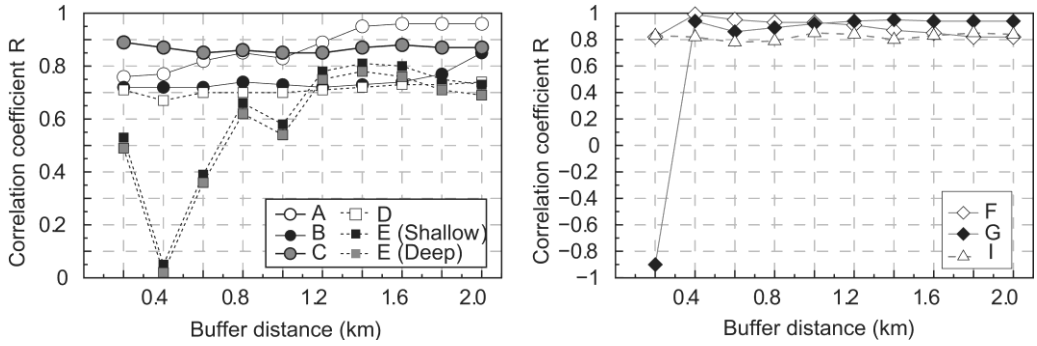

(a) (b)

Figure 4-5 Changes in correlation coefficients for different buffer distances. Only wells with high positive correlations are shown: (a) Changes in lower part, and (b**)** in middle part.

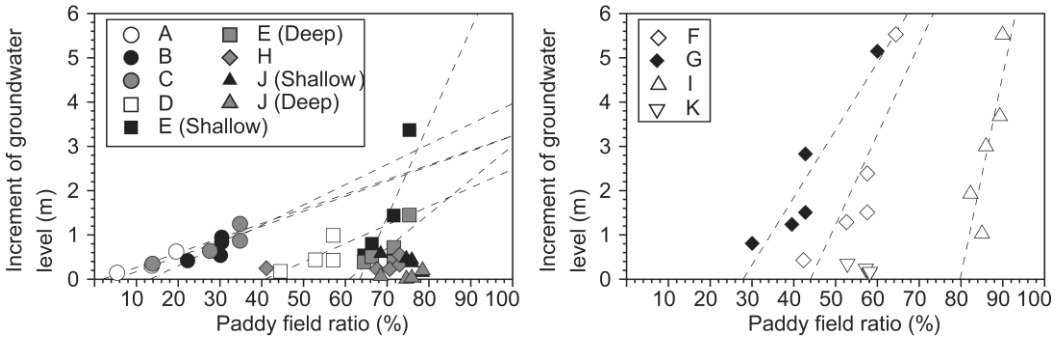

(a) (b)

Figure 4-6 Increments of groundwater levels and paddy field ratios (Buffer distance is 1.6 km). Fitted lines are shown only for wells in which the correlation coefficient exceeds 0.7: (a) Relationships in lower part, and (b) in middle part.

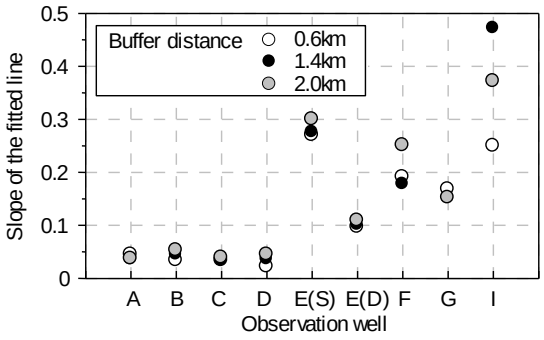

Figure 4-7 Changes in the slope of fitted linear correlations for three buffer distances (0.6, 1.4, and .2.0 km).

Note: E (S) means shallow well and E (D) means deep well.

the H and J (Deep) wells in which groundwater levels did not show the seasonal changes, correlation coefficients were low. In addition, J (Shallow) and K wells showed a negative relationship despite the paddy field area ratios being relatively high (J well around 70% and K well 60%) probably because the three H, J and K wells were influenced by infiltration of river water and the K well was also influenced by heavy groundwater use by pumping ((Figure 3-6).

Correlation coefficients between the increments of groundwater levels and the paddy field area ratio were calculated for the wells which have high positive relationships as shown in Figure 4-5. When the buffer distance increased from 0.2 km to 2.0 km, the coefficients mostly exceeded 0.7. However, when the buffer distance was less than 1.0 km, for instance in both the shallow and deep wells at the E well, correlation coefficients were low. It is considered that the buffer circle with the radius of 0.2 km cannot explain the decreasing of amount of water level rises at the E well. However, as the radius of the buffer circle is taken larger, the correlation between increment of groundwater level and the paddy field area ratio becomes more significant, showing that 1.0 km correlation is higher than 0.2 km. This result indicates that changes in paddy area within more than 1.0 km from the well have led to the groundwater level rising at the beginning of the irrigation period. Furthermore, Figure 4-5 (b) shows that the G well has a negative correlation coefficient at a 0.2 km buffer distance. The same reason as for the E well is suggested as the reason for this. At G well, the paddy fields influencing the groundwater increment are over 0.4 km from the well. The paddy field area ratios did not change significantly when the buffer distance increased, so the range which affects the groundwater level cannot be clarified. Overall then, paddy fields at least 1.0 km from observation wells affected the groundwater level rise at the start of the irrigation but this result can be significantly influenced by the location of the well on the fan.

Therefore, I explored the impact of land use conditions relative to position of the well. Linear relationships exist between the increment of groundwater level and the paddy field area ratio as shown in Figure 4-6. For those wells with high positive correlations, the slope of the fitted line was calculated for three different buffer distances as shown in Figure 4-7. The value of the slope implies the degree of the influence of a unit change in the paddy field area on the increment of the groundwater level. At F, G, and I wells which are located in the middle part of the fan, slopes are greater than for other wells in the cases of the three circular buffer zones. Additionally, the slope at E (Shallow) well was comparatively high. This is considered to be because the groundwater level at this well reflects the shallow groundwater in the unconfined aquifer which is more affected by infiltration water from paddy fields.

The increments of groundwater levels caused by infiltration of the paddy water were more affected by changes in the paddy field area in the middle part of the fan. One reason for this is that the groundwater catchment area may be limited in the middle part of the fan relative

to the lower part.

4.4 Conclusions

The effects of paddy field on groundwater level in the Tedori Alluvial Fan were evaluated by the spatial analysis. This study examined the relationship between the increments of groundwater levels at the sampled wells and paddy field area within buffer circles whose radius ranged from 0.2 km to 2.0 km from each sampled well. Noticeable results in the hydrological observations were as follows:

1) A positive relationship between the increments of groundwater levels at the sampled wells and paddy field area was found at almost all wells and the paddy fields at least 1.0 km from observation wells affected the increments.

2) The effect of changes in paddy field area on groundwater level at a given well is greater in the middle part of the fan than in the lower part. It is confirmed that paddy fields have a profound effect on groundwater levels during the irrigation period.

3) To raise the groundwater level during the irrigation period, conservation of paddy fields is very important, especially in the middle and upper parts of the alluvial fan.

References

Hokuriku Regional Agricultural Administration Office. 1977. Hydraulic geology and groundwater in the Ishikawa prefecture (in Japanese).

Ministry of Land, Infrastructure. 2011. Transport and Tourism, National Land Numerical Information Download Service. http://nlftp.mlit.go.jp/ksj/.

CHAPTER 5

Assessment of factors influencing groundwater level changes during irrigation based on steady state groundwater flow analysis

5.1 Introduction

In this chapter, a steady state model during the irrigation period was developed considering the observed groundwater-level contour maps and the measured interaction water flow between groundwater and the river. Steady numerical analysis during the irrigation period was performed using several scenarios to assess groundwater-level influencing factors such as land use and pumping schemes and to examine effective measures for maintaining groundwater levels.

5.2 Groundwater Flow Model

5.2.1 Governing equations of groundwater flow

A 3-D centered finite difference numerical model was developed based on MODFLOW 2005 (Harbaugh, 2005). The MODFLOW series (Harbaugh and McDonald, 1996; Harbaugh et al., 2000; Harbaugh, 2005) developed by the United States Geological Survey is the most reliable among existing groundwater flow models. Considering mass balance law of water and the Darcy's gradient type relationship, the governing equation for the 3-D groundwater flows for isotropic aquifers is:

$$S_s \frac{\partial h}{\partial t} = \frac{\partial}{\partial x}\left(K_s \frac{\partial h}{\partial x} \right) + \frac{\partial}{\partial y}\left(K_s \frac{\partial h}{\partial y} \right) + \frac{\partial}{\partial z}\left(K_s \frac{\partial h}{\partial z} \right) + q \tag{5-1}$$

where, K_s is the saturated hydraulic conductivity (L/T), h is the potentiometric head (L), S_s is the specific storage of the porous medium (1/L), and q is the flux per unit volume representing

sources and/or sinks of water; $q > 0$ for inflow and $q < 0$ for outflow, and x, y, z are coordinate (L).

5.2.2 Model discretization

The model domain is the right bank of the Tedori River, with the area of 140 km^2. The Tedori River, the Sai River, the Sea of Japan, and Hakusan Mountains are boundaries to south, northeast, west, and east, respectively (Figure 5-1). The sandy gravel layer and the sandy gravel and clay layer were modeled as the shallow and deep aquifer, respectively.

In MODFLOW, an aquifer system is approximated as a discretized domain that consists of an array of nodes and associated finite difference blocks (cells). A schematic sketch of the grids and layers used in this study is shown in Figure 5-2. The model domain was discretized into grid dimensions of 400 m × 400 m. and contained 897 cells for each layer and four layers, giving a total of 3,588 cells. The first to third layers represented the shallow aquifer, and a part of the second layer was the coastal clay zone. The fourth layer represented the deep aquifer. The surface elevation of the upper layer was derived from digital elevation model (DEM) data with a ground resolution of 50 m, while the bottom of the fourth layer was defined horizontally at -200 m from sea level. The second and third layers were determined based on information derived from borehole geological data (Hokuriku Regional Agricultural Administration Office 1977).

5.2.3 Boundary conditions and input data

Steady state calibration was conducted to determine the hydraulic conductivities and hydraulic conductance of riverbed materials through two calibration phases. To estimate hydraulic conductivities, steady state calibration was first carried out under the following conditions. Cells in layer 1 were grouped into three zones (northern, southern and coastal) based on the surface geology to consider the spatial distribution of the hydraulic conductivity over the shallow aquifer. The same zones were also applied to layers 2 and 3. The part of layer 2 corresponding to the coastal clay zone had different hydraulic properties. Layer 4 (deep aquifer) was not divided. The zone settings are shown in Figure 5-3. Consequently, five hydraulic parameter zones were set up. No flow boundary condition was applied to the eastern mountain-front boundary of aquifers and the bottom of the model domain. Constant head boundary conditions were set along the rivers (the Tedori River and the Sai River) using interpolated measured groundwater levels (2010 June) and the Sea of Japan using the mean sea-level surface. The interpolated groundwater levels were not obtained at the downstream

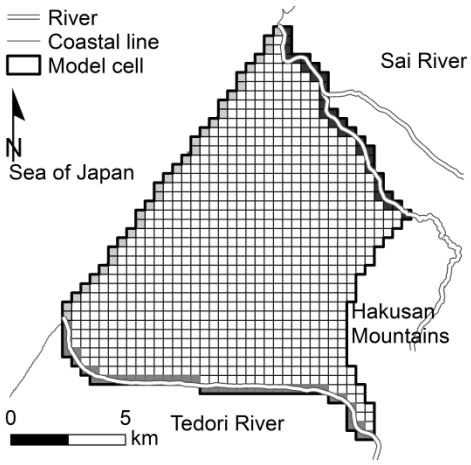

Figure 5-1 Horizontal discretization of the model domain.

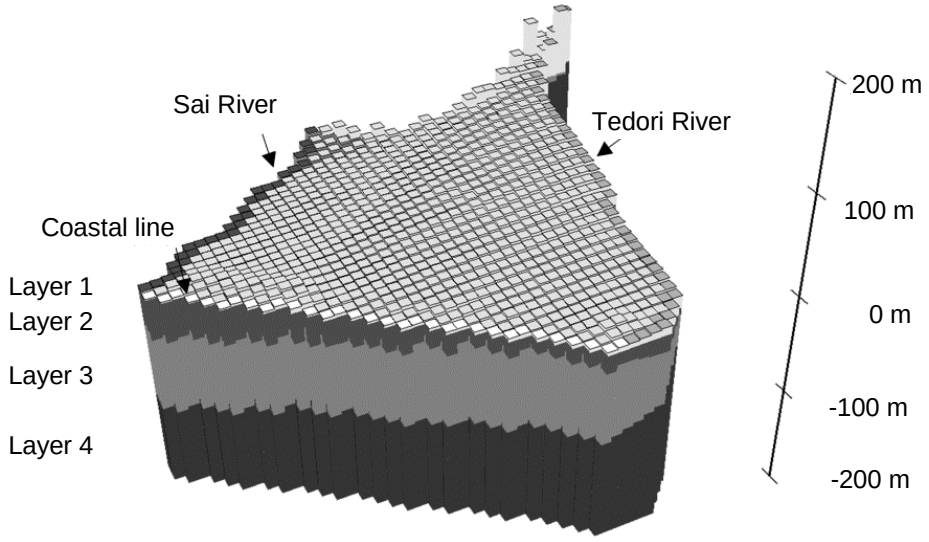

Figure 5-2 Schematic sketch of the grids and layers.

section of the Sai River due to the shortage of observation points. Thus, the constant head boundary was set based on the linear interpolation between the interpolated groundwater level at the nearest cell from the river mouth and the sea-level surface. The sea-level surface at Kanazawa Bay is available in NOWPHAS (Ministry of Land, Infrastructure, Transport and Tourism, 2011). Internal boundary conditions such as rivers and lakes, which significantly influence groundwater, do not exist in the study area. The recharge flux, which is specified as the upper boundary condition for MODFLOW, was given by field measurements of the paddy water percolation rate. Murashima (2013) investigated the 12-hour interval water requirement rate in 36 paddy plots in the fan from 11 May to 10 August 2008 and calculated the daily water requirement with depth. The mean water requirements were 10.9 mm/d before and 24.7 mm/d after the mid-summer drainage, and standard deviations of the water requirements after the drainage were larger than before. The averaged water requirement weighted days during after

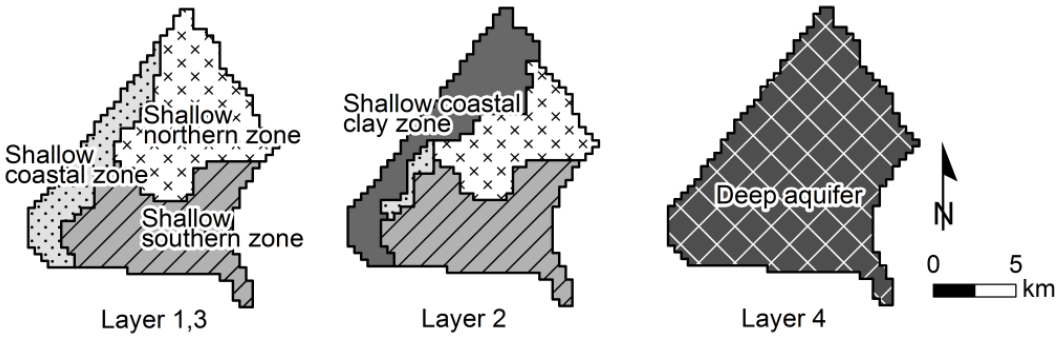

Figure 5-3 Zoning to determine hydraulic conductivities.

Table 5-1 Optimized hydraulic conductivities using MODFLOW.

Zone		Hydraulic conductivity (m/d)
Shallow aquifer	Northern zone	8.6×10^{2}
	Southern zone	4.8×10^{1}
	Coastal zone	7.4×10^{2}
	Coastal clay zone	1.1×10^{-3}
Deep aquifer		1.2×10^{0}

and before the mid-summer drainage was15.6 mm/d. The mean water requirements before and after the mid-summer drainage did not differ significantly at a P-value of 0.05 between the three zones associated with the hydraulic conductivities of the model domain. Water percolation rates before and after the mid-summer drainage, which were calculated by subtracting the evapotranspiration during the irrigation period from the mean water requirement, were 7.4 mm/d and 10.9 mm/d, respectively. The interpolated groundwater levels (2010 June), which is used to the boundary condition, was measured in duration of before the mid-summer drainage. Thus, the water percolation before the mid-summer drainage (7.4 mm/d) is used for estimation of the groundwater recharge. All of the percolated water are considered to be recharged to the aquifer in steady state during the irrigation period (Maruyama et al., 2014). Upland and crop-rotated paddy fields are also considered as the recharge area. The crop rotated area ratio to the total study area was 14%, which was estimated by the ratio of crop rotation in the study area in 2005 (27%) and the paddy fields area ratio to the total study area in 2006 (51%). The upland field ratio was 2% of the total area. The recharge area except rice-planted paddy was 16% of the total area. For the study area, there has been no investigation to clarify rate of precipitation, which contributes to the groundwater recharge. Maruyama et al. (2014) estimated the groundwater recharge from the upland cultivation areas

expect for the rice-planted paddy fields using the relationship the direct surface runoff and precipitation amount investigated in the Nobi Plain in the central Japan. This estimation indicated that the groundwater recharge from the upland cultivation area was accounted for 10% of that from the rice-planted paddy fields. The simulation results of the present groundwater level (described in detail below), taking into consideration of the groundwater recharge from all of the agricultural fields, shows the relatively little differences (within 0.3 m) from that assuming the groundwater recharge from the only irrigated rice-planted paddy fields. During the irrigation period (from May to August), clear relationship between the mean groundwater levels and monthly precipitations. From the above reasons, recharge area was set to only the irrigated rice-planted paddy fields. The recharge fluxes from each cell were calculated by multiplying the percolation water rate from a cell in which rice-planted paddy occupies (7.4 mm/d) by both the paddy field area ratio in each cell and the area ratio of rice-planted fields to the total paddy fields. Groundwater use data for each cell was created considering the spatial distribution (1 km grid) of annual groundwater in 2008 and the monthly ratio of groundwater use in June (irrigation period) to the annual groundwater use (8.1%).

A steady state calibration for the hydraulic conductivities of five zones was performed by trial and error and the inverse method using PEST (Doherty 2004). The PEST automatically adjusts model parameters until the difference between model outputs and observations is minimized. In this study, the observed data consisted of groundwater levels during the irrigation period (June 2010) at 38 wells which the depths of strainers or well bottoms were known. The results of the optimized hydraulic conductivities is shown in Table 5-1. The conductivities of the shallow aquifer in the southern zone and deep aquifer from pumping tests were 4.0×10^{1} m/d and 1.7×10^{0} m/d, respectively. Okuyama (2013) reported that the conductivity of the shallow aquifer (northern zone) from a laboratory permeameter test was 2.3×10^{2} m/d. The calibrated results were sufficiently close to the estimated values from the field and laboratory tests. The mean error between the simulated and measured (ME) groundwater levels was 0.9 m, while the root mean square error (RMS) and normalized RMS (NRMS) were 2.1 m and 3.3%, respectively. Groundwater level contours from the simulated heads agreed with those of the observed levels in June of 2010. The calibrated hydraulic conductivities are considered reasonable.

To calculate the water exchange between the Tedori River and the aquifer, a second steady-state calibration was carried out by taking into account head-dependent boundary conditions using the MODFLOW river package (Harbaugh, 2005). The groundwater is hydraulically connected to the river if the water table is above the elevation of the base of the streambed sediments of the river. In this case, the river package calculates the recharge through the river bed using the following equation:

$$Q = C\left(H - h\right) \tag{5-2}$$

where Q is the exchange flow between the groundwater and river water (L^3/T), C is the hydraulic conductance of the riverbed (L), and H is the river water table (L). The conductance is calculated from:

$$C = \frac{K_r LW}{M} \tag{5-3}$$

where L is the length of the river along a cell (L), W is the width of the river in the cell (L), M is the thickness of the riverbed (L) and K_r is the vertical hydraulic conductivity of the riverbed material (L/T).

The river water levels and width of the river were obtained from observation of the discharge of the Tedori River in June of 2009. The recharge through the river bed was calculated using equation (5-2) under the assumption that the thickness of the riverbed was 15 m for descriptive purposes. The vertical hydraulic conductivities of the riverbed materials were determined so that water flow from the river to the groundwater, which is calculated in second model calibration, was equal to that calculated in the first model calibration. In the downstream the section along the river in which groundwater flowed into the river, the constant head boundary was specified.

Figure 5-4 shows comparisons of the calculated and observed head. The groundwater contours of simulated groundwater heads agreed well with those of the observed heads. The ME, RMS and NRMS were 0.9 m, 2.1 m and 3.4%, respectively. The calculated flow from the river to the right side groundwater of the river was 43% of the total observed flow from the river to groundwater during the irrigation period, which does not contradict the observed results; therefore, the model calibration result is considered reasonable.

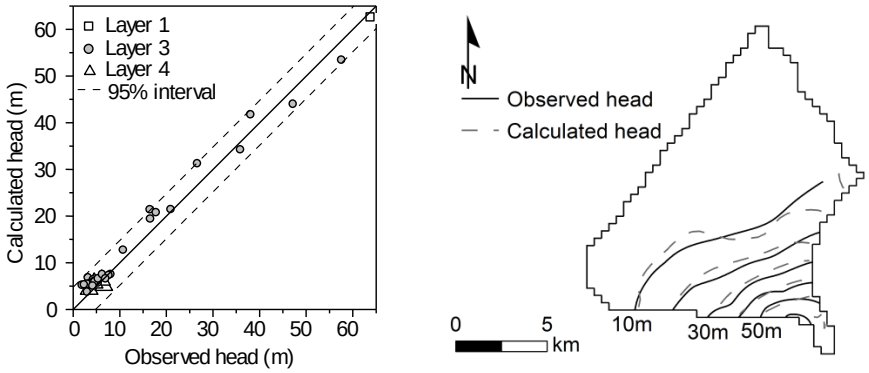

(a) (b)

Figure 5-4 Comparison of the calculated and observed head: (a) correlation diagram, and (b) contour map.

5.3 Results and Discussions

5.3.1 Water balance

To evaluate the recharge sources of the groundwater and flow paths, the annual water balance during the irrigation period was calculated considering the study area as a groundwater basin. Because the water balance analysis was conducted under the steady state condition at the irrigation period, it should be noted that these results differ from the water balance estimated by Maruyama et al. (2014). Table 5-2 shows water balances of the groundwater basin during the irrigation period. The ratios of the inflow water to from the Tedori River, Sea of Japan (the neighborhood area of border with the rivers) and the Sai River, and irrigated paddy to the total inflow were 18%, 44%, and 38%, respectively. The ratios of the outflow water from the Tedori River, Sea of Japan, the Sai River, and irrigated paddy were 4%, 52%, 28%, and 16%, respectively. These inflow and outflow water ratios at the Sai River were larger than the other water components. The groundwater thus flowed from coastal area to the Sai River. Because the interpolated groundwater levels was not obtained at the downstream section of the Sai River , a constant head boundary was set based on the linear interpolation between the interpolated groundwater level at the nearest cell from the river mouth and the sea-level surface. This approximated boundary conditions at the downstream section affected relatively large inflow and outflow water amount. However, the flow directions from the coastal area to the Sai River did not seem to have much influence on the groundwater levels for the entire model domain and the groundwater-level contours were well reproduced. It was thought that there was little problem for using this model if the mass balances around the coastal zone near the Sai River are appropriately handled. Furthermore, both the Tedori River and the surface boundary were net inflow sources; the ratios to total net inflow were 27% (1.4×10^5 m^3/d) and 73% (3.8×10^5

Table 5-2 Water balances of the groundwater basin during the irrigation period.

	Inflow (m^3/d (mm/d))	Outflow (m^3/d (mm/d))	Net inflow・Outflow* (m^3/d (mm/d))
Tedori River	1.8×10^5 (1.3)	3.9×10^4 (0.3)	1.4×10^5 (1.0)
Sai River	3.9×10^5 (2.7)	4.6×10^5 (3.2)	-7.0×10^4 (-0.5)
Sea of Japan	5.0×10^4 (0.3)	2.4×10^5 (1.7)	-1.9×10^5 (-1.4)
Irrigated paddy	3.8×10^5 (2.7)	-	3.8×10^5 (2.7)
Groundwater use	-	1.4×10^5 (1.0)	-1.4×10^5 (-1.0)

*(astrisk) Positive value indicates net inflow and negative value indicates net outflow.

m^3/d), respectively. Net outflow sources were groundwater use, outflow to the Sea of Japan, and the Sai River. The ratios to total net outflow were 35% (7.0×10^4 m^3/d), 48% (1.9×10^5 m^3/d), and 17% (1.4×10^5 m^3/d), respectively. These results suggest that each recharge source was non-negligible to the formations of groundwater levels.

5.3.2 Impact of land use and groundwater use change on groundwater levels

Possible factors influencing groundwater level changes in the study area were detected to be land use, groundwater use, and river water level. However, changes in the river water levels in the Tedori River and the Sai River have been small. Steady state groundwater flow simulations in the irrigation period for several scenarios of land use and groundwater use, which were set based on the past and the present, were calculated in order to assess decrease of the groundwater levels. Land use data were available in 1976, 1987, 1991, 1997, and 2006. Distributions (1km grid) of annual groundwater use were obtained for 1987, 1993, and 2008, respectively. Crop rotated paddy fields were variable for each year. Three scenarios based on the available data sets were generated as shown in Table 5-3. Case A1, which was the oldest combination, is the control simulation. Figure 5-5 shows the groundwater drawdowns from the condition of case A1 (the control simulation). In order to pay attention to “drawdown”, the positive values indicate decrease in groundwater levels and vice versa. The groundwater levels decrease in the most part of the model domain in the cases of A2 and A3. The decrease in groundwater level is noticeable at the area from the upper zone of this fan to middle zone, near the Tedori River. The maximum drawdown is 0.9 m in the case of A2 and 2.4 m in the case of A3, respectively. One reason is that the groundwater catchment area is limited in the upper and middle part of this fan relative to the lower part. At the lower zone of this fan, the groundwater levels slightly rise because of the decrease in the groundwater use. Figure 5-6 shows a comparison of the calculated and observed groundwater levels at the wells G, H, and I. The observed values were the mean values from May to August in 1986, 1997, and 2006, respectively. There are differences between the calculated and observed results. This was partly due to the differences in the period of the land use and groundwater use data. The temporal patterns of the groundwater levels were reasonably reproduced. The largest groundwater decreasing among the observation wells was 1.9 m during 1987-2006 at the well I. The observed groundwater drawdowns among the wells qualitatively agreed with the drawdown distributions of the computed groundwater levels. The developed groundwater flow model can be utilized for examining protections of groundwater levels because this model can simulate the relative changes in the groundwater level appropriately.

Table 5-3 Combination of land use and groundwater use data for simulations based on the past and the present data.

Case	Land use	Groundwater use	Rate of crop-rotated paddy to total paddy
A1	1987	1987	23%
A2	1997	1993	24%
A3	2006	2008	27%

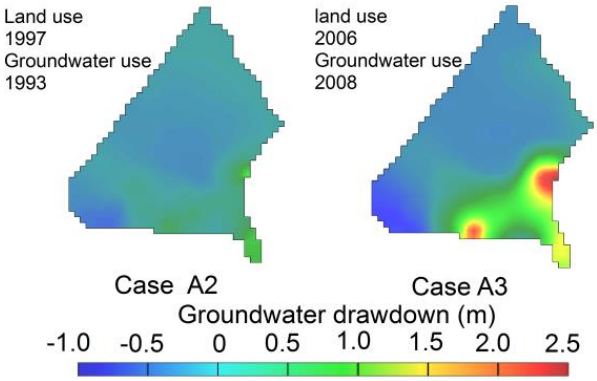

Figure 5-5 Groundwater drawdown by the land use and groundwater use changes in the irrigation period (Drawdown from the condition in case A1).

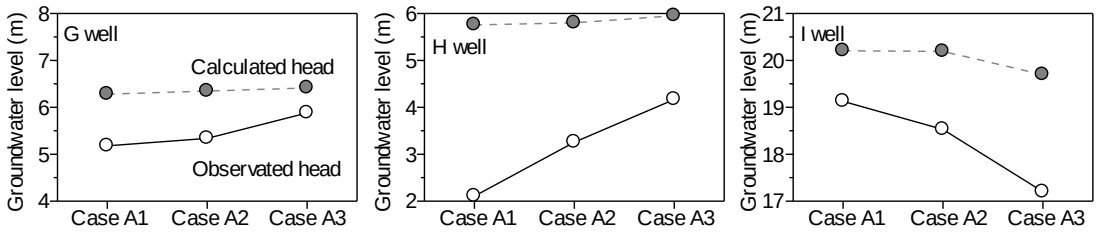

Figure 5-6 Comparison changes in the calculated and observed head in the irrigation period using the past data of land use and groundwater use.

There is a possibility that the paddy field area decreases over time. To assess the impact of decreasing the paddy field, groundwater levels were simulated with hypothetical land use changes; decline ratios of the paddy field were set 10%, 30%, 50%, and 70% relative to the paddy field area in 2006, assuming no distribution change in paddy field (Table 5-4). Figure 5-7 shows groundwater drawdown from the current condition (case A3). Figure 5-7 reveals that groundwater depressions occur at the upper zone of the fan. The maximum drawdowns for the cases B1, B2, B3, and B4 are 0.5 m, 2.0 m, 3.6 m, and 5.2 m, respectively. The groundwater depression at the upper zone of the fan is due to limitation of the groundwater catchment area and the much decrements of the rice-planted paddy area owing to having larger paddy field area

Table 5-4 Combination of land use and groundwater use data for simulations based on hypothetical land use changes.

Case	Land use (Decline ratio)	Groundwater use	Rate of crop-rotated paddy to total paddy
B1	2006 (10%)	2008	27%
B2	2006 (30%)	2008	27%
B3	2006 (50%)	2008	27%
B4	2006 (70%)	2008	27%

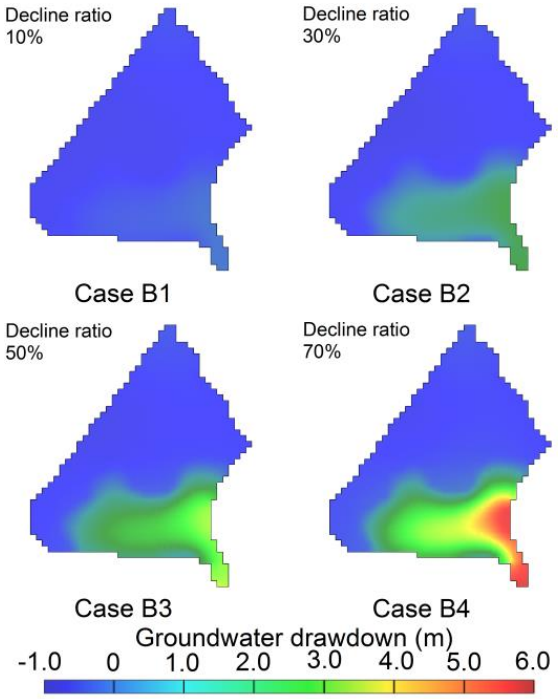

Figure 5-7 Groundwater drawdown by decreasing of paddy field area in the irrigation period (Drawdown from the condition in case A3).

at the upper zone.

5.3.3 Protections of groundwater level

To protect of groundwater level during the irrigation period, a pumping regulation is thought one of the effective methods. Required regulation ratios of pumping were estimated based on several simulations by reducing the groundwater use under hypothetical decreasing of paddy field (case B1 - B4). The spatial distribution of pumping remains in that of 2008. If the difference between the calculated groundwater levels and the current groundwater levels (the result of case

Table 5-5 Combination of land use and groundwater use data for simulations based on and groundwater use changes in each zone.

Case	Land use (Decline ratio)	Groundwater use (Change volume)	Rate of crop-rotated paddy to total paddy
C1	2006 (-30%*)	2008	27%
C2	2006 (-70%*)	2008	27%
C3	2006 (-100%*)	2008	27%
D1	2006	2008 (+1.0 × 10^4 m^3/d*)	27%
D2	2006	2008 (+3.0 × 10^4 m^3/d*)	27%
D3	2006	2008 (+5.0 × 10^4 m^3/d*)	27%

*(astrisk) The changes occur only in each zone (See Figure 5-8).

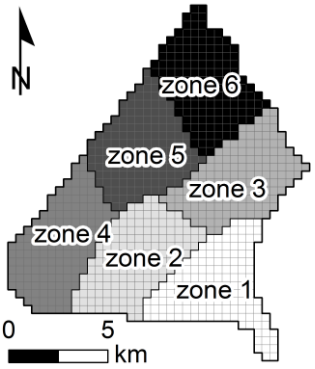

Figure 5-8 Partitions of the model domain.

A3) was less than 0.1 m, the current groundwater levels were judged to be maintained by the pumping regulation. As a result, pumping regulation by 20% enabled to maintain groundwater levels under the paddy field was decreased by 10%. When the paddy field was decreased by greater than 30%, the ground water level could not be maintained by pumping regulation. Total amount of groundwater use was equivalent to the amount of 40% of groundwater recharges based on the water balances (Table 5-2). The larger intensity of groundwater use was observed at the northeast part of this fan and the paddy field mainly distributed at the southern part. Differences in spatial distributions of the pumping and the paddy field caused the result that the pumping regulations cannot maintain the groundwater level, which cannot be explained by the water mass balances. It should be notated the groundwater drawdowns by decreasing the paddy field were possibility overestimation because the simulations was conducted under the assumption that the source of the groundwater recharge was only the irrigated paddy field during the irrigation period.

Several scenario simulations were performed to reveal spatial sensitivity of the groundwater level in response to changes in land use and groundwater use. Firstly, the fan was divided into 6

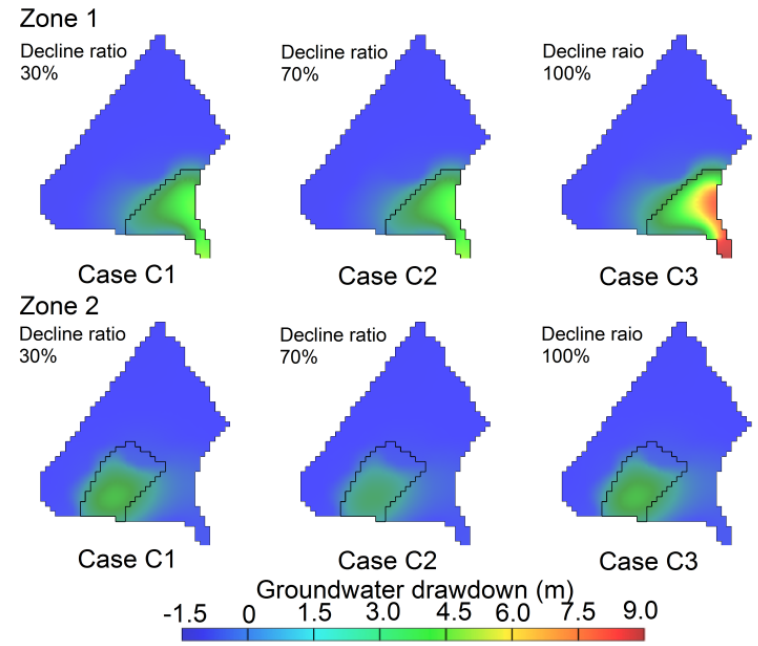

(a)

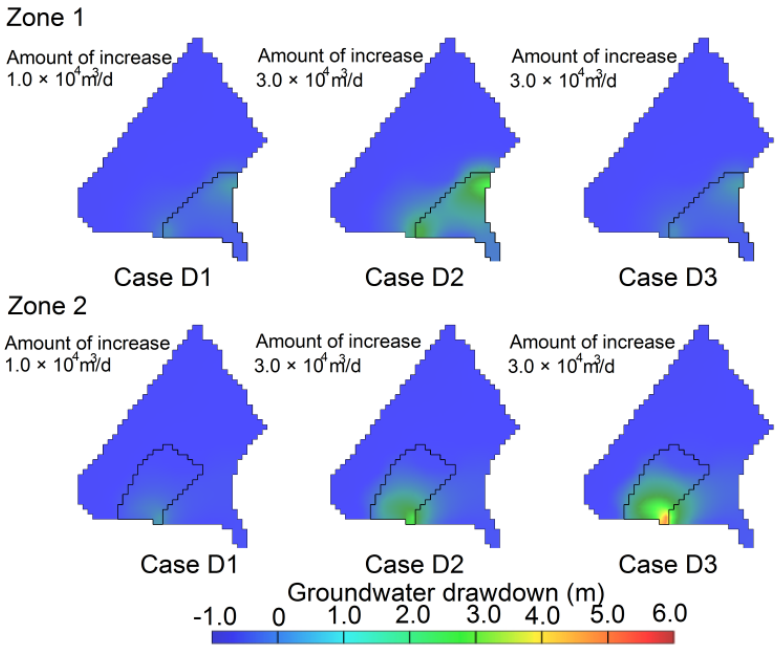

(b)

Figure 5-9 Groundwater drawdown for hypothetical changes in (a) the land use, and (b) the groundwater use at the range surrounded by the solid line in the irrigation period.

Note: Drawdown from the condition in case A3: upper, zone 1; lower, zone 2.

zones with approximately equal area, which are shown in Figure 5-8. The divided areas are hereafter called as zone. The scenarios considering the land use changes were conducted with three different decrement ratios of the paddy field to the current condition(2006): 30%, 70%, and 100% (Table 5-5). The scenarios considering the groundwater use changes were conducted with three different increment amounts of the pumping to the current condition (2008): 1.0×10^4 m^3/d, 3.0×10^4 m^3/d, and 5.0×10^4 m^3/d (Table 5-5). These increments of groundwater use were determined in consideration of a range of actual groundwater use in each zone from 1.3×10^4 m^3/d to 4.0×10^4 m^3/d. For all scenarios, the changes occur only in each zone. Figure 5-9 shows groundwater drawdowns for hypothetical changes in zone 1 and zone 2 from the current condition; case A3 was applied to the control simulation. The groundwater drawdowns for decreasing the paddy field are relatively large at zone 1 (the upper part of the fan) and zone 2 (the middle part of the fan near the Tedori River). The maximum drawdowns are 8.6 m for changing in zone 1 and 3.4 m for changing in zone 2 in the case A3. However, the maximum drawdowns remain low (less than 0.3 m) in the case of hyporgetical changes in zone 3-6 located around the lower parts of the fan and the urban area even in the case C3. These spatial charcterstics of the groudnwater drawdowns are also observed at the drawdowns for groudnwater use. The maximum drawdowns are 5.1 m for changing in zone 1 and 4.7 m for changing in zone 2 in the case D3. The maximum values are less than 1.0 m for changing in other zones. These results revealed that the spatial sensitivities of groundwater level for changes in the land use and groundwater use were different by the changeable locations. These changes within the upper part and the middle part the Tedori River are more affective to the groundwater level. It was concluded that the groundwater level protecions which carried out within these areas are more effective.

5.3.4 Effect of water level in the Tedori River

The seepage water to the shallow groundwater was observed along the almost of the Tedori River and amount of this water was one of the net inflow sources. Noto et al. (2013a; 2013b) predicted that the river water level would decline due to the decreasing in the snowfall. The hypothetical simulations were conducted for the three scenarios, the river water levels at the Tedori River would decline by 0.1m (case E1), 0.2m (case E2), and 0.3m (case E3) relative to the current river water level. The current river water levels were the observation values in the irrigation period in 2009 and ranged from 0.38 m to 0.87 m. Figure 5-10 shows groundwater drawdowns for hypothetical changes in the river water levels in the irrigation period from the current condition; case A3 was applied to the control simulation. The groundwater drawdowns were relatively large at the upper parts of the fan along the Tedori River. The maximum

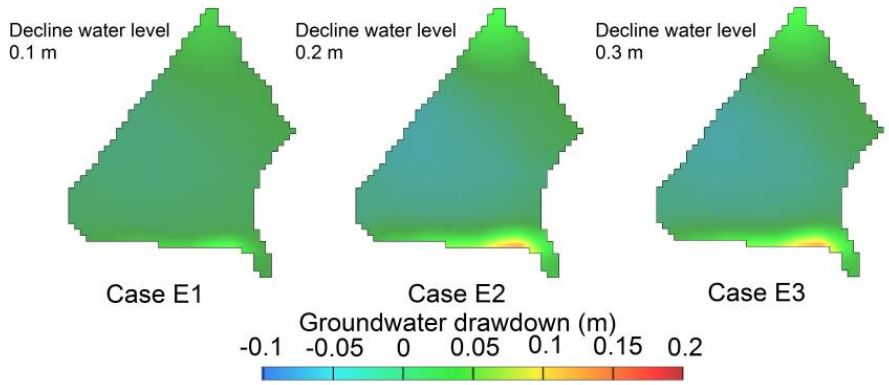

Figure 5-10 Groundwater drawdown for hypothetical changes in the river water levels in the irrigation period (Drawdown from the condition in case A3).

drawdowns are 0.05 m, 0.1 m, and 0.2 m in the cases E1, E2, and E3, respectively. The net inflow water to the groundwater in these cases were reduced by 1.3%, 2.5%, and 3.5%, respectively.

5.4 Conclusions

In this chapter, the numerical simulations was developed using the steady state groundwater flow analysis based on the hydrogeological conditions and hydrological observation results to assess the factors influencing groundwater level changes during irrigation in the Tedori River fan. Steady state groundwater flows in the irrigation period simulated several scenarios of land use and pumping schemes based on the past, the present, and the predicted future human activities. Noticeable results in the steady state simulations were as follows:

1) Groundwater levels in the upper and middle parts of the fan is affected considerably by paddy area and pumping discharge.

2) In cases where the paddy field area is smaller by more than 30% from the present condition, the groundwater level would not be maintained by pumping regulations. This result was influenced by the difference in spatial distribution of the land use and groundwater use.

3) Drawdown of the water level of the Tedori River also causes a slight groundwater level decline along the river.

In the study area, the decrements of the paddy field during 1987-1997 and 1997-2006 were 6.5% relative to 1987 and 10.5% relative to 1997, respectively. More reduction of paddy field area in the further requires another protections of groundwater levels in addition the pumping regulation.

Reference

Harbaugh AW. 2005. MODFLOW-2005, The U.S. Geological Survey Modular Ground-Water Model - the Ground-Water Flow Process. U.S. Geological Survey Techniques and Methods 6-A16, http://water.usgs.gov/nrp/gwsoftware/modflow2005/modflow2005.html.

Harbaugh AW, Banta ER, Hill MC, McDonald MG. 2000. MODFLOW-2000, the U.S. Geological Survey Modular Ground-Water Model - User guide to modularization concepts and the ground-water flow process. U.S. Geological Survey Open-File Report 00-92, p. 121

Harbaugh AW, McDonald MG. 1996. User's documentation for MODFLOW-96, an update to the USGS modular finite-difference ground-water flow model: USGS Open-File Report 96. p. 485.

Hokuriku Regional Agricultural Administration Office. 1977. Hydraulic geology and groundwater in Ishikawa prefecture (in Japanese).

Khan S, Rana T, Carroll J, Gabriel H. 2010. Assessment of rice hydraulic loading impacts on groundwater and salinity levels. Paddy Water Environ 8: 23-29.

Maruyama T, Noto F, Yoshida M, Horino H, Nakamura K. 2014. Analysis of water balance in the Tedori river alluvial fan areas of Japan: focused on quantitative analysis of groundwater recharge from river and ground surface, especially paddy fields. Paddy Water Environ 12: 163–171.

Ministry of Land, Infrastructure, Transport and Tourism. 2011. The Nationwide Ocean Wave information network for Ports and HArbourS, (NOWPHAS) http://www.mlit.go.jp/kowan/nowphas/index_eng.html.

Murashima K .2009. Investigation and change prediction of irrigation water use. Normal hydrological cycle as a core of irrigation water, Annual Report 2008. Ishikawa Prefectural University, Japan (in Japanese).

Noto F, Maruyama T, Hayase Y, Takimoto H, Nakamura K. 2013a. Evaluation of water resources by snow storage using water balance and tank model method in the Tedori River basin of Japan. Paddy Water Environ 11: 113-121.

Noto F, Maruyama T, Hayase Y, Takimoto H, Nakamura K. 2013b. Prediction of water resources as snow storage under climate change in the Tedori River basin of Japan. Paddy Water Environ 11: 463–471.

Okumoto T. 2013. Elucidation of hydrogeological structure in the Tedori River alluvial fan. In Normal hydrological cycle in the Tedori River Alluvial Fan areas as a core of irrigation water - Case study in the Tedori River basin assuming the climate change -, Maruyama T. and Hayase Y. (eds.). Ishikawa Prefectural University Press: Ishikawa, pp. 137-144 (in Japanese).

CHAPTER 6

Assessment of factors influencing groundwater level change using groundwater flow simulation, considering vertical infiltration from rice-planted and crop-rotated paddy fields

6.1 Introduction

In this chapter, a steady state model was extended to a transient model to determine the quantitative effects of different land use conditions, such as paddy and upland fields (including crop-rotated paddy fields) on the groundwater recharge and groundwater level. The transient model consists of a 1-D unsaturated model (HYDRUS-1D) for estimation of groundwater recharge and a 3-D groundwater model (MODFLOW). Based on groundwater flow simulation from 1975 to 2009, evaluation of relationships between changes in groundwater levels over time and changes in artificial or natural factors was then performed.

6.2 Summary of the analysis

In this study, groundwater recharge was calculated with the HYDRUS-1D 1-D unsaturated flow model and adapted to the upper boundary condition of the MODFLOW 3-D groundwater flow model. Recharge areas were set as the paddy field and upland field, including crop-rotated paddy fields. Other land use conditions were considered as non-recharge areas. MODFLOW's domain arrays were identified as calculation cells. Each unsaturated soil profile was set for each calculation cell assigned to recharge area. The bottom water flux at each calculation cell in the recharge area was determined by HYDRUS-1D under a time variable atmospheric boundary condition.

6.3 Unsaturated Flow Model

6.3.1 Governing equations

Water movement in the unsaturated zone was assumed to occur only in the vertical direction, which is described by a modified form of the Richards equation:

$$\frac{\partial \theta}{\partial t} = \frac{\partial}{\partial z}\left[K \frac{\partial h}{\partial z} + K \right] - S \tag{6-1}$$

where θ is the volumetric soil water content, which is a function of the pressure head for a given material (dimensionless), *t* is time (T), *z* is the vertical coordinate (L) (positive upward), *K* is the unsaturated hydraulic conductivity at the current pressure head (L/T), *h* is the water pressure head (L), and *S* is the sink term by plant roots (1/T).

The unsaturated soil hydraulic properties, θ and *K*, are highly nonlinear functions of the pressure head. In this study, the hydraulic properties were calculated using the equations described by van Genuchten (1980). The soil water retention, θ(*h*), and hydraulic conductivity, *K*(*h*), functions are given by:

$$\theta = \frac{\theta_s - \theta_r}{\left[1 + |\alpha h|^n\right]^m} + \theta_r \ (h < 0), \quad \theta = \theta_s \ (h \geqq 0) \tag{6-2}$$

$$K(h) = K_s S_e^l \left[1 - (1 - S_e^{1/m})^m\right]^2 \tag{6-3}$$

$$S_e = \frac{\theta - \theta_r}{\theta_s - \theta_r} \tag{6-4}$$

where n is a pore-size distribution index (dimensionless) (*m*=1-1/*n*, *n* >1), *l* is a pore-connectivity parameter (dimensionless), α is the inverse of the air-entry value [1/L], θ_r is the residual water content (dimensionless), θ_s is the saturated water content (dimensionless) and S_e is the effective water content (dimensionless). The pore-connectivity parameter l in the hydraulic conductivity function is estimated to be about 0.5 for many soils (Mualem, 1976). Five parameters (K_s, θ_s, θ_r, α, n) are required for the calculations.

The numerical model used was Version 4.0 of HYDRUS-1D, a software package for simulating water, heat, and solute movement in one-dimensional variably saturated media based on finite element representation of the governing equations (Šimůnek et al., 2008).

6.3.2 Model discretization

The soil profiles were set from the soil surface to 5 m below the water table considering the fluctuation in groundwater level. The depth of the water table was determined from the difference between ground surface elevation and interpolated groundwater levels during the non-irrigation period in 1993 (Figure 6-1(b)). The depth varied from 2 m to 45 m, and was deeper in the upper region of the fan than the lower region. The soil profile was vertically discretized into two layers. The upper layer from the surface to 0.3 m depth, was the low permeability layer (plow sole), which occurred under the puddled top soil. The plow sole is the major factor controlling the infiltration rate and groundwater recharge in paddy fields (Chen et al., 2002). The lower layer, from 0.3 m depth to the bottom of the vertical calculation domain, was the subsoil under the plow sole. As shown in Figure 6-1(c), the hydraulic parameters were initially grouped into three zones considering the shallow aquifer zoning (described in detail below). Parameters of the soil water retention curve were calibrated to fit the groundwater fluctuation. Optimized parameters are shown in Table 6-1. Optimized saturated conductivities of the plow sole layers were relatively large. This reason is explained as follows. Soil water flows in unsaturated condition in an open system with negative pressure because the soil surface infiltration is given by prescribed water flux (Table 6-2) and depths of groundwater level are around 5–40 m (Figure6-1(b)). The unsaturated conductivity becomes low significantly under the unsaturated condition. The groundwater recharge (bottom flux) at the rice-planted paddy fields was simulated reasonably (as mentioned below). Optimized saturated conductivity is therefore nothing more than one parameter to determine the shape of the unsaturated hydraulic conductivity function based on the van Genuchten-Mualem model.

The recharge areas were paddy and upland crop-rotated paddy fields. Buildings and roads constitute possible land uses for the recharge area, apart from the agricultural fields. However, roads are regarded as impermeable because they are usually made of asphalt. The ratio of the floor space to the total building space is around 33 % in Kanazawa City. When about two-thirds of the building field was set as the recharge area, the simulated groundwater-levels had lower reproducibility of the seasonal fluctuations than simulations the building field set as totally impermeable area. Thus, land use conditions other than agricultural fields were considered as non-recharge areas. For each year, a cell was assigned as either a paddy cell, upland cell, or a non-recharge cell as follows: all cells were ranked in ascending order according to the paddy field area ratio in each cell. The cells having larger paddy field area rates were then specified to be uniform paddy field cells in decreasing order. The number of specified paddy cells was set so that the sum of their areas was equal to the actual paddy field area. A similar method was used to determine the upland cells. The cells specified as

Table 6-1 Hydraulic parameters in HYDRUS-1D.

Zone	θ_r	θ_s	α (1/m)	n	K_s (m/d)	l
Plow layer in northern zone	0.0500	0.3710	1.10	1.30	10.0	0.5
Subsoil in northern zone	0.0501	0.3810	2.51	2.50	70.1	0.5
Plow layer in southern zone	0.0587	0.3660	0.964	1.40	6.74	0.5
Subsoil in southern zone	0.0527	0.411	3.36	2.71	100	0.5
Plow layer in coastal zone	0.0501	0.3700	0.998	1.50	9.94	0.5
Subsoil in coastal zone	0.0500	0.3980	3.01	2.72	70.5	0.5

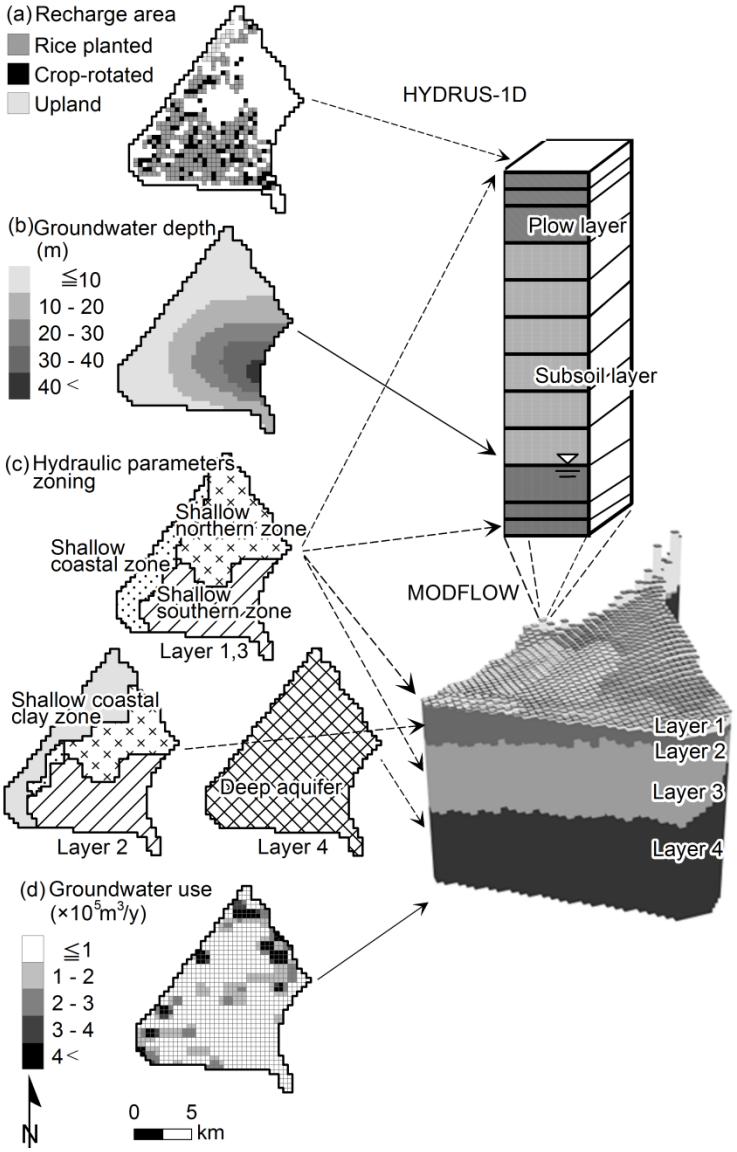

Figure 6-1 Input data for HYDRUS-1D and MODFLOW: (a) recharge areas in 2009, (b) groundwater-level depth (non-irrigation period in 1993), (c) hydraulic parameters zoning, (d) annual groundwater use in 1993.

neither paddy cells nor upland cells were set as non-recharge area cells. Among the paddy cells, the crop-rotated paddy cells were randomly reconfigured considering the ratio of paddy rice-upland crop rotation in each year and assuming that the rotation was not carried out for two years running. Figure 6-1(a) shows the recharge area in 2009. Temporal variations for the paddy and upland field areas were obtained using a linear interpolation method and land use data available in 1976, 1987, 1991, 1997, 2006 and 2009. The ratio of paddy rice-upland crop rotation in this area was available for each year. Land use conditions were changed from November considering the cropping schedule for each year (one hydrological year in this study was from November to October).

6.3.3 Boundary conditions and input data

The upper boundary condition was set to be a time variable atmospheric boundary condition and the lower boundary condition was set to be a free drainage condition because of the relatively deep water tables. HYRDUS-1D requires the precipitation, potential evaporation, and potential transpiration data, which were obtained from the Kanazawa meteorological station for the present study. Potential evapotranspiration was calculated according to the Penman method. Monthly albedo for paddy and upland fields were based on Kotoda (1989). Potential evapotranspiration was partitioned into an evaporation component and a root water uptake component (transpiration). Potential transpiration rates, T, were derived from the following equation (Campbell, 1985):

$$\frac{T}{ET} = 1 - \exp\left(-0.82\mathrm{LAI}\right) \tag{6-5}$$

where, LAI is the leaf area index defined as the total one-sided leaf area per unit ground area (dimensionless). In this study, LAI was multiplied by the vegetation cover ratio (defined as the percentage of area covered with plants per ground area) considering the furrow area. A month is divided into three parts (decade days): early of month (10 days), middle of month(10 days), and end of month (remaining days). Values of LAI were derived on a decade days basis for rice, soybeans, and barley seeds using values reported by Shibayama et al. (2011), Shimada et al. (1990), and Takeda and Udagawa (1976), respectively. Values of the vegetation cover ratio for soybeans were obtained on a decade days basis from Satoh (2002), while those for rice and barley seeds were estimated using an empirical model between the vegetation cover ratio and LAI by Nakamura et al. (2007) and Fukushima et al. (2003), respectively.

Water extraction in the root zone was calculated from the potential transpiration and root-length density by the Feddes root water uptake model (Feddes et al., 1978). Root water

Table 6-2 Irrigation water managemet and amount of irrigation water.

Term	Irrigation water management	Amount of irrigation water (mm/d)
Late April	Soil puddling	60
Early May to late May	-	20
Early June to mid-June	Mid-summer drainage	Precipitation
Late June to late July	Intermittent irrigation	20
Early August to late August	Intermittent irrigation	5
Early September	Ponding water release	Precipitation

uptake parameters of the Feddes model for soybean and barely were used as database values of HYDRUS-1D, while those reported by Phogat et al. (2010) were used for rice. The depth of the root zone was 0.2 m below the soil surface and the root-length density in the root zone was assumed to be uniformly distributed.

The initial conditions were considered to be a uniform pressure head (-1 m) throughout the vertical soil profile. Leterme et al. (2013) indicated that relatively long warm-up periods were necessary to avoid oscillations of calculation (at least several years), even while the numerical solution eventually stabilized. This was partly due to the presence of zones with a deep water table, which resulted in atmospheric input taking several years to migrate through the unsaturated zone. Since Lererme et al. (2013) used a warming-up period of 10 years to ensure results independent of the initial conditions, the same warming-up period was used in this study. During the warming-up period, weather data from October 1975 to November 1976 were used because the weather data in this duration were similar to the averaged value during 1980-2010.

According to Noto et al. (2013), snowmelt water amount was calculated by the following model to the Tedori River basin:

$$S = m_s T + \frac{RT}{80} \tag{6-6}$$

where, S is the daily snowmelt (L/T), m_s is the snowmelt coefficient (L/(°C T)), R is the daily precipitation (L/T), and T is the daily mean temperature (°C). The coefficient m_s was estimated to demonstrate short-term groundwater fluctuations by trial and error (m_s=7 mm/(°C d)). Snowmelt was set to 0 mm when snowfall were observed and the snowmelt model was used when snowfall was not observed. Snowfall data used was obtained from the Kanazawa meteorological station. Evaporation at the surface was not considered during application of the model because the model considers snowmelt at the snow surface based on evaporation.

Table 6-3 Hydraulic conductivities and storage coefficients using MODFLOW.

Zone		Hydraulic conductivit	Specific storage	Specific yield
Shallow aquifer	Northern zone	8.6×10^{2}	1.0×10^{-4}	0.05
	Southern zone	4.8×10^{1}	1.0×10^{-4}	0.05
	Coastal zone	7.4×10^{2}	6.6×10^{-5}	0.05
	Coastal clay zone	1.1×10^{-3}	1.0×10^{-3}	0.03
Deep aquifer		1.2×10^{0}	1.0×10^{-4}	0.05

Since HYDRUS-1D does not include an irrigation management model, some irrigation scenarios were set that considered both the observed irrigation practices and volume of water rights for puddling purposes in the study area. Table 6-2 summarizes the paddy irrigation management settings. The maximum ponding depth for paddy fields was set at 0.15 m during the irrigation period, while that of upland fields (including crop rotated fields) and paddy fields during the non-irrigation period was set at 0.03 m.

HYDRUS-1D was run using daily stress periods. Decade-days recharge values were derived by averaging daily recharge values from HYDRUS-1D and used for the upper boundary condition for the groundwater flow model to reduce computational efforts.

6.4 Groundwater flow model

In Chapter 5, the groundwater flow model at steady state using MODFLOW developed. The model was extended to a transient model to determine. The groundwater flow model was calibrated under both steady state and transient state conditions. Steady state calibration was conducted to determine the hydraulic conductivities and hydraulic conductance of riverbed materials, which mentioned above (5.2.3). Transient state simulation was optimized by adjusting the storage coefficients. The latter calibration is explained in the following sections.

6.4.1 Boundary conditions and input data

Specific coefficients were determined by a transient state calibration. The hydraulic conductivities and conductances, which were estimated from the steady state calibration, were used in the transient calibration. The transient simulation spanned a 35-year period (1975-2009) and the storage coefficients were assigned based on the hydraulic conductivity zones.

Along the Sai River and downstream section of the Tedori River, constant head boundary conditions were set using interpolated water levels in December of 1993

(non-irrigation period) because groundwater levels near these sections changed only slightly both seasonally and over the long term. Other boundary conditions were the same as those in the above second steady state calibration. This can be justified because of the small changes in river water levels in the Tedori River and mean sea level at the Sea of Japan during the simulation period.

Fine spatial and temporal distributed groundwater use data were not available. Accordingly, datasets with monthly intervals for the period from 1975 to 2009 were created considering the spatial distribution of the annual groundwater in 1993 and temporal variation of annual and monthly groundwater use in 2005. Monthly-based groundwater use in each cell was applied for the transient groundwater flow simulations.

The map of groundwater levels in December of 1993 was used to set the initial heads for the transient state calibration. The computational time step was set as digital elevation model. The groundwater levels in the eight monitoring wells (wells C-I in Figure 3-9) were used for model calibration. Optimized storage coefficients are shown in Table 6-3.

6.5 Results and Discussion

6.5.1 Seasonal and annual changes in groundwater level

Figure 6-2 shows a comparison of the decade-average of the calculated and observed groundwater levels in D well. The seasonal pattern of fluctuation, which is considered to be typical of groundwater level changes in the paddy irrigation area, was reasonably well reproduced. Initially, there was a substantial increase in the groundwater level from the end of April to early May (the beginning of the irrigation period) due to paddy fields being plowed and irrigated before transplantation of the rice seedlings. From July to September (the irrigation period), groundwater levels remained high and stable. From September to October (the beginning of the non-irrigation period), groundwater levels decreased dramatically. Overall, the model was able to reasonably compute seasonal fluctuations, which were significant in response to paddy irrigation such as the increase of groundwater levels at the beginning of the irrigation period. Other observation wells also showed fluctuations with the difference in the degree of increase of groundwater levels. Figure 6-3 shows comparisons of the calculated and observed groundwater-level contour maps. The observed groundwater-level contours were based on simultaneous observations of groundwater level in early December 1993, mid-November 2009, and early June 2010. Because the simulation period is until November of 2009, the simulation results did not provide the contours in November of 2009 and June of 2010. The contours in November of 2008 and June of 2009 were used instead of

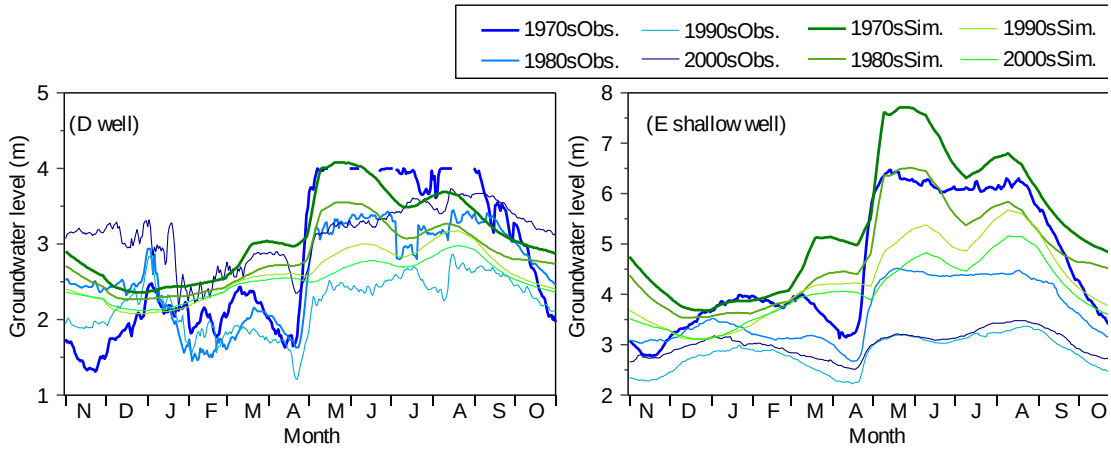

Figure 6-2 Calculated and observed groundwater levels averaged by decade in D and E (shallow) wells.

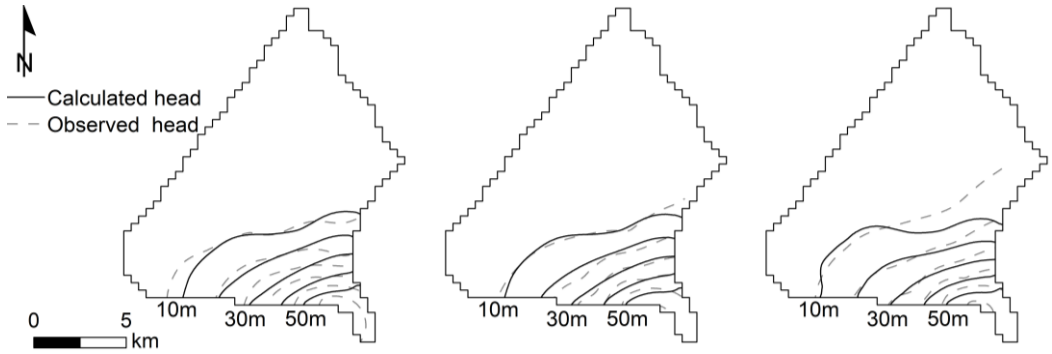

(a) (b) (c)

Figure 6-3 Calculated and observed groundwater-level contour maps: (a) non-irrigation period in December 1993, (b) non-irrigation period in November 2009, and (c) irrigation period in June 2010.

those of November of 2009 and June of 2010. Simulated groundwater levels were averaged for decade days and shallow simulated groundwater-level contours approximately fit the observations of the three periods.

There were some differences between the predicted and the observed results. Specifically, the absolute values between the observed and calculated groundwater levels varied. This was partly due to the resolution of the MODFLOW cells (based on a 400-m grid). There were also sluggish decreases in calculated groundwater levels after the irrigation period. Namely, there was a lag time in groundwater recharge because the groundwater depth was relatively deep and the infiltration water did not contribute to the groundwater recharge promptly. Moreover, temporal and local groundwater changes in winter did not respond to groundwater use for melting snow because of lower-resolution input data in space (based on a 1 km grid) and time (monthly). Figure 6-4 shows the observed groundwater levels at E, F, I,

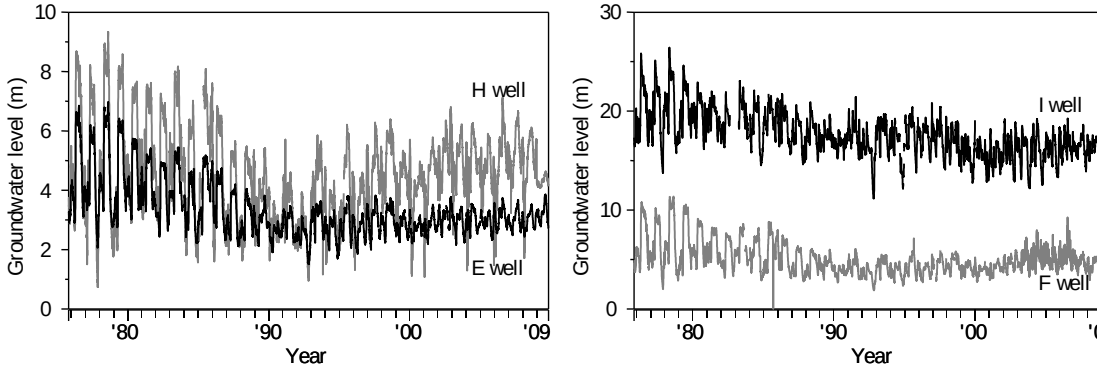

(a) (b)

Figure 6-4 Temporal changes in observed groundwater levels from 1976 to 2009: (a) E and H wells, and (b) I and F wells.

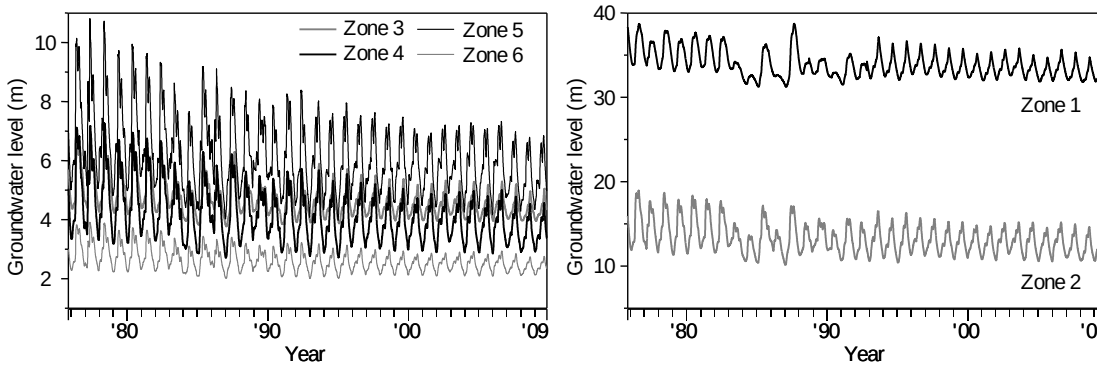

(a) (b)

Figure 6-5 Temporal changes in calculated groundwater levels from 1976 to 2009averaged in each zone: (a) zones 3, 4, 5 and 6, and (b) zones 1 and 2

Table 6-4 Change rate of annual groundwater levels.

Zone	Change rate of annual groundwater levels (m/y)	
	Hydrological year	Irrigation period
Zone 1	-0.07	-0.08
Zone 2	-0.07	-0.10
Zone 3	-0.03	-0.04
Zone 4	-0.05	-0.08
Zone 5	-0.04	-0.06
Zone 6	-0.02	-0.03

Note: Positive value indicates groundwater level rise and negative value indicates groundwater level depression.

and H wells. The lowest decade-averaged groundwater level was observed in the 1990s, while the groundwater levels increased slightly during the 2000s, probably because of a reduction in annual groundwater use. However, the lowest calculated value was in the 2000s, which was likely due to the low spatial and temporal resolution of the groundwater use setting. Based on the above results, this model could calculate changes in groundwater reasonably, despite the limitations of the model structure and data. The ME, RMS and NRMS were 0.5 m, 1.8 m and 5.4%, respectively.

The fan was divided into 6 zones with approximately equal area, which are shown in Figure 5-8. Figure 6-5 shows the average calculated groundwater level in each zone. The decreasing trends of groundwater levels in each zone were similar to temporal changes in some observed wells (Figure 6-4). Groundwater levels averaged over the hydrological year (from November to October) declined from 1975 to 2009, with a maximum decrease of 3.5 m being computed in zone 1. Change rates of groundwater levels averaged over the hydrological year or the irrigation period (from mid-April to early September) are shown in Table 6-4. Positive values indicate the rate of groundwater increase, while negative values indicate groundwater depression. In zone 1 (the upper zone of this fan) and zone 2 (the middle zone of this fan, near the Tedori River), the groundwater levels decreased by an average of -0.07 m/y, which was larger than in other zones. During the irrigation period, the greatest rate of decrease was -0.10 m/y in zone 2, and relatively small values are -0.08 m/y in zone 1 and 4. The annual changes in groundwater levels caused by changing the paddy field area were more affected by changes in the paddy field area in the middle part of the fan. One reason for this is that the groundwater catchment area is limited in the upper and middle part of the fan relative to the lower part.

6.5.2 Seasonal changes in groundwater recharge

Figure 6-6 shows the mean of seasonal precipitation, snowmelt water, evaporation, transpiration and groundwater recharge from the paddy and upland fields, including the rotated paddy fields over 35 years and the standard deviations. The recharge value at the paddy fields was relatively large (average, 10.2 mm/d) from early May to early June owing to the beginning of paddy irrigation. The averaged recharge values in the period influenced by the mid-summer drainage (mid-June to early July) and after that period (mid-July to the end of August) were 6.5 mm/d and 10.8 mm/d, respectively. Maruyama et al. (2014) estimated the water percolation to be 10.7 mm/d by subtracting evapotranspiration from the water requirement rate observed during mid-May to early August in 2008. The ratio of calculated recharge to water percolation was 90%. Measured water percolation may contain water

components that do not contribute to groundwater recharge such as the volume of water that flows to the sea. These findings suggest that the groundwater recharge estimated using HYDRUS-1D had reasonable precision. The recharge amounts in the non-irrigation period from both paddy and upland fields were relatively high in the snowfall and spring snowmelt periods, with the largest value of 5.8 mm/d being observed from early to mid-March. The average recharge from mid-September to the end of November, which accounts for 35% of the rainfall, is 1.1 mm/d and the groundwater level is approximately constant.

The annual recharge in the hydrological year from the paddy and upland fields was 1,819±202 mm and 886±287 mm, respectively. The total recharge during the irrigation period from the paddy and upland fields was 1,207±57 mm and 220±106 mm, respectively. The annual recharge at the upland field was mean 36% of the annual precipitation. In paddy fields, the ratio of the irrigation period to a year was about 74%. Taken together, these findings indicate that irrigated rice-planted paddy fields have a 5.5-fold greater ability to recharge groundwater than upland fields.

6.5.3 Annual changes in groundwater recharge

The annual net water balances for 35 years were calculated considering the study area as a groundwater basin (Figure 6-7). Both the Tedori River (the head-dependent boundary) and the surface boundary were net inflow sources, and the ratios for total net inflow were 70% and 30%, respectively. Net outflow sources were groundwater use and outflows to the sea and the Sai River (the constant head boundary), and the ratios for total net outflow were 40% and 60%, respectively. The ratios for total net inflow were 40% and 60%, respectively. These results suggest that the groundwater recharge from agricultural fields has a greater effect on groundwater levels than groundwater use.

Figure 6-8 shows the annual changes in precipitation and the agricultural area ratios, as well as the recharge for the entire model domain. Groundwater recharge is divided into two recharge fields, rice-planted paddies and upland (including rotated) fields. Ratios of each agricultural (paddy, rice-planted paddy, and upland) area to the total study area are shown. Ratios of rice-planted paddies to total groundwater recharge ranged from 80%–96%, indicating that rice-planted paddies are the dominant groundwater recharge source. The ratio of paddy area (including the crop rotation) and rice-planted paddy area decreased by 34% and 48%, respectively, from 1976 to 2009. Total recharges at rice-planted paddies and upland paddies ranged from 7.17×10^7 m^3 in 2008 to 1.95×10^8 m^3 in 1977 and from 6.13×10^6 m^3 in 1976 to 2.89×10^7 m^3 in 1983, respectively. Regional groundwater recharges ranged from 7.93×10^7 in 2009 to 2.03×10^8 m^3 in 1977. Under the influence of decreased rice-planted paddies

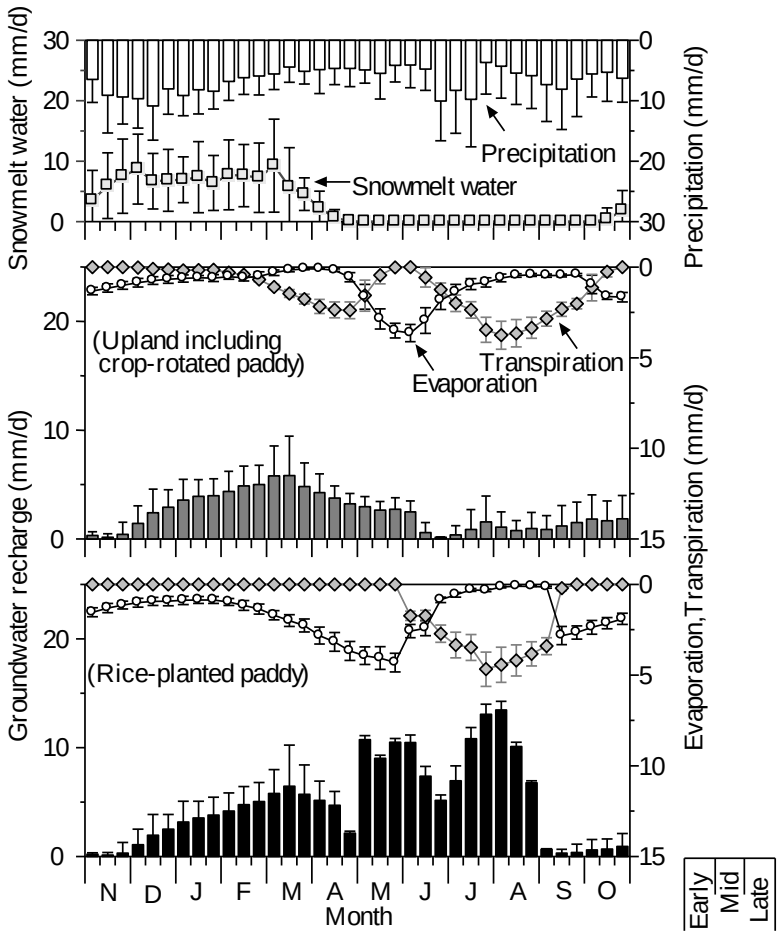

Figure 6-6 Seasonal changes in precipitation, snowmelt water, evaporation, transpiration, and groundwater recharge at the unit recharge area.

Note: Bars indicate one standard deviation.

and precipitation, the amount of regional groundwater recharge is decreasing, with a total decrease to 61% of the peak in 1977. The Mann-Kendall test (P = 0.05) revealed that agricultural area ratios (rice-planted, paddy, and upland fields), precipitation, snowfall, and groundwater recharge from 1975 to 2009 showed significantly decreasing trends. There was no change in the ratio of paddy rice-upland crop rotation and groundwater use.

Groundwater storage was estimated from annual average groundwater levels and effective porosities. Effective porosities were used to determine the approximate specific yield (Table 6-3). The average groundwater storage was 2.9×10^9 m^3 over 35 years, with a decrease of 2.4×10^7 m^3 occurring from 1976 to 2009. The annual groundwater recharge was comparable to about 4.8% (from 2.8% to 7.0%) of groundwater storage. The influence of rice-upland crop rotation on groundwater recharge was evaluated by simulation using the hypothetical land use scenario without paddy rice-upland crop rotation. The simulation revealed that groundwater recharge would decrease by 68－95% for paddy fields and 73－

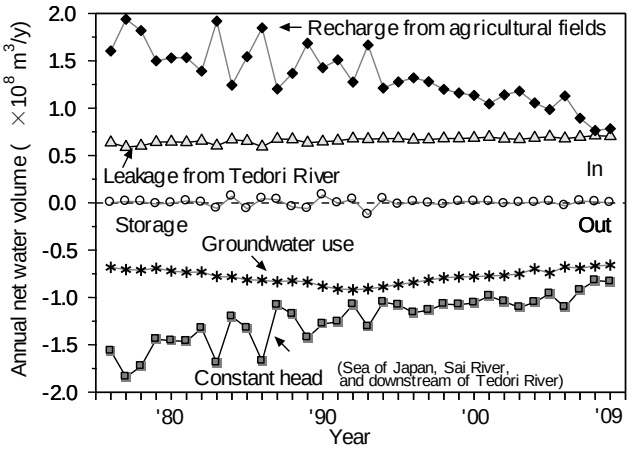

Figure 6-7 Annual net water balances for the entire model domain.

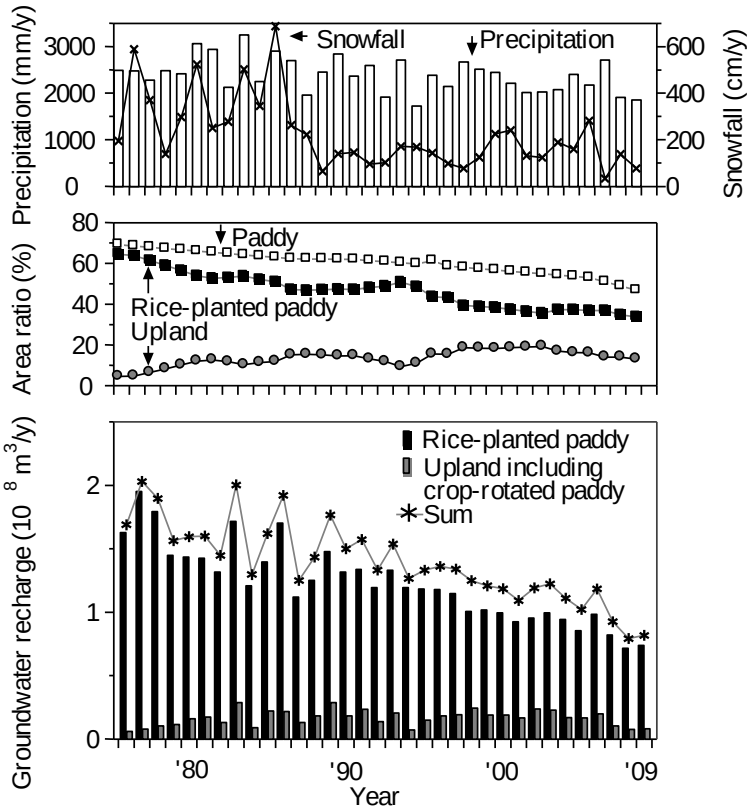

Figure 6-8 Annual changes in precipitation, snowfall, area ratio, and groundwater recharge for the entire model domain.

98% for the whole model. Under no crop-rotation systems, change rates of groundwater levels for each zone ranged from -0.02 to -0.05 m/y, with a maximum drawdown of 1.3 m occurring from 1975.

The decrease in groundwater storage over 35 years was 1% of the total storage. However, groundwater recharge was 5% of the storage and 1.1–2.8 times the amount of groundwater use. Hence, it was confirmed that the conservation of paddy fields is of

importance for sustainable groundwater use. Furthermore, the effects of the crop rotation on groundwater recharge were non-negligible; however, additional studies are warranted.

6.6 Conclusions

This study was conducted to develop a groundwater model that considered unsaturated flow to compute water-table fluctuations in the Tedori River fan in response to paddy irrigation management, rainfall, snowfall, snowmelt, and evapotranspiration. The model consisted of the 1-D unsaturated water flow model (HYDRUS-1D) for estimating groundwater recharge and a 3-D groundwater flow model (MODFLOW). The fine distribution of agricultural fields was modeled by coupling the 1-D unsaturated flow model to the 3-D groundwater flow model through simulating groundwater recharge for each 3-D model grid (400 m × 400 m). This technique enabled spatial and temporal groundwater levels to be estimated reasonably and groundwater recharge to be estimated appropriately, although some improvements could be made to enable more accurate simulation. Noticeable results in the transient simulation during 1975 to 2009 were as follows:

1) Annual groundwater recharge decreased over time. Regional groundwater recharges ranged from 7.93×10^7 m^3 in 2009 to 2.03×10^8 m^3 in 1977. The total amount of regional groundwater recharge decreased to 61% of the peak in 1977 because of declines in rice-planted field area and precipitation. Thus, annual averaged groundwater levels have decreased to 3.5 m in the upper zone over 35 years.

2) Irrigated rice-fields have a 5.5-fold greater ability to recharge the groundwater than upland fields. The rice-upland crop rotation system could possibly decrease groundwater recharge by 73%－98% relative to the current situation.

Next chapter, quantitative assessments of the impact of predicted climate change on groundwater recharge and groundwater levels using the developed transient model are carried out.

References

Campbell GS. 1985. Soil physics with basic transport models for soil-plant system. Elsevier, Amsterdam.

Feddes RA, Kowalik PJ, Zaradny H. 1978. Simulation of field water use and crop yield, Simulation of field water use and crop yield, PUDOC, Wageningen, Simulation Monographs, p, 189.

Fukushima A, Kusuda O, Furuhata M. 2003. Relationship of vegetation cover to growth and

yield in wheat. Rep Kyusyu Br Crop Sci Soc Japan 69: 33–35 (in Japanese).

Kotoda K. 1989. Estimation of river basin evapotranspiration from consideration of topographies and land use conditions. IAHS Publ 177: 271–281.

Leterme B, Gedeon M, Jacques D. 2013. Groundwater recharge modeling in the Nete catchment (Belgium) with HYDRUS-1D – MODFLOW package, In: Šimůnek J van Genuchten M TH, Kodešová R (eds) Proc. of the 4th International Conference "HYDRUS Software Applications to Subsurface Flow and Contaminant Transport Problems", March 21-22, 2013, Dept. of Soil Science and Geology, Czech University of Life Sciences, Prague, Czech Republic, ISBN: 978-80-213-2380-3, pp. 235–244,

Liu CW, Chen SK, Jou SW, Kuo SF (2001) Estimation of the infiltration rate of a paddy field in Yun-Lin Taiwan. Agricultural Systems 68: 41–54.

Maruyama T, Noto F, Yoshida M, Horino H, Nakamura K. 2014. Analysis of water balance in the Tedori river alluvial fan areas of Japan: focused on quantitative analysis of groundwater recharge from river and ground surface, especially paddy fields. Paddy Water Environ 12: 163–171.

Mualem Y. 1976. A new model for predicting the hydraulic conductivity of unsaturated porous media. Water Resour Res 12: 513–522.

Nakumura S, Yudate T, Uchino H, Iwama K, Jitsuyama Y, Ichikawa S. 2007. Effect of vegetation cover ratio in maize and soybean on weed growth and crop yield: relations to planting density and varieties. Report of the Hokkaido Branch, the Japanese Society of Breeding and Hokkaido Branch, the Crop Science Society of Japan 48: 51–52 (in Japanese).

Noto F, Maruyama T, Hayase Y, Takimoto H, Nakamura K. 2013. Evaluation of water resources by snow storage using water balance and tank model method in the Tedori River basin of Japan. Paddy Water Environ 11: 113–121.

Phogat V, Yadav AK, Malik RS, Kumar S, Cox J. 2010. Simulation of salt and water movement and estimation of water productivity of rice crop irrigated with saline water. Paddy Water Environ 8: 333–346.

Satoh T. 2002. Studies on techniques for lodging prevention of rice variety “Koshihikari” based on growth diagnosis. Hokuriku Sakumotsu Gakkaiho 37: 4–9 (in Japanese).

Shibayama M, Sakamoto T, Takada E. Inoue A, Morita K, Takahashi W, Kimura A. 2011. Estimating paddy rice leaf area index with fixed point continuous observation of near infrared reflectance using a calibrated digital camera. Plant Prod Sci 14(1): 30–46.

Shimada S, Hirokawa F, Miyagawa T. 1990. Effects of planting data and planting density on a high yielding soybean cultivar grown at drained paddy field in Sanyo District. Jpn J Crop Sci 59(2): 257–264 (in Japanese with English abstract).

Šimunek J, Bradford SA. 2008. Vadose zone modeling: introduction and importance. Vadose

Zone J 7(2): 581–586.

Takeda G, Udagawa T. 1976. Ecological studies on the photosynthesis of winter cereals. III. Changes of the photosynthetic ability of various organs with growth. Jpn J Crop Sci 45(2): 357–368 (in Japanese with English abstract).

van Genuchten MTh. 1980. A closed-form equation for predicting the hydraulic conductivity of unsaturated soils. Soil Sci Soc Am J 44: 892–898.

CHAPTER 7

Numerical assessments of the impacts of climate change on regional groundwater systems

7.1 Introduction

Quantifying the impact of climate change on groundwater resources requires not only reliable forecasting of changes in major climate variables, but also adequate estimation of various factors reflecting climate change. However, for this first stage of more complicated prediction of groundwater level change, the direct impacts of climate change were focused; accordingly, land use conditions, groundwater pumping amount, and river and sea water levels, were assumed to remain unchanged.

This study presents quantitative assessments of the effects of climate change on groundwater recharge and level in a paddy field area of Japan. The goals of this study are (1) to project changes in groundwater levels under future climate variations from 2010 to 2090, including quantification of the ranges of uncertainty in groundwater level projections; (2) to investigate which meteorological factors are sensitive to groundwater levels in paddy-dominated areas.

7.2 Materials and Methods

7.2.1 Climate change scenarios

Future projections of groundwater level should be conducted under as many different GCMs as possible. The ELPIS-JP datasets (Iizumi et al., 2012) were selected because the combination of seven GCMs and three scenarios of GHG (GreenHouse Gas) emissions produced daily meteorological data; namely, air temperature, precipitation, humidity, solar radiation, and wind speed. The seven GCMs are BCCR, CGCM-T47, CGCM-T47, CGCM-T63, GISS-AOM, INMCM3, IPSL, MIROC-H, MIROC-M, and MRI and the three emission scenarios are B1,

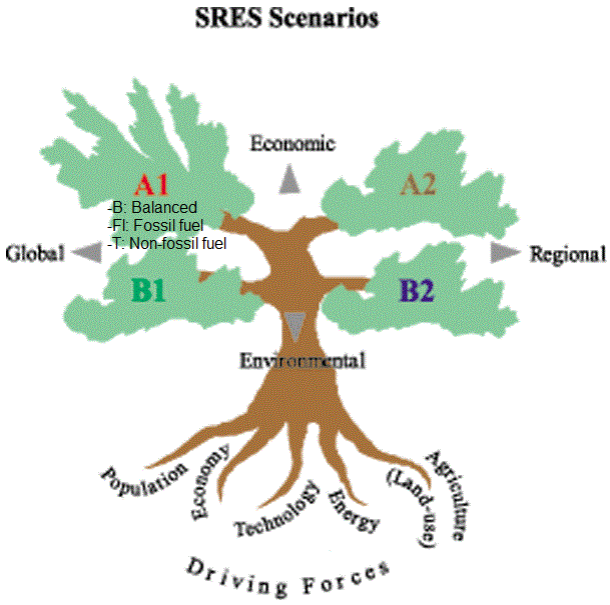

Figure 7-1 The four main families for the emission scenario. The A1 scenario develops into three groups in response to directions of technological change in the energy system (partly revised, Nakicenovic et al., 2000).

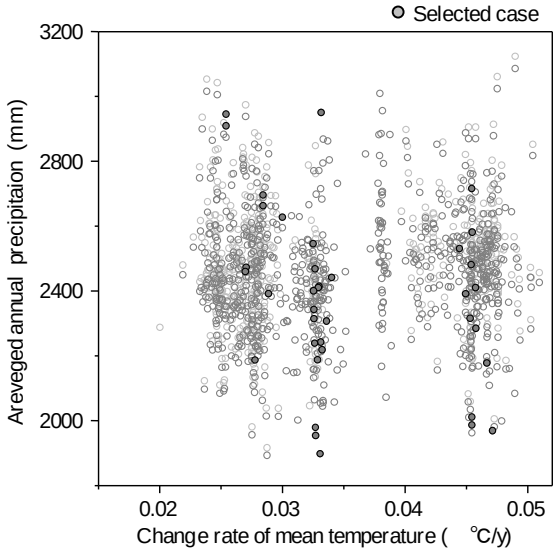

Figure 7-2 Annual precipitation averaged over 80 years and change rate of annual temperature for 1,350 cases.

A1B, and A2. Figure 7-1 outlines emission scenarios (Nakicenovic et al., 2000). The A1B scenario has alternative directions of technological change in the energy system, with a balance between fossil fuel and non-fossil fuel. The B1 scenario simulates reduction of material demand and clean and efficient technologies. Global population in this scenario is predicted to peak in

the mid-21st century and decline thereafter. The B1 and A1B scenarios were used most in the IPCC Fourth Assessment Report (IPCC, 2007). The A2 scenario is regional and economic development scenario and the global population increases slowly and comes to a peak by the end of this century (IPCC, 2007). The ELPIS-JP includes the datasets of 50 daily meteorological time-series data during 1971 to 2091 (some exceptions until 2090) for each combination of GCM and emission scenario computed using a weather generator, which enables the stochastic generation of a large number of statistically uniformly-distributed climate time series (Semenov and Stratonovitch, 2010). Computed climatic variables include the daily mean, maximum and minimum temperatures, precipitation, solar radiation, relative humidity, and wind speed. A total number of 1,350 cases (7 GCMs ×3 GHG emission scenarios × 50 generator estimations) are available for 938 sites in Japan.

To consider the various future changes in temperature and precipitation, three GCMs were selected based on the change rates of mean temperature during 2011-2090, which were estimated as follows. First, daily temperatures were averaged into annual temperatures, after which the temporal change rates were calculated as the gradient of the linear regression. The selected GCMs included BCCR by the Bjerknes Center for Climate Research in Norway (Déqué et al., 1994), IPSL by the Institute Pierre Simon Laplace in France (Houerdin et al., 2006), and MRI by the Meteorological Research Institute in Japan (Yukimoto and Noda, 2002). Four of 50 generated results (cases) for each combination of the GCM and emission scenarios were selected to ensure a broad of impacts from temperature and precipitation change based on the average annual precipitation over 80 years. Additionally, six cases generated by the combination of BCCR and A2 were selected due to having a large range of precipitation, giving 12, 12 and 14 cases for B1, A1B, and A2 scenarios, respectively. The uncertainty of climate change projections is assessed with 38 cases. Figure 7-2 shows the average annual precipitation and change rate of temperature of all 1,350 cases.

7.2.2 Model analysis

The transient state groundwater flow model, which consisted of the 1-D unsaturated water flow model (HYDRUS-1D) for estimating groundwater recharge and a 3-D groundwater flow model (MODFLOW), was developed in Chapter 6. The model reasonably simulated seasonal fluctuations and long-term changing trends in both groundwater recharge and groundwater level during 1975-2009, showing its validity for application to predictive simulation in the study area.

Main points of modification in the input data and boundary condition since the transient simulation were mentioned below.

(1) Unsaturated model

The calculation cells are classified into paddy, upland, and non-recharge cells, which have different recharge patterns. Classification is based on paddy field and upland field area ratios in each cell. Among the paddy field cells, those that are crop-rotated were randomly reconfigured in each year during 2010–2090 based on the ratio of crop-rotated paddy area (25%) under the assumption that rotation was not implemented for two consecutive years. The rest of the paddy field cells were classified as rice-planted fields. The number of cells for rice-planted, crop-rotated, upland, and non-recharge areas was 302, 101, 17, and 477, respectively. Vegetation in the upland field was set to be the same as that of the crop-rotated paddy field because the upland field area was significantly smaller than the crop-rotated paddy area. Future forecasts of groundwater level were calculated under the condition that land use area would be unchanged. However, there is fear that the discharge water amount of the Tedori River would decrease by the climate change, especially during early spring, and the possible cropping paddy field area would also decrease. The required discharge of the Tedori River for early irrigation purpose is estimated. The required irrigation water for the soil puddling is 60 mm/d, as shown in Table 6-2, and water delivery loss ratio of the irrigation concrete canal is assumed to be 10% (Watanabe, 1998). Amount of the required irrigation water for the entire the study area, in which paddy fields area ratio is 45% and the rate of paddy rice-upland crop rotation is 25%, is calculated to be 3.2×10^6 m^3/d. Noto et al. (2013) predicted that the discharge of the Tedori River in 2050 would be 4.7×10^6 m^3/d. Thus, the required irrigation water could be supplied by river water. The fact is consistent with the calculation scenario that the present land use condition does not change in the future simulations.

The upper boundary condition was forced with climate data using an atmospheric boundary condition and the lower boundary condition was free drainage, consistent with previous studies of the impact of climate change on recharge (Crosbie et al., 2013). HYRDUS-1D requires the precipitation, potential evaporation, and potential transpiration data. Snowmelt water was calculated by degree-day analysis (equation (6-6)). Noto et al., (2013) applied this model to the Tedori River basin. Daily precipitation was specified as being either rain or snow depending on the average temperature. Snowmelt water was calculated when the temperature beyond 4.5 °C and was assumed to zero when the temperature blow 4.5 °C. In Chapter 6, the simulation was carried out from 1975 to 2009 considering temporal changes in methodological elements, land use conditions, and groundwater use. Final time result provided the initial groundwater level distribution for HYDRUS-1D and MODFLOW in this future simulation. The first year (from November 2009 to October 2010) was used as the warm-up period. HYDRUS-1D was run using daily stress periods.

(2) Groundwater model

The boundary conditions were set using the same boundary conditions in the transient state simulation during 1975-2009 (6.4.1). Head-dependent boundary condition was applied to the along the Tedori River expecting for the downstream of the river. At the boundary condition, the seepage water through the river bed was calculated using the groundwater level, river water level, and riverbed conductance parameter. Constant head boundary conditions were set along the rivers (downstream of the Tedori River and the Sai River) with interpolated groundwater levels. The Sea of Japan was also applied to constant head boundary with the mean sea-level surface at Kanazawa Bay. No flow boundary condition was applied to the eastern mountain-front and the bottom of the model domain.

Groundwater uses were given over a month long period based on the distribution of the groundwater use with 1 km grid. MODFLOW was run using monthly stress periods with a daily time step. In the future prediction, groundwater use, water level of the river and groundwater, and sea as boundary conditions were kept constant during the simulated period.

7.3 Results

7.3.1 Methodological element change

Figure 7-3 shows several annual changes in precipitation, potential evapotranspiration, and mean temperature. The non-irrigation period, which is defined as the period without paddy irrigation, lasted from early September to mid-April (Table 6-2). The irrigation and non-irrigation periods were 146 and 219 days, respectively. The annual mean temperature showed an increasing trend from 2.0 to 3.9°C over 80 years. Other meteorological elements showed various changes. Figure 7-4 shows histograms of the future temporal change rates of mean temperature, precipitation during a year, precipitation during the irrigation period, precipitation during the non-irrigation period, and potential evapotranspiration at rice-planted fields for each emission scenario. The temporal change rates in temperature became progressively larger following B1, A1B, and A2. The change rate in almost of cases ranged from 0.03 to 0.05°C/y. Precipitation during the three periods would show an increasing trend rather than a decreasing trend. The temporal change rates of precipitation during a year and during the non-irrigation period ranged from -4 to 4 mm/y/y (mm/duration of non-irrigation period/y). The temporal change rate of precipitation during the irrigation period ranged from -2 to 2 mm/duration of the irrigation period/y. All cases using scenario B1 showed a temporal

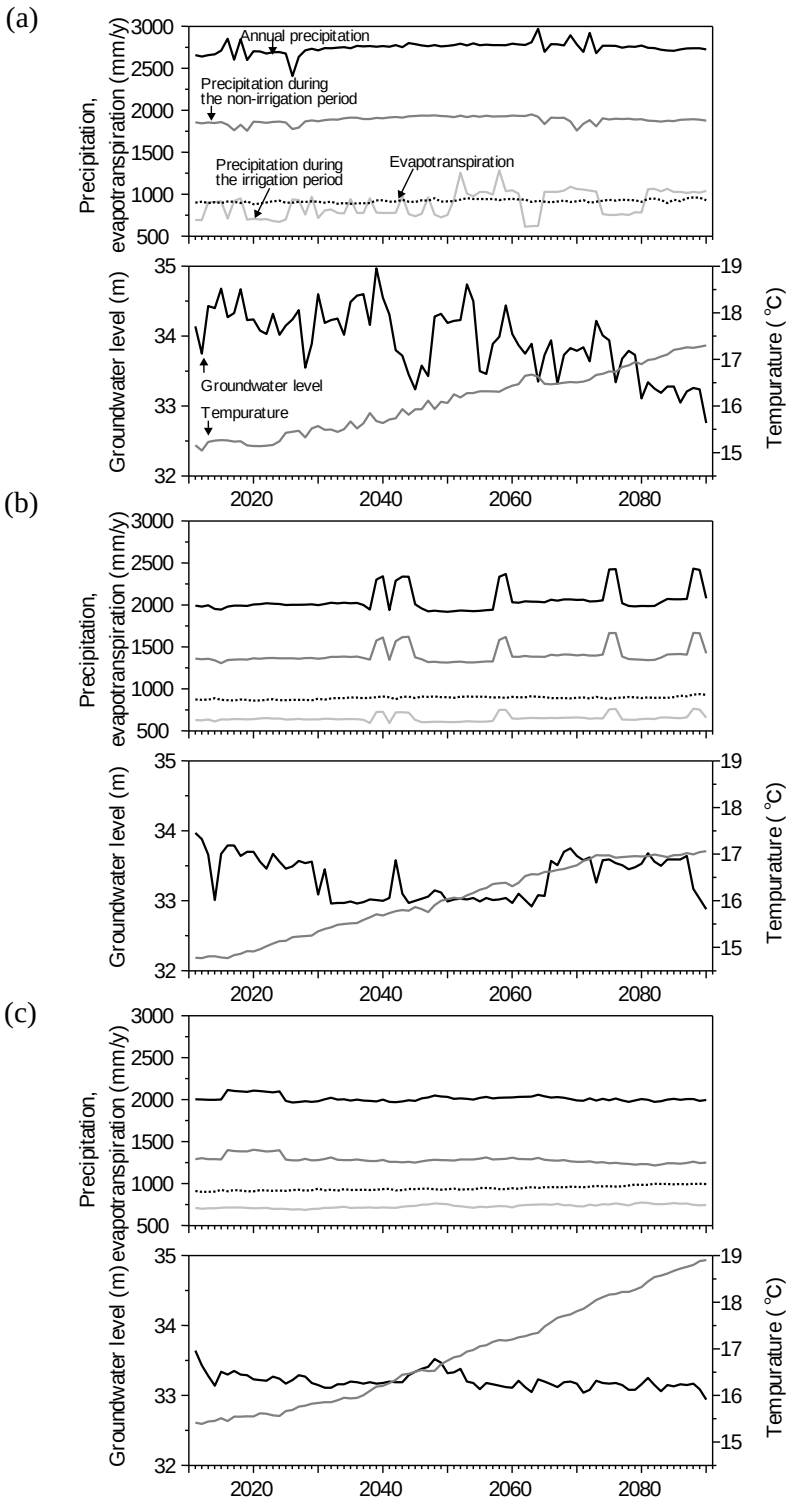

Figure 7-3 Annual changes in mean groundwater level in zone 1, mean temperature, precipitation, and potential evapotranspiration at the paddy fields from 2010 to 2090: representative case based on (a) combination of the BCCR model and A1B emission scenario, (b) a combination of the MRI model and B1 emission scenario, (c) a combination of the IPSL model and A2 emission scenario.

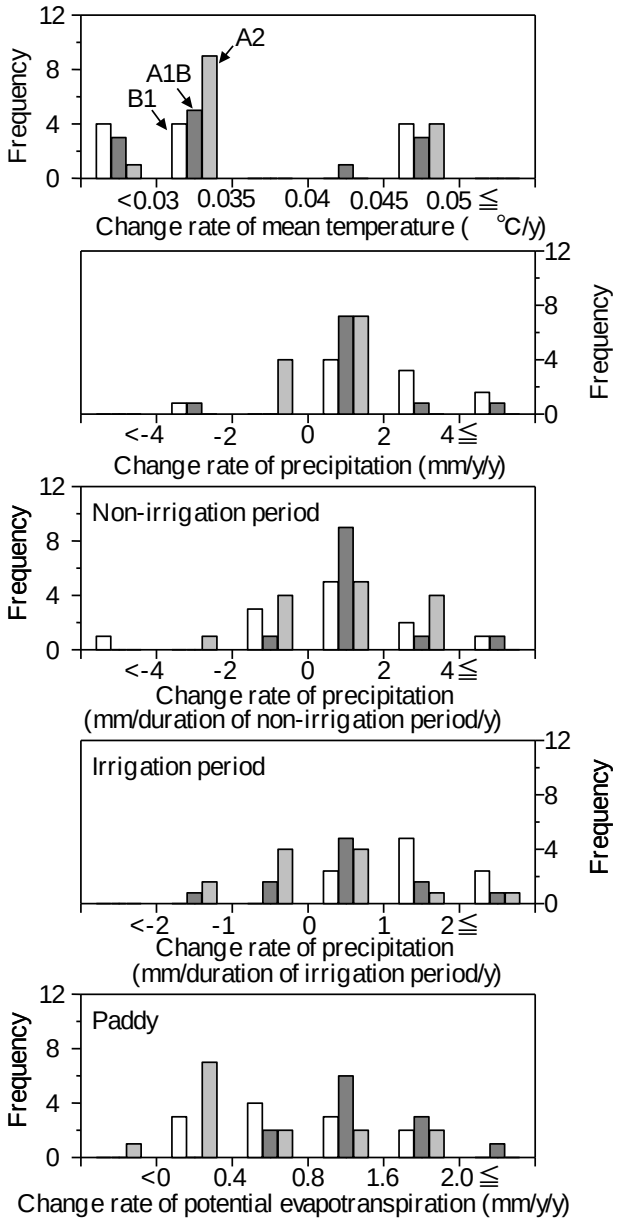

Figure 7-4 Histogram of change rate of mean temperature, precipitation, and potential evapotranspiration in paddy fields.

increasing trend of precipitation during the irrigation period. The temporal change rates of precipitation during the non-irrigation period do not show a clear characteristic of the frequency distribution among the three emission scenarios. Over 80 years, the averaged variations of precipitation based on the change rates during a year, during the irrigation period, and during the non-irrigation period were 135 mm/y (from -165 to 1092 mm/y), 50 mm (from -159 to 247 m/duration of the irrigation period), and 85 mm/duration of non-irrigation period (from -327 to 974 mm/duration of non-irrigation period), respectively. The average precipitation and standard

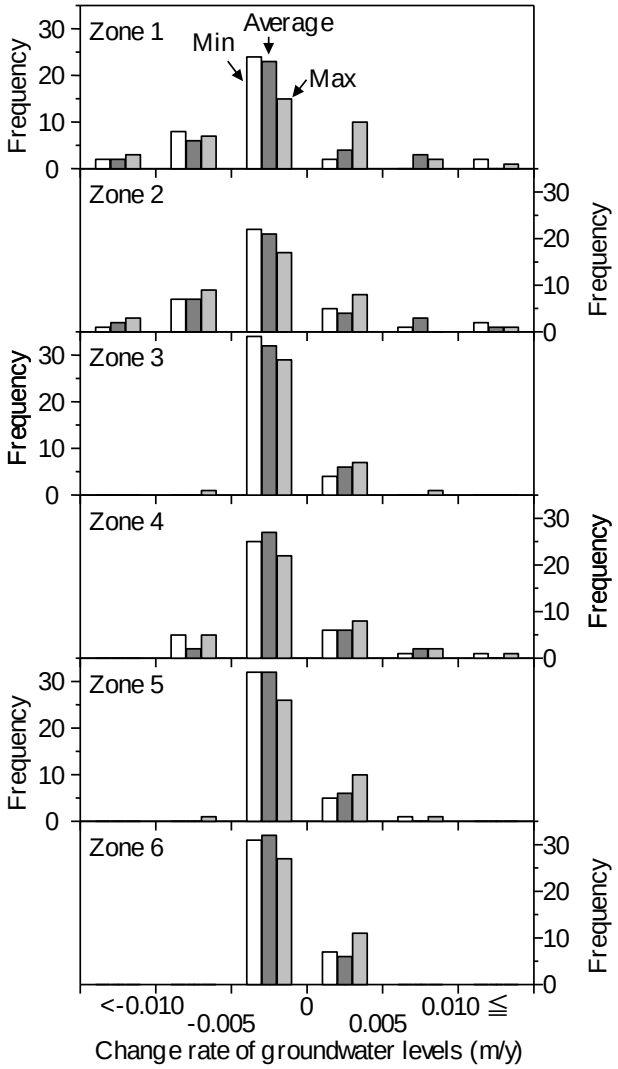

Figure 7-5 Histogram of change rate of groundwater levels (minimum, average, maximum).
*Positive (negative) values indicate increasing (decreasing) trend.

deviation from 2011 to 2020 (10 years) for three durations were 2,362±267 mm/y, 740±116 mm/duration of the irrigation period, and 622±229 mm/duration of the non-irrigation period. The temporal variations of precipitation were comparable, with approximately 10% of the amount averaged for the last 10 years. Potential evapotranspiration from paddy fields showed an increasing trend for all cases. The temporal change rate of potential evapotranspiration was mostly in the range of 0.4-2.0 mm/y/y. The predicted amount of change in the annual potential evapotranspiration at paddy fields over the 80 years was 61 mm/y (from -11 to 133 mm/y). This temporal variation was less than that of precipitation.

7.3.2 Groundwater level change

To evaluate local changes in groundwater level in the study area, the fan was divided into six zones with approximately equal areas (Figure 5-8). Simulated annual mean groundwater levels were calculated as the average of daily groundwater levels in each zone. The temporal change rates in the minimum or maximum decade-days averaged groundwater levels were also estimated. Figure 7-3 shows several annual changes in groundwater levels averaged in zone 1. The groundwater levels showed decreasing or no clear trends in response to various meteorological changes. Figure 7-5 shows histograms of the rates for each zone. The largest frequency was distributed in the range of -0.005 to 0.000 m/y for all zones, and the frequency of cases with temporal decreasing trends was larger than that of cases with increasing trends. Groundwater levels showed a seasonal pattern of fluctuation affected by paddy irrigation. Specifically, the groundwater level increased substantially at the beginning of the irrigation period before rice transplanting, remained at a high level during the irrigation period, dramatically decreased from September to October (after the irrigation period), and then fluctuated in response to precipitation, snowfall, and snowmelt from November to April. The minimum groundwater levels were predicted during snowmelt season or before the irrigation period (April or May). Maximum groundwater levels were primarily predicted during the irrigation period (August or September). The temporal change rate of the maximum groundwater level showed increasing trends in all six zones in most cases, while that of the average groundwater level showed a slight decreasing trend. Absolute values of the change rates in zones 1 and 2 were larger than those of the others because the recharge area for zones 1 and 2 is relatively small. The groundwater catchment area is limited in the upper and middle areas of the fan relative to the lower area. The greatest rates of decrease of minimum, average, and maximum groundwater levels in zones 1 and 2 were -0.013 m/y, -0.014 m/y, and -0.016 m/y, respectively. Over 80 years, the largest minimum, average, and maximum groundwater drawdowns in zone 1 were -1.0 m, -1.1 m, and -1.3 m, respectively.

7.4 Discussions

The annual net water balances were calculated from 2011 to 2020 (10 years) for the cases with the three greatest increasing rates of groundwater level and the three greatest decreasing rates among the 38 total cases. The Tedori River and the groundwater surface boundary were the net inflow sources, and their rates to the total net inflow were 64±2% and 35±2%, respectively. The net outflow boundaries were the Japan Sea and Sai River and groundwater use by pumping was the outflow source. The rate of sea and the Sai River to the total net outflow was 36±1%, while

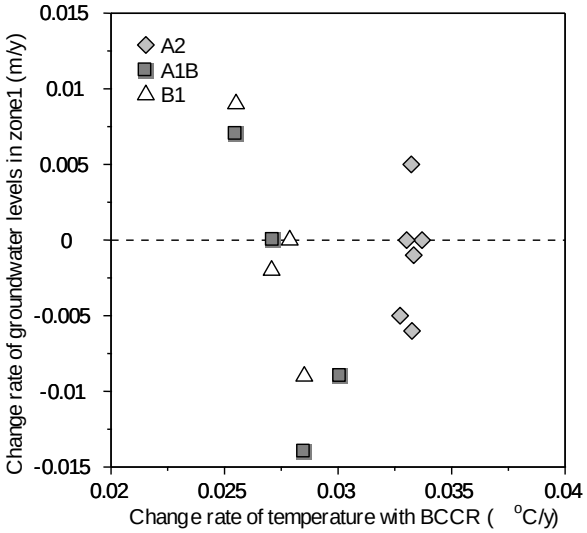

Figure 7-6 Change rate of annual groundwater levels averaged in zone 1 and change rate of annual temperature (BCCR).

Table 7-1 Correlation coefficients between change rate of groundwater level in each zone and each meteorological element.

Meteorological element		Zone 1	Zone 2	Zone 3	Zone 4	Zone 5	Zone 6	Ave.
Change rate of mean temperature (°C/y)		0.19	0.20	0.16	0.21	0.19	0.19	0.19
Change rate of precipitation	whole year (mm/y/y)	0.56	0.63	0.54	0.67	0.62	0.62	0.61
	non-irrigation period (mm/duration of non-irrigation/y)	0.66	0.82	0.64	0.74	0.71	0.70	0.69
	irrigation period (mm/duration of irrigation/y)	-0.16	-0.11	-0.17	-0.07	-0.12	-0.12	-0.13
Rate of change in days of precipitation within range (d/duration of non-irrigation /y)	< 10 mm/d	-0.59	-0.62	-0.57	-0.63	-0.61	-0.61	-0.61
	10 - 20 mm/d	0.19	0.18	0.18	0.17	0.17	0.17	0.18
	20 - 30 mm/d	0.36	0.36	0.34	0.36	0.36	0.36	0.36
	30 - 40 mm/d	0.16	0.18	0.17	0.18	0.18	0.17	0.17
	40 ≤ mm/d	0.19	0.24	0.20	0.26	0.24	0.23	0.23

that to groundwater use was 64±2%. During the irrigation period per unit recharge area (520 cells), the groundwater recharges for the six cases were estimated to be 1,423±142 mm/y and 797±69 mm/duration of the irrigation period, respectively. Although the groundwater recharge was mainly fed by paddy irrigation water, the influence of predicted variations in annual precipitation (135 mm/y) was not negligible.

Simulation of groundwater levels from 1975 to 2009 considering temporal changes in methodological elements, land use conditions, and groundwater use revealed a change rate in zone 1 of -0.07 m/y (6.5.1). The change rates obtained in this study (Figure 7-6) were smaller than -0.07 m/y; however, the results of the present study do not cover future variations in artificial factors such as changes in paddy field area or groundwater use.

The sensitivities of groundwater level to the meteorological elements were examined. The meteorological elements were mean annual temperature, as well as precipitation during a year, during the irrigation period, during the non-irrigation period, and on days in which there were 0-10, 10-20, 30-40, and above 40 mm/d precipitation. The correlation coefficients among these factors are listed in Table 7-1. The correlation between the change rate of mean temperature and that of groundwater level was low. Figure 7-6 shows the relationship between the change rate of the average groundwater levels in zone 1 and that of the annual temperature obtained with the BCCR. All emission scenarios revealed no relationship between change rates of annual groundwater levels and change rates of annual temperature and that the temporal change rate of groundwater level was independent of changes in annual temperature. The correlation coefficient between the change rate of groundwater level and that of precipitation during the non-irrigation period was highest. The relationship to the change rate of precipitation days on which there was less than 10 mm precipitation/d showed a negative relationship and a relatively high correlation coefficient. This was likely because there was a highly negative relationship between the change rate of precipitation during the non-irrigation period and that of days on which there was less than 10 mm precipitation/d ($R = 0.83$), demonstrating that days with less than 10 mm/d precipitation would increase when precipitation during the non-irrigation period decreased. As shown in Table 7-1, the change rate of days of 10－20, 20－30, and above 40 mm precipitation/d was not related to that of groundwater level as shown in Table 7-1. Thus, variations in relatively high-intensity precipitation days have little effect on groundwater level.

This study predicted that the maximum decrease in groundwater level was about 1 m based on the predicted variation in precipitation, which was 135 mm/y (from -165 to 1092 mm/y). These findings indicate that climate change would have a slight effect on groundwater levels if the cultivated paddy field area did not change. However, Noto et al. (2013) simulated the effects of climate change on water resources stored as snow using a RCM (Regional Climate

Model) and found that a shortage of irrigation water during the paddy puddling period would occur. Furthermore, they predicted that it would be impossible to cultivate paddies using currently employed practices under climate change effects. Accordingly, it is necessary to evaluate the impact of climate change on groundwater level while taking into account changes in paddy irrigation practices when conducting modeling.

7.5 Conclusions

This study was conducted to assess the impacts of climate change on groundwater level in an alluvial fan containing high areas of irrigated paddy fields. To accomplish this, the response of the groundwater level to predicted climate change based on multi GCMs and GHG emission scenarios was simulated using a coupled model of a 1-D unsaturated water flow model (HYDURS-1D) to estimate groundwater recharge and a 3-D groundwater flow model (MODFLOW). Noticeable results in response to climate change and simulated groundwater levels during 2010 to 2090 are as follows:

1) From the predicted results of the ELPIS-JP data sets, the amount of precipitation has changed over 80 years in the range of -165 to 1092 mm/y (mean 135mm/y) in response to temperature increases of 2.0°C to 3.9°C.

2) Simulation results revealed that groundwater levels would have both decreasing and increasing trends in response to climate changes. The frequency of decreasing trends would be larger than that of increasing trends. The predicted maximum drawdown of the groundwater level during 2010-2090 was approximately 1 m, and the groundwater level was the most sensitive to changes in the amount of precipitation during the non-irrigation period. The change rate of days with precipitation at levels of 10－20, 20－30 and above 40 mm/d had little relationship to that of groundwater levels.

References

Déqué M, Dreveten C, Braun A, Cariolle D. 1994. The ARPEGE/IFS atmosphere model: acontribution to the French community climate model. Clim Dyn 10: 249-266.

Hourdin F, Musat I, Bony S, Braconnot P, Codron F, Dufresne JL, Fairhead L, Filiberti MA, Friedlingstein P, Grandpeix JY, Krinner G, Levan P, Li ZX, Lott F. 2006. The LMDZ4 general circulation model: climate performance and sensitivity to parameterized physics with emphasis on tropical convection. Clim Dyn 27: 787–813.

Intergovernmental Panel on Climate Change (IPCC). 2007. Climate change 2007: the Physical Science Basis. Cambridge University Press, Cambridge.

Iizumi T, Semenov MA, Nishimori M, Ishigooka Y. Kuwagata T. 2012. ELPIS-JP: a dataset of local-scale daily climate change scenarios for Japan. PhilTrans R Soc A 370: 1121-1139.

Nakicenovic N, Alcamo J, Davis J, de Vries B, Fenhann J, Gaffin S, Gregory K, Grübler A, Jung TY, Kram T, La Rovere El, Michaelis L, Mori S, Morita T, Pepper W, Pitcher H, Price L, Riahi K, Roehrl A, Rogner H, Sankovski A, Schlesinger M, Shukla P, Smith S, Swart R, van Rooijen S, Victor N, Dadi Z. 2000. Special Report on Emissions Scenarios: A Special Report of Working Group III of the Intergovernmental Panel on Climate Change. Cambridge University Press, Cambridge. http://www.grida.no/climate/ipcc/emission/index.htm.

Noto F, Maruyama T, Hayase Y, Takimoto H, Nakamura K. 2013. Prediction of water resources as snow storage under climate change in the Tedori River basin of Japan. Paddy Water Environ 11: 463-471.

Semenov MA, Stratonovitch P (2010) Use of multi-model ensembles from global climate models for impact assessments of climate change. Clim Res 41: 1-14.

Yukimoto S, Noda A. 2002. CGCR Supercomputer Activity Report, No.10. National Institute for Environmental Studies, Tsukuba.

Watanabe T .1998. Paddy irrigation. In: Maruyama T and Nakamura R (ed) Water utilization - environmental engineering. Asakura Publishing Co., Ltd, pp. 58-74 (in Japanese).

CHAPTER 8

Evaluation of river and paddy water impacts on groundwater using water and Sr isotopes

8.1 Introduction

In the study area, some researchers have examined the interactions between groundwater and river water; studies have focused on both river water infiltration to groundwater, and groundwater flow to the river through hydrological observations (Futamata et al., 2005; Morita et al., 2008; Tsujimoto et al., 2005; this study). Maruyama et al. (2012; 2014) estimated the water balance in the area. Ishida and Tsuchihara (2013) investigated the river water contribution ratios to shallow groundwater by end member mixing analysis based on oxygen and hydrogen isotopes, and the age of shallow and deep groundwater using tritium. Hayase (2013) pointed out that a large amount of snowmelt runoff contributed to low concentrations of nitrogen in groundwater, and that paddy irrigation water had little effect on the nitrogen concentration in groundwater. Yonebayashi and Minami (2013) examined groundwater quality using cluster analysis and a nitrogen isotope. They reported that domestic sewage and livestock wastewater had little effect on groundwater quality, and groundwater quality in the fan was categorized spatially by the cluster analysis, which were similar to the geographic divisions. The steady state and transient state numerical flow simulations developed based on observed groundwater level contour maps and the measured water flow between groundwater and the river. However, groundwater flow paths and the validity of the model simulated results remain unclear.

The objectives of this study were: (1) to identify characteristics of groundwater recharge and groundwater flow paths in the shallow aquifer using multiple water quality indicators, and (2) to confirm the consistency between hydrolochemical observations and the hydrological observations, and numerical flow simulations conducted in the study area.

8.2 Multi tracer observation

8.2.1 Sampling method

Water quality measurements were carried out in June of 2011 during the irrigation period. Figure 8-1 shows the locations of the sampling points. The number of samples of groundwater, spring water, river water, and paddy ponding water were 63, 2, 13, and 5, respectively. Groundwater samples were obtained from wells owned by public and private sectors.

River water samples were collected from the Tedori River and the Sai River, including some branches in lowland and hinterland areas of the basin. According to the strainer depths of sampling wells and borehole geological data (Hokuriku Regional Agricultural Administration Office, 1977), 48 and 4 groundwater samples were obtained from the shallow aquifer and from the deep aquifer, respectively. 11 samples were not classified because of lack of information about the wells.

8.2.2 Water quality analysis

Water temperature and EC were measured on site. Major cation (K^+, Ca^{2+}, Mg^{2+}, and K^+) and anion (SO_4^{2-} and Cl^-) concentrations, NO_3^--N, and NO_2^--N were analyzed in the laboratory by

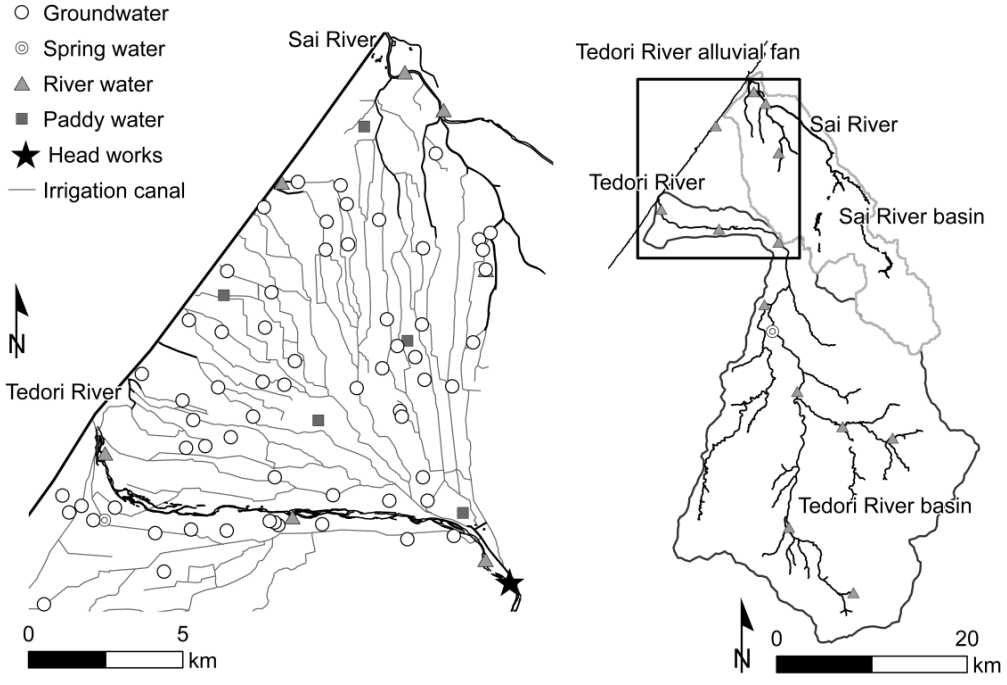

(a) (b)

Figure 8-1 Maps of the locations of water sample sites in (a) the Tedori River alluvial fan, and (b) the Tedori River Basin.

ion chromatography (LC-10A, Shimadzu Corp., Japan). According to Nakano et al. (2008), the HNO_3 concentration was determined in terms of the difference between the total equivalent concentrations of cations and anions. A large number of elements (Cd, Cr, Se, Pb, As, B, Zn, Al, Fe, Cu, Mn, Sb, Ni, Ba, Mo, Li, Sr) were determined by ICP-MS (7500cx, Agilent Technologies, USA). The δD and $\delta^{18}O$ values were determined using a water isotope Analyzer (L2120-I, Picarro Inc., USA). The δD and $\delta^{18}O$ values were determined relative to internal standards that were calibrated using Vienna-Standard Mean Ocean Water (V-SMOW). It is convenient and common to multiply the δ values by 1000 to express the values as ‰ difference from the standard being used. The $^{87}Sr/^{86}Sr$ ratios were analyzed by a thermal ionization mass spectrometer (TRITON, Thermo Fisher Scientific Inc., USA).

8.3 Results and Discussions

8.3.1 Isotopes of water

The δD and $\delta^{18}O$ values ranged between -68.0‰ and -24.5‰ and between -11.1‰ and -2.9‰, respectively. The mean $\delta^{18}O$ values for shallow groundwater, Tedori River water including the upper stream, Sai River water, and paddy water were -9.28‰, -10.55‰, -9.53‰, -4.56‰, respectively. The mean δD values for the shallow groundwater, Tedori River water, Sai River water, and paddy water were -53.2‰, -61.57‰, -54.1‰, -33.8‰, respectively. Figure 8-2 shows δD and $\delta^{18}O$ in the shallow groundwater, river water, spring water, paddy water, and precipitation. The weighted mean (weighing by the amount of precipitation) of $\delta^{18}O$ and δD for precipitation water, which was collected in the fan, were -8.07‰ and -43.94‰ (Ishida and Tsuchihara, 2013). The δD and $\delta^{18}O$ values of paddy water were larger than in the other waters because of the strong effect of evaporation on paddy water (Komiya et al., 2003; Mizutani et al., 2001). Figure 8-3(a) shows the spatial distribution of $\delta^{18}O$ in the shallow water and $\delta^{18}O$ values for river water and paddy water. The $\delta^{18}O$ values of groundwater near the Tedori River are lower than those near the northeastern part of the fan. The isotopic values of river water were lower than those of precipitation (-8.07‰) because of the elevation effect on the isotopes. The $\delta^{18}O$ averages of Tedori River water and Sai River water are -10.55‰ and -9.53‰ respectively. The mean $\delta^{18}O$ value for the Tedori River is lower than that of Sai River in the fan because the catchment area of the Tedori River includes high-elevation areas. Spatial distribution of the $\delta^{18}O$ of groundwater shows that inflow water from the Tedori River to shallow groundwater strongly influences groundwater qualities. A similar distribution was observed for the δD values.

The result of linear regression analysis suggests a clear correlation between δD and$\delta^{18}O$ (the correlation coefficients were larger than 0.97), and the slopes of the regression

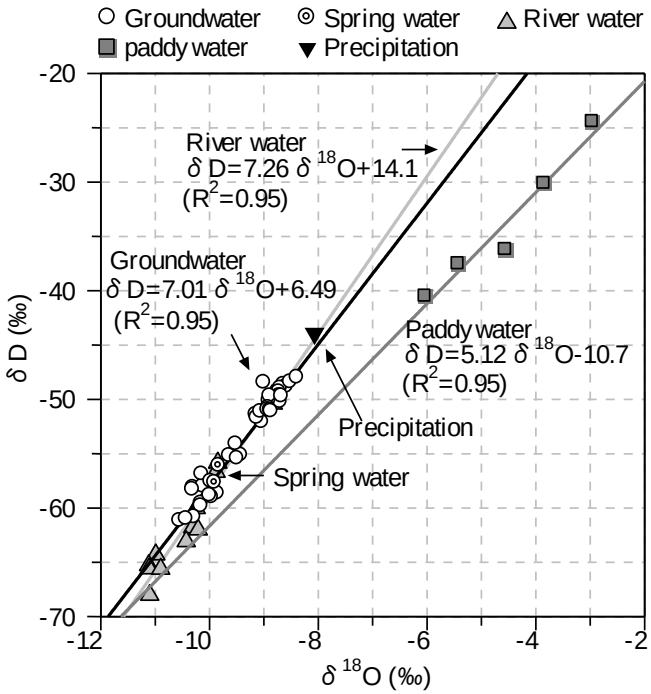

Figure 8-2 The relationship between δD and $\delta^{18}O$ in shallow groundwater, spring water, river water, and paddy water.

Note: Precipitation values were obtained from Ishida and Tsuchihara (2013).

lines are 7.01, 7.26 and 5.12 for the shallow groundwater, river water, and paddy water, respectively (Figure 8-2). The local meteoric water line (LMWL), which was reported by Ishida and Tsuchihara (2013), was $\delta D=8.05\delta^{18}O+19.52$. The slopes are smaller than the slope of the LMWL. Furthermore, the paddy water samples were plotted almost linearly. This line is regarded as the evaporation line (EL). This indicates the influence of evaporation on paddy water. Furthermore, almost all shallow groundwater samples were plotted in a line between the values for the river water and the weighted mean precipitation. Such a trend suggests that river water and precipitation contribute more to groundwater recharge than does paddy water. The area of irrigated paddy fields (33% of the total area in 2009) has been decreasing in recent years because of urbanization, an increase in the area of fallow fields, and the use of a rice-upland crop rotation system (the ratio of crop-rotated paddy tot the total paddy field area was 25% in 2009). This decrease in the area of rice-planted paddy fields is partly responsible for the lower contribution of paddy water to groundwater recharge.

Deuterium excess values (d-excess) were calculated as d-excess=$\delta D-8\delta^{18}O$. The d-excess values in the shallow groundwater decreased with distance from the Tedori River, and ranged from 24.2‰, to 19.1‰. The d-excess values in the Tedori River, the Sai River, and precipitation were 22.7‰, 22.1‰ 20.6‰, respectively. Lin and Yamanaka (2012) suggested

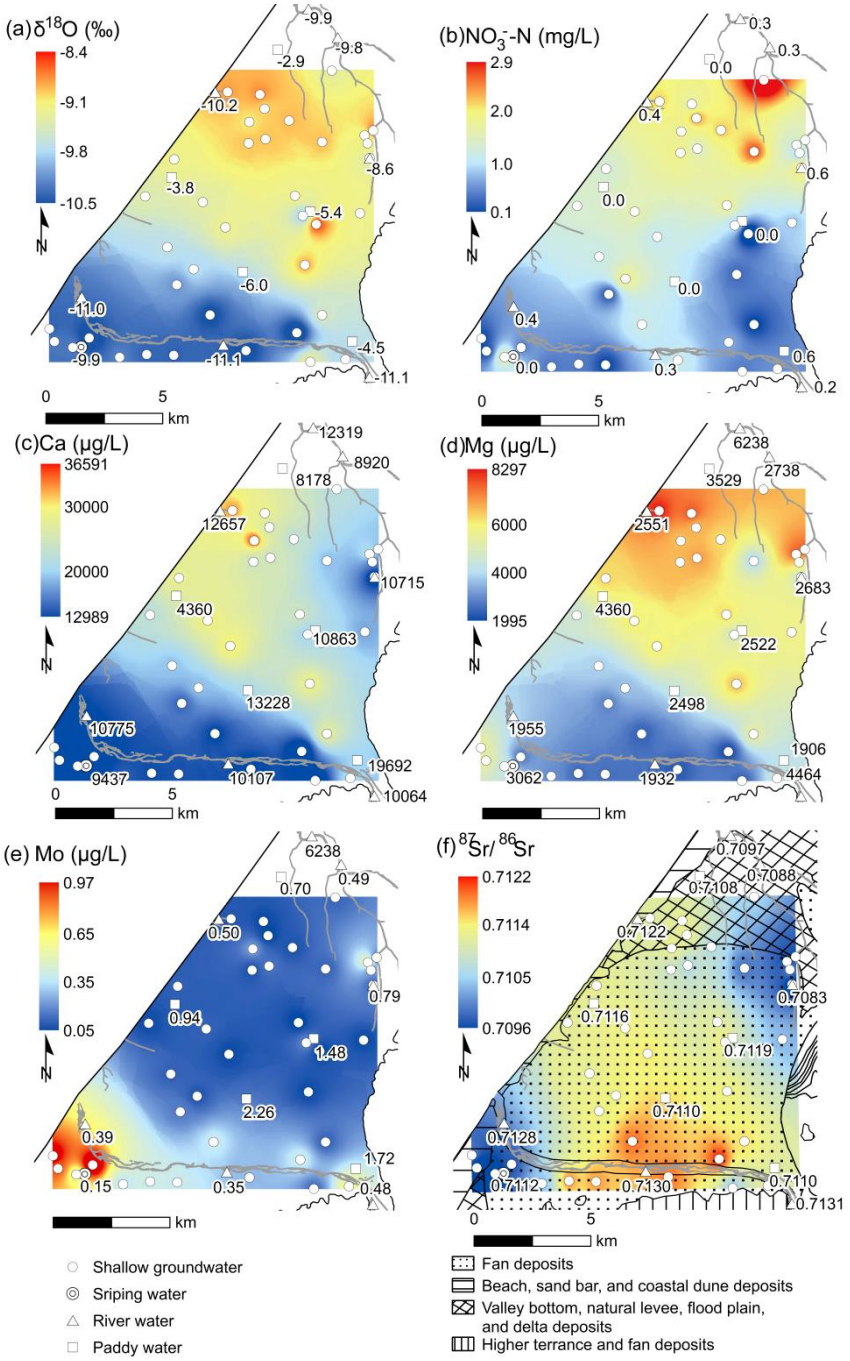

Figure 8-3. Spatial distribution of multiple tracers in the shallow groundwater: (a) $\delta^{18}O$, (b) NO_3^--N, (c) Ca, (d) Mg, (e) Mo, and (f) $^{87}Sr/^{86}Sr$ ratio.

Note 1:Circle, double circle, triangle, and square represent the sampling points for groundwater, spring water, river water, and paddy water, respectively.

Note 2: The values in the figures represent the concentrations present in the spring water, the river water, and the paddy water.

Note 3: The surface geology (Geological Survey of Japan, AIST (ed.), 2012) is shown in (f).

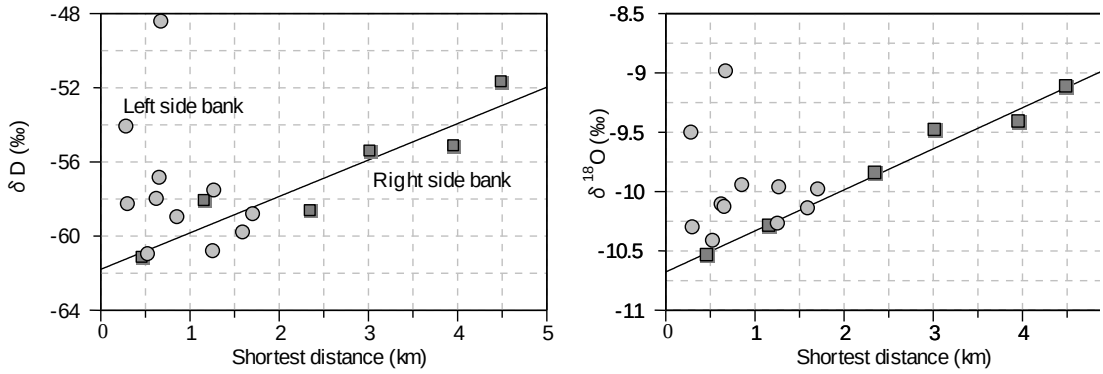

Figure 8-4 Relationship between δD and $\delta^{18}O$, and the shortest distance from the Tedori River to the groundwater sampling point.

that the d-excess value in paddy water decreases in response to evaporation. The changes in d-excess of shallow groundwater with distance from the Tedori River is therefore supported influenced by mainly river water seepage and precipitation infiltration, and by partly paddy water infiltration.

Liu and Yamanaka (2012) demonstrated that factors controlling the contribution ratio to groundwater were the distance from the river, the topographic gradient, and geological conditions. Figure 8-4 shows the relationship between the δD and $\delta^{18}O$ values, and the shortest distance between the groundwater sampling point and the Tedori River. There are positive linear relationships at the right bank within 5 km of the river for both δD and $\delta^{18}O$ (correlation coefficients were 0.93 and 0.99, respectively). However, a clear relationship was not observed at the left bank. It is considered that the contribution of river seepage water flow to the right bank was higher than to the left bank.

The δD - $\delta^{18}O$ diagram (Figure 8-2) shows that the river water and precipitation provides more recharge to the groundwater than does the paddy water. According to the net water balance analysis based on the transient unsaturated/saturated water flow simulation, with MODFLOW and HYDRUS-1D (6.5.3), both the Tedori River and the paddy water were net inflow sources. The proportions of the groundwater recharges from the river water, from the rice-planted (irrigated) paddy field during the irrigation period, and from the rice-planted paddy field during the non-irrigation period and upland field including crop-rotated paddy field to the total net inflow to groundwater were approximately 41%, 35%, and 24%, respectively, in recent 10 years. It was concluded that the recharge from the river water and precipitation at agricultural fields except for the irrigated paddy field have more influence to groundwater than that of the irrigated paddy field quantitatively. The recharge water from the rice-planted paddy field during the non-irrigation period and from upland field is considered to have similar δD and $\delta^{18}O$ values to precipitation (Figure 8-2). Thus, the result of water balance analysis was consistent with the

δD - $\delta^{18}O$ diagram characteristic of the groundwater, river water, paddy water, and precipitation.

8.3.2 Dissolved ions and multi-element concentrations

Water isotopes and water balance analysis with the numerical simulations revealed that the river water and precipitation provides more recharge to the groundwater than does the paddy water. In this section, the estimated result is confirmed based on the distribution characteristics of the dissolved ions and multi-element concentrations. Figure 8-5 depicts stiff diagrams of the groundwater, river water, and paddy water in the fan. Most of the shapes of the stiff diagrams are classified as the Ca-HCO_3 type. The Ca-HCO_3 type is generally regarded as shallow groundwater that has been not polluted. Dissolved substances are relatively low in the river waters except for the site in the downstream section of the Sai River. A comparison of the Stiff diagrams of the groundwater at the right and left banks of the Tedori River indicates that concentrations of dissolved substances in groundwater in the left bank are lower than those of the right bank. Except for the groundwater in left bank be located near the Tedori River, the stiff diagrams in the shallow groundwater become Ca - HCO_3 richer than that of the river water. The dissolved substances in precipitation is generally regarded as the lower than that of river water. These results suggested that the groundwater was affected by water of different origin from the Tedori River water and precipitation.

Figure 8-3 (b), (c), (d), and (e) show spatial distributions of NO_3^--N, Ca, Mg, and Mo concentrations in the shallow groundwater. The distributions of the dissolved ions and multiple elements in shallow groundwater samples can be divided into 3 groups as follows:

(1) Relatively low concentration of Cl^-, SO_4^{2-}, NO_3^--N, NH_4-N, Mg, and Na occurred near the Tedori River and relatively high concentrations occurred around the upper area of the Sai River.

Inflow from the Tedori River to groundwater caused a significant decrease in the concentrations of the above elements in shallow groundwater along the Tedori River through dilution.

(2) Relatively low concentrations of Ca, Ba, Sr, Se, Li occurred near the Tedori River and the northeastern part of the fan, and higher concentrations occurred around the center of the fan where the paddy field area was relatively large.

Inflow water and infiltration water from the paddy fields affected the spatial distributions of groundwater qualities.

(3) Relatively high concentrations of B, Sb, and Mo occurred near the Tedori River.

The distributions of the other elements (K^+, As, Mn, Ni, Cr, Pb, Zn, Cu, and Fe) do not show clear spatial distributions. NO_2^--N was not detected in almost all of the groundwater samples and was not detected in any paddy waters. The NO_2^--N concentrations in some river

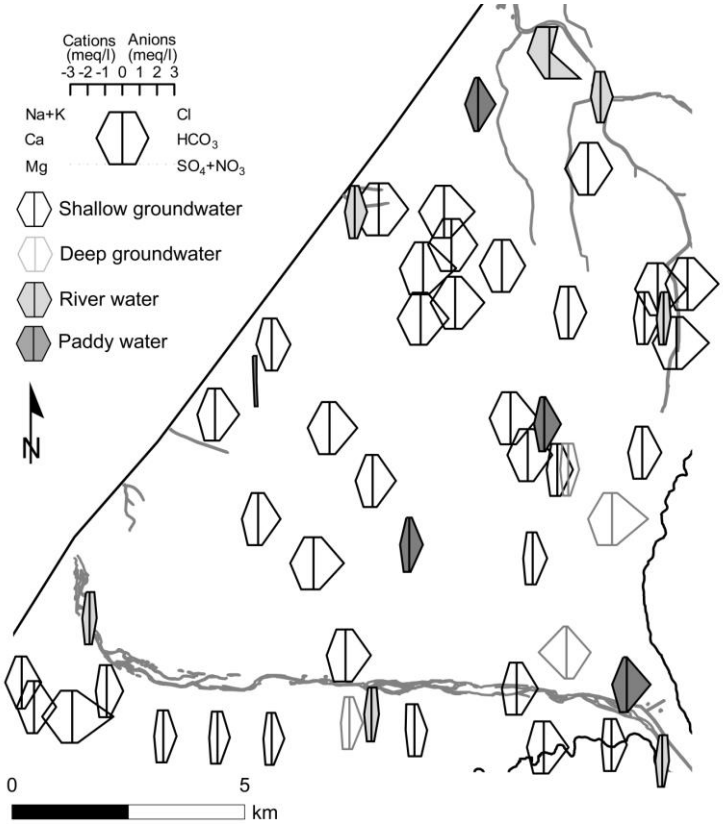

Figure 8-5 Stiff diagrams of shallow groundwater, deep groundwater, river water, and paddy water.

Note: The black line, light gray line, black line inside light gray, and black line inside dark gray represent the shallow groundwater, the deep groundwater, the river water, and the paddy water, respectively.

water samples were less than 0.56 mg/l. The maximum NO_3^--N concentration in groundwater was 2.92 mg/l in the northeast urban area. Yonebayashi and Minami (2013) reported that NO_3^--N concentrations in groundwater near the Tedori River were affected by the nutrient load from agriculture.

8.3.3 Isotopes of strontium

The $^{87}Sr/^{86}Sr$ ratios in all water samples ranged from 0.7083 to 0.7172 while the ratios in the shallow groundwater ranged from 0.7087 to 0.7122. The concentrations of Ca and Mg were positively correlated with Sr (correlation coefficients were 0.97 and 0.77, respectively). These correlations suggest that the three elements have a similar origin (rocks) (Nakano et al., 2008). The Sr concentration in shallow groundwater increased as a result of elution from the soil that occurs with agricultural activities (Hosono et al., 2007). Figure 8-3(f) shows the spatial

distribution of $^{87}Sr/^{86}Sr$ ratios in shallow groundwater, river waters, and paddy water. The surface geology distribution is also illustrated in the figure. The lower ratios of shallow groundwater are observed in the downstream section of the Tedori River and the northeastern parts of the fan. This distribution slightly is reflected by the local geology in the downstream of the Tedori River and the Sai River water in the northeastern parts of the fan. The ratios ranged from 0.7085 to 0.7172 in the Tedori River and from 0.7083 to 0.7097 for the Sai River. The $^{87}Sr/^{86}Sr$ ratios in the Tedori River water were comparatively high, depending on older geological features at the upper basin. The $^{87}Sr/^{86}Sr$ ratio of upper spring water (elevation 196 m) was 0.7106; the $^{87}Sr/^{86}Sr$ ratio of this water is generally regarded to reflect little interaction with the aquifer rocks because of the relatively short residence time of the water. The $^{87}Sr/^{86}Sr$ ratios in the paddy water ranged from 0.7108 to 0.7118, which were relatively low. The $^{87}Sr/^{86}Sr$ ratios of shallow groundwater decrease slightly with distance from the Tedori River. Additionally, the distributions indicate that the river seepage water, which mainly occurred in the middle sections of the Tedori River, flowed to the northwest towards the coastal area in the center of the fan, and there was little seepage water in the downstream section of the Tedori River. Spatial distributions of ion and element concentrations and δD, and $\delta^{18}O$ values in groundwater (Figure 8-3 (a)), cannot be used as indicators of seepage water flow from the Tedori River to groundwater. Information on the groundwater flow paths was successfully gained from the observed $^{87}Sr/^{86}Sr$ ratios.

Figure 8-6 shows the relationship between $^{87}Sr/^{86}Sr$ ratios and 1/Sr values of the shallow groundwater of the right side bank (in near the Sai River, in center of the fan, and in near the Tedori River), the Tedori river water, and paddy water. From the Tedori River, and from the Sai River, to the center of the fan, the Sr concentrations in the shallow groundwater become linearly larger with flow distance and the $^{87}Sr/^{86}Sr$ ratios converge to close range of values (0.711－0.712) (see dash lines in Figure 8-6). The increasing trend of Sr concentration indicated the Sr concentrations were affected by the eluviation from of Sr from the soil, which comes from the geological origin (fan deposits). The close range of $^{87}Sr/^{86}Sr$ ratio values revealed that the $^{87}Sr/^{86}Sr$ ratios, of the fan deposits in the study area, have in the range of 0.711－0.712. The $^{87}Sr/^{86}Sr$ ratios in the paddy water also show the similar range values. It was inferred that the eluviation from the geology was encouraged by the agricultural activities including the cation exchange reaction at the paddy field and the $^{87}Sr/^{86}Sr$ ratios in the paddy water therefore reflect that of the fan deposits-origin. Furthermore, the $^{87}Sr/^{86}Sr$ ratios in the paddy water were lower than in the Tedori River water. Hosono et al. (2007) reported that $^{87}Sr/^{86}Sr$ ratios of basal and supplemental fertilizers used in Shiga Prefecture, Japan, ranged between 0.708 and 0.7102. Therefore, it is possible that the $^{87}Sr/^{86}Sr$ ratios in paddy water may be lower partly because of the use of fertilizers. Consequently, the distribution characteristics of $^{87}Sr/^{86}Sr$ ratios in the

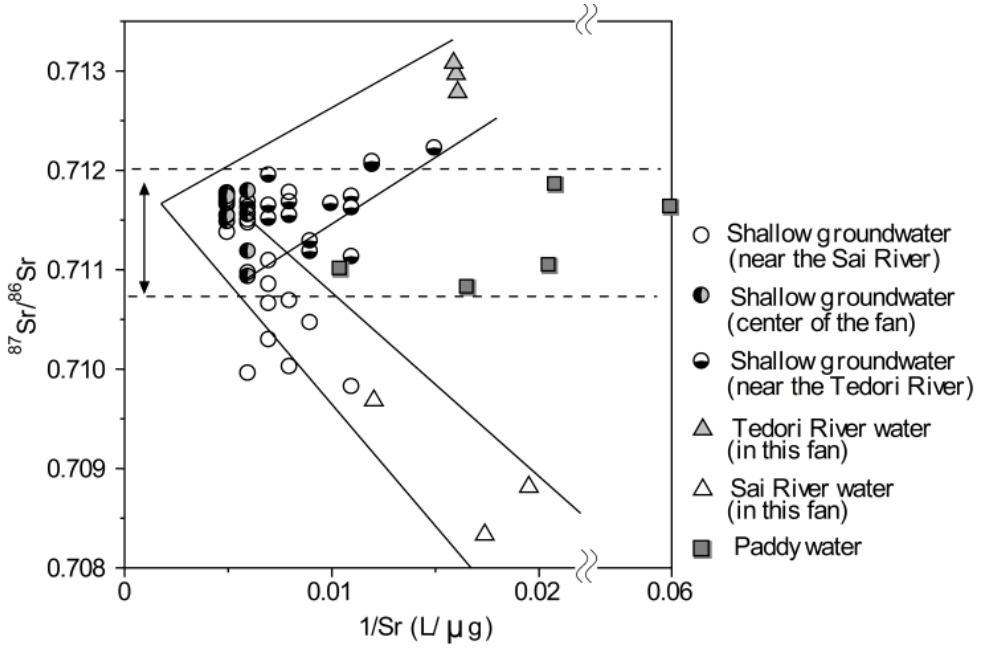

Figure 8-6 Relationship between $^{87}Sr/^{86}Sr$ ratio and 1/Sr of shallow groundwater in the right side, Tedori River water in the fan, the Sai River in the fan, and paddy water.

shallow groundwater could be mainly explained by the mixing process with $^{87}Sr/^{86}Sr$ derived from river waters (the Tedori River and the Sai River) and that of derived from the fan deposits-origin.

8.3.4 River water-groundwater interaction

In this section, we examine the consistency with the hydrochemical observation and several hydrological observation results. To determine water-groundwater exchange volumes in the Tedori River, river flow amounts and inflow amounts entering the river were measured (3.5). The net exchange water volume between groundwater and the Tedori River per km along the river during the irrigation period in 2009 is shown in Figure 3-13(a). Groundwater flowed to the river in the downstream section located between 1.1 km and 2.2 km from the river mouth, and in the section located between 11.8 km and 14.3 km from the river mouth. Seepage water recharged to the groundwater in the sections located between 2.2 km and 11.8 km and between 14.3 km to 16.4 km from the river mouth. Total inflow from the river to groundwater was 4.1×10^6 m^3/d and total outflow from groundwater to the river was 1.1×10^6 m^3/d during the irrigation period. A substantial amount of water flow from the river to groundwater was observed in the section located between 2.2 km and 8.0 km from the river mouth. These results

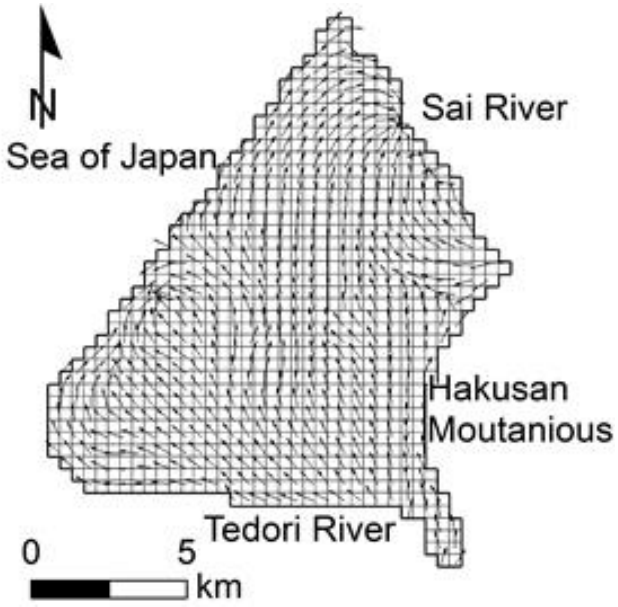

Figure 8-7 Steady-state simulated groundwater flow directions during the irrigation period.

mostly agreed with the groundwater flow path near the Tedori River estimated with the $^{87}Sr/^{86}Sr$ ratios. The groundwater-level contour, as shown in Figure 3-12, obtained from mapping and kriging of groundwater levels, which were observed simultaneously at 86 wells in June of 2010 (3.4). Flow lines are perpendicular to the contours and go northeastward, which indicates that seepage water from the Tedori River flows along the topographic gradient (1/140) of the land surface. Lateral flow from the mountain front is not observed. These results are consistent in principle with the tendency of groundwater flow paths observed by multiple water quality indicators.

Figure 8-7 shows steady-state simulated groundwater flow directions during the irrigation period. The flow direction of seepage water from the river is predominately toward the center of the fan. Seepage water occurring in the upper sections of the Sai River flows to both the sea and the lower part of the Sai River. Thus, the groundwater flow simulation results indicate that the influence of the seepage water from the Sai River to the groundwater was limited. The hydrological observation and simulation results were in reasonable agreement with the distributions of multiple water quality indicators. The observed spatial distribution showed validity of model boundary conditions.

8.5 Conclusions

This study applied a multi-tracer technique to investigate the sources and flow paths of groundwater under an alluvial fan where irrigated paddy fields dominate the land use condition.

Spatial distribution of certain ions and elements, $\delta^{18}O$, δD, and $^{87}Sr/^{86}Sr$ ratios, were examined by conducting simultaneous sampling at 83 sites including 63 groundwater sites, 12 river water sites, 2 spring water sites, and 5 paddy water sites. Analysis of hydrochemical and hydrological characteristics of waters revealed the following:

1) The δD and $\delta^{18}O$ values suggest that the river water and precipitation at the agricultural field except for the irrigated paddy field provided more recharge to the groundwater than did the paddy water at the irrigated paddy field. The result was consistent with the water balance analysis.

2) Several water quality indicators (including Mg, Na, NO_3^--N, δD, $\delta^{18}O$, and the $^{87}Sr/^{86}Sr$ ratios) exhibit similar spatial distributions, with low concentrations occurring along the Tedori River and concentrations increasing with distance from the river. This indicates that seepage water from the Tedori River to the shallow groundwater, which has a dilution effects on the groundwater. Some tracers (Ca, and Sr) occurred in low concentrations near both rivers and high concentration around the center of the fan where the paddy field area ratios were relatively large, indicating that the paddy water affects groundwater qualities. There is no clear evidence of lateral flow from the mountain front.

3) Distributions of the $^{87}Sr/^{86}Sr$ ratios reflected the groundwater flow paths, which cannot be estimated by other water quality parameters. Seepage water from the river, which mainly occurred in the middle sections of the Tedori River, flowed to the northwest towards the coastal area in the center of the fan. There was little seepage water at the downstream section of the Tedori River. The seepage water from the Sai River affects to the groundwater flow only neat the Sai River.

4) Groundwater flow and sources of groundwater recharge estimated from water qualities of various water sources agreed reasonably well with the groundwater level contours map and the estimated water exchange volume along the Tedori River. These results are consistent with the flow direction obtained from the numerical simulation during the irrigation period. Water quality indicators support the validity of the numerical model established.

References

Futamata K, Takahashi I, Inoue M. 2005. Influence of river stream on groundwater and recharge in the Tedori River alluvial fan areas. Research Report of the Hokuriku Regional Office, Ministry of Construction 209–212 (in Japanese).

Geological Survey of Japan, AIST (eds.). 2012. Seamless digital geological map of Japan 1: 200,000. Jul 3, 2012 version. Research Information Database DB084.

Hayase Y. 2013. Fluctuation in characteristic and amount of nitrogen with hydrologic cycle in

Tedori River Basin, In Normal hydrological cycle as a core of irrigation water - Case study in the Tedori River basin assuming the climate change -, Maruyama T. and Hayase Y. (eds.). Ishikawa Prefectural University Press: Ishikawa, pp. 1-10 (in Japanese).

Hosono T, Nakano T, Igeta A, Tayasu I, Tanaka T, Yachi S. 2007. Impact of fertilizer on a small watershed of Lake Biwa: use of sulfur and strontium isotopes in environmental diagnosis. Science of the Total Environment 384: 342-354.

Ishida S, Tsuchihara T. 2013. Stable isotope-based investigation of hydrological aspects of groundwater flow mechanism in Tedori Alluvial Fan, In Normal hydrological cycle as a core of irrigation water - Case study in the Tedori River basin assuming the climate change -, Maruyama T. and Hayase Y. (eds.). Ishikawa Prefectural University Press: Ishikawa, pp. 162-171 (in Japanese).

Hokuriku Regional Agricultural Administration Office. 1977. Hydraulic geology and groundwater in Ishikawa prefecture (in Japanese).

Komiya H, Malaya S, Masuda H, Kusakabe M. 2003. Groundwater flow system in the central and south part of Matumoto basin, Nagano, estimated from oxygen and hydrogen stable isotope ratios and water quality. Journal of Groundwater Hydrology 45(2): 145-168 (in Japanese with English abstract).

Liu Y, Yamanaka T. 2012. Tracing groundwater recharge sources in a mountain-plain transitional area using stable isotopes and hydrochemistry. Journal of Hydrology 464-465: 116-126.

Maruyama T, Noto F, Yoshida M, Horino H, Nakamura K. 2014. Analysis of water balance in the Tedori river alluvial fan areas of Japan: focused on quantitative analysis of groundwater recharge from river and ground surface, especially paddy fields. Paddy Water Environ 12: 163–171.

Maruyama T, Noto F, Yoshida M, Nakamuara K, Horino H, Murashima K, Takimoto H .2012. Analysis of water balance at the Tedori River alluvial fan areas in Japan. J Jpn Soc Hydrol Water Res 25(1): 20–29 (in Japanese with English abstract).

Mizutani Y, Satake H, Yamabe A, Miyachi H, Mase N, Yamayura K. 2001. Hydrogen and oxygen isotope ratios of groundwater in shallow aquier beneath the alluvial fan. Journal of Groundwater Hydrology 43(1): 3-11 (in Japanese with English abstract).

Morita K, Honda T, Nishiura T. 2008. For planning of normal discharge of Tedori River. Technical Report of Hokuriku Regional Office of Construction, Ministry of Construction and Transportation. http://www.hrr.mlit.go.jp/library/kenkyukai/h20/pdf/c/cj_15kanazawa.pdf. (in Japanese).

Nakano T, Tayasu I, Yamada Y, Hosono T, Igeta A, Hyodo F, Andoo A, Saitoh Y, Tanaka T, Wada E, Yachi S. 2008. Effect of agriculture on water quality of Lake Biwa tributaries, Japan.

Science of the total environment 389: 132-148.

Tsujimoto T, Futamata H, Qing X, Sumi T. 2005. Relation between instream flow and underground water in fluvial fan discussed in river management of the Tedori River. Journal of River Engineering 11: 529–534 (in Japanese with English abstract).

Yonebayashi K, Minami Y. 2013. Dynamical clarification of groundwater quality, In Normal hydrological cycle as a core of irrigation water - Case study in the Tedori River basin assuming the climate change -, Maruyama T. and Hayase Y. (eds.). Ishikawa Prefectural University Press: Ishikawa, pp. 172-180 (in Japanese).

CHAPTER 9

Summary and Conclusions

To accomplish sustainable groundwater use, groundwater environments and related processes, such as recharge, flow, and storage, must be well understood. This thesis presents an assessment of the groundwater environment in a paddy-dominated alluvial fan using integrated unsaturated/saturated zone modeling, and hydrological and hydrochemical observations. The present study was conducted in the Tedori River alluvial fan, where paddy-upland crop rotation has been carried out since the 1970s. From the results of this study, the following conclusions can be drawn:

In Chapter 3, the distribution of the groundwater levels and the groundwater flow paths were clarified using simultaneous groundwater-level observations from 1993, 2009, and 2010. The groundwater level during the irrigation period is about 5 m higher than during the non-irrigation period, which implies that paddy irrigation water contributes significantly to groundwater level. Results show that the groundwater levels in the upper and middle parts of the fan during the non-irrigation period declined by 5 m from 1993–2009. Discharge observations of the Tedori River show that there is significant infiltration of river water into shallow groundwater along almost the entire river, except the downstream section.

Chapter 4 includes a discussion of the direct relationship between groundwater levels and paddy field areas that fall within a distance of 0.2–2.0 km from the sampled well, based on results from spatial analysis. There was a positive relationship between the increments in groundwater levels at the beginning of the irrigation period and paddy field area at almost all of the wells, and a noticeable influence on groundwater levels when the paddy fields were at least 1.0 km from observation wells. The effect of changes in the paddy field area on groundwater levels at a given well is greater in the middle part of the fan than in the lower part. These results confirm that, to conserve the paddy fields, it is very important to raise the groundwater level during the irrigation period, especially in the middle and upper parts of the alluvial fan.

Chapter 5 describes how the groundwater model using MODFLOW was developed from hydrological observations. A steady state simulation was used to assess the factors influencing groundwater level, and the effectiveness of groundwater-level protection schemes was evaluated using several actual and hypothetical scenarios of land use and pumping regimes. The groundwater level in the upper and middle parts of the fan was affected considerably by the paddy area and pumping discharge. Analysis of the water balance showed that the net inflow

sources are the Tedori River and the surface boundary, while the net outflow sources are groundwater use, outflows to the Sea of Japan and the Sai River. In cases where the paddy field area was up to 30% less than the present area, it was impossible to maintain the groundwater levels by pumping regulations because of spatial variations in land use and groundwater use. Drawdown of the water level of the Tedori River (0.1–0.3 m) would result in a slight decrease in the groundwater level along the river. If the river water level declines by 0.3 m, the net inflow water to the groundwater will also decrease by 3.5%.

In Chapter 6, the steady state model was extended to include the transient model through coupling of HYDRUS-1D, which simulated the unsaturated flow with MODFLOW. To ensure that high-resolution data of agricultural fields (rice-planted paddy, crop-rotated paddy, and upland) were considered in the model, groundwater recharge was estimated with HYDRUS-1D for each groundwater flow model grid square (400 m × 400 m). Based on groundwater flow simulations for 1975–2009, annual groundwater recharge decreased to 61% of the peak, mainly because of declines in the rice-planted paddy field area and precipitation. Irrigated rice-planted fields have a 5.5-fold greater ability to recharge groundwater than upland fields. The rice-upland crop rotation system could possibly decrease groundwater recharge by between 73－98% of present levels.

In Chapter 7, the response of groundwater levels to predicted climate changes for 2010–2090 was calculated using the transient coupled (unsaturated/saturated) model. The climate change scenarios result from a combination of multiple GCM and GHG emission scenarios, which were provided by ELPIS-JP. In the study area, the amount of precipitation was predicted to change by between -165 and 1092 mm/y (mean 135 mm/y) over the 80 years from 2011–2090 in response to temperature increases of between 2.0 °C and 3.8 °C. Simulation results revealed that groundwater levels would both decrease and increase in response to climate changes, and that groundwater levels were more likely to decrease than increase. The maximum drawdown of the groundwater level was predicted to be approximately 1 m until 2090, and the groundwater level was most sensitive to changes in precipitation during the non-irrigation period. The change rates per day with precipitation amounts of 10–20, 20–30 and above 40 mm/d had little relation to change rates in groundwater levels.

In Chapter 8, the sources and flow paths of groundwater were investigated using a multi-tracer technique. The spatial distribution of certain ions and elements, namely $\delta^{18}O$, δD, and $^{87}Sr/^{86}Sr$ ratios, was examined by collecting samples at 83 sites, including 63 groundwater sites, 12 river water sites, two spring water sites and five paddy water sites. The δD and $\delta^{18}O$ values indicated that the river water provided more recharge to the groundwater than the paddy water. Several water quality indicators, including Mg, Na, δD, $\delta^{18}O$, and the $^{87}Sr/^{86}Sr$ ratios, showed similar spatial distributions; concentrations were relatively low along the Tedori River

and increased with distance from the river. These results suggested that water from the Tedori River seeps into the shallow groundwater, and has a dilution effect on the groundwater. Concentrations of some tracers (NO_3^--N, Ca, and Sr) were relatively low near both the Tedori River and the Sai River. Concentrations, however, were relatively high around the center of the fan where the paddy field area ratios were relatively large, indicating that the paddy water affected groundwater qualities. The groundwater flow paths were identified from distributions of the $^{87}Sr/^{86}Sr$ ratios. Groundwater flow and sources of groundwater recharge estimated from water quality properties of various water sources agreed reasonably well with the groundwater-level contour map and the estimated water exchange volume along the Tedori River. These results are consistent with the net mass balance and the flow direction obtained from numerical simulations during the irrigation period. Water quality indicators support the validity of the newly developed numerical model.

This study quantitatively evaluated the groundwater environment in a paddy-dominated alluvial fan using a combination of hydrological and hydrochemical observations, and numerical simulations that considered unsaturated flow in the paddy field area under a rice-upland crop rotation. Within the spatial and temporal resolution limitations of the model structure and model input data, the developed model produced reasonable estimations of groundwater recharge and levels in a relatively large model domain. The general framework (integrated approach) and computer programs (MODLFOW and HYDRUS-1D) in the present study could be used to illustrate case studies of paddy fields.

Results from the integrated approach clearly showed that river water and precipitation contributed to groundwater levels and groundwater quality in the alluvial fan, where paddy fields dominated. Results also reconfirmed that paddy fields have a significant role in areas recharged by precipitation. Thus, to protect groundwater levels through surface water and groundwater interactions, it is important to maintain the paddy field area and the river's flow. Maintaining the river's flow also contributes to cleaning up groundwater that is contaminated by paddy agriculture. In the study area, irrigation water shortages are predicted to occur during the paddy puddling period because of a decline in snowfall. In the future, it will be increasingly important to allocate river water for paddy irrigation in such a way that the meteorological conditions and paddy farming requirements are both considered. I hope that the findings of this thesis will make a useful contribution to ensuring that river water is distributed in the most suitable way.

Quantitative assessments of the factors influencing recharge and groundwater-level changes for the past, present, and future, such as those in this study, could be used to support groundwater management decision-making processes. Numerical simulations in this study only included natural (meteorology and river water level) and manmade (land and

groundwater uses) processes. To more accurately evaluate groundwater environments, (1) human decision-making processes for irrigation management at the field scale and (2) the influence of socioeconomic factors on agricultural land and water use should be included in future groundwater flow models.

Acknowledgement

First, my deepest appreciation goes to Associate Professor Kimihito NAKAMURA, Graduate School of Agriculture, Kyoto University, for providing me the path of researching and scholarship. Without his the continuing guidance and persistent help this thesis would not have been possible.

I would like to offer my special thanks to Professor Shigeto KAWASHIMA, Graduate School of Agriculture, Kyoto University, for making enormous contribution to my research work and chairperson of the examination committee of this thesis. I would like to thank especially to Professor Satoshi HOSHINO and Professor Masayuki FUJIHARA, Graduate School of Agriculture, Kyoto University, for becoming the member of the examination committee and for their valuable discussions and advice for this research.

I reserve much gratitude to Professor Haruhiko HORINO, Graduate School of Life and Environmental Sciences, Osaka Prefecture University, for his valuable guidance, suggestions, and scientific comments throughout my research work. I am grateful for Mr. Masashi OZAKI who worked on the construction of the numerical model together.

This research was supported by a subsidy from the Ministry of Agriculture, Forestry and Fisheries of Japan entitled “Investigation of the normal hydrological cycle in the Tedori River alluvial fan areas as the core of irrigation water”. I am pleased to acknowledge the encouragement of Dr. Toshisuke MARUYAMA. The author would like to express thanks to the Ishikawa Prefectural government and Ishikawa Prefectural University for helping conduct field observations and providing statistical datasets. Some water quality analyses were conducted at the Research Institute for Humanity and Nature. I received generous support from Professor Takanori NAKANO and Dr. Satoko HASHIMOTO, Research Institute for Humanity and Nature, and Professor Tsugihiro WATANABE, Graduate School of Global Environmental Studies, Kyoto University.

I have plenty of thanks to all members of Hydrological Environment Engineering Laboratory for all the good and rough times we shared and for their sincere cooperation. Last, my heartfelt appreciation goes to Mr. Hidekazu YOSHIOKA and my family, always with me even through my difficult time and fun times.

May, 2014
Yumi IWASAKI